TABLE OF CONTENTS

Table of Contents (Continued)

LIST OF TABLES

List of Tables (Continued)

LIST OF FIGURES

List of Figures (Continued)

2.5.2   VIBRATORY GROUND MOTION

VCS SUP 2.5-2   Insert the following subsections following Subsection 2.5.2 of the DCD.

The vibratory ground motion assessment for the Units 2 and 3 site is described in this section. This assessment was performed in conformance with the guidance in Regulatory Guide 1.208, *A Performance-Based Approach to Define the Site-Specific Earthquake Ground Motion,* March 2007. Regulatory Guide 1.208 incorporates developments in ground motion estimation models; updated models for earthquake sources; methods for determining site response; and new methods for defining a site-specific, performance-based earthquake ground motion that satisfy the requirements of 10 CFR 100.23 and led to the establishment of the safe shutdown earthquake ground motion. The purpose of this section is to develop the Ground Motion Response Spectra (GMRS) characterized by horizontal and vertical response spectra determined as free-field motions on hard rock using performance-based procedures.

The GMRS represents the first part in development of a safe shutdown earthquake for a site as a characterization of the regional and local seismic hazard under Regulatory Position 5.4 of Regulatory Guide 1.208. In the case of the Units 2 and 3 site, the GMRS is used to supplement the certified seismic design response spectra for the AP1000 DCD. The certified seismic design response spectrum is the safe shutdown earthquake for the site for lower frequency ground motions and the site-specific GMRS is the safe shutdown earthquake for higher frequency ground motions. The safe shutdown earthquake defined in this way comprises the vibratory ground motion for which certain structures, systems, and components are designed to remain functional, pursuant to Appendix S to 10 CFR Part 50.

The starting point for this site assessment is the EPRI Seismicity Owners Group PSHA evaluation (Reference 232 and Subsection 2.5.2.2.1).

Subsections 2.5.2.1 through 2.5.2.4 document the review and update of the available EPRI seismicity, seismic sources, ground motion models, and PSHA. Subsection 2.5.2.5 discusses the seismic wave transmission characteristics of the site, wherein, given the implicit uncertainty of the hard rock conditions of the ground motion models used in the PSHA and the detailed discussion in Subsection 2.5.4 of the engineering aspects of the geotechnical investigation, it is concluded that the Units 2 and 3 site is a hard rock site and no site response analyses are required for input to development of the GMRS.

Subsection 2.5.2.6 describes the development of the horizontal GMRS for the Units 2 and 3 site based on the approach in Regulatory Guide 1.208. The vertical GMRS is developed from the vertical-to-horizontal ratios described in Subsection 2.5.2.4.7.

VCS COL 2.5-2   2.5.2.1   Seismicity

The seismic hazard analysis conducted by EPRI (Reference 232) relied on an analysis of historical seismicity in the CEUS to estimate seismicity parameters (rates of activity and Richter b-values) for individual seismic sources. The historical earthquake catalog used in the EPRI analysis was complete through 1984. Data from earthquakes that occurred within the site region since 1984 were reviewed and used to update the EPRI catalog.

2.5.2.1.1   Regional Seismicity Catalog Used for 1989 EPRI Seismic Hazard Analysis Study

Many seismic networks record earthquakes in the CEUS. A large effort was made during the EPRI seismic hazard analysis study to combine available data on historical earthquakes and to develop a homogeneous earthquake catalog that contained all recorded earthquakes for the region. "Homogeneous" means that estimates of body-wave magnitude, m_b, for all earthquakes are consistent, that duplicate earthquakes have been eliminated, that non-earthquakes (*e.g.,* mine blasts and sonic booms) have been eliminated, and that significant events in the historical record have not been missed. Thus, the EPRI catalog (Reference 235) forms a strong basis on which to estimate seismicity parameters.

2.5.2.1.2   Updated Seismicity Data

NRC Regulatory Guide 1.206, *Combined License Applications for Nuclear Power Plants*, Revision 0, June 2007, specifies that earthquakes of MMI greater than or equal to IV or a magnitude greater than or equal to 3.0 should be listed "that have been reported within 200 miles (320 kilometers) of the site." In updating the EPRI catalog, a latitude-longitude window of 30° to 38° N, 77° to 89° W was used. This window incorporates at least a 200-mile (320- kilometer) radius "site region" and all seismic sources contributing significantly to the Units 2 and 3 site earthquake hazard.

The updated catalog was compiled from the following sub-catalogs:

*   EPRI Catalog. The various data fields of the EPRI catalog are described in Reference 235.

*   SEUSSN Catalog. The Southeastern United States Seismic Network catalog is available from the Virginia Tech Seismological Observatory FTP site (Reference 268). In the August 2006 catalog update, the SEUSSN catalog contained 3,131 records dating from March 1698 to December 2004 within the site region latitude-longitude window.   Of these, 1,681 records occurred in 1985 or later.

*   ANSS Catalog. The Advanced National Seismic System (ANSS) catalog (Reference 202) was searched on August 16, 2006 for all records within the site region latitude-longitude window from 1928 to August 7, 2006,

resulting in 2,357 records. Of these, 1,872 records occurred in 1985 or later.

The SEUSSN and ANSS catalogs were used for the temporal update (1985 to present) of the EPRI seismicity catalog. The SEUSSN has coverage over the entire site region (defined above) and is the primary catalog used to compile the national ANSS seismicity catalog. While the SEUSSN catalog is taken as the preferred catalog, some additional events listed only in the ANSS catalog are also included in the update.

The magnitudes given in both catalogs were converted to EPRI *best or expected estimate* of m_b magnitude ($E[m_b]$, also called Emb in Reference 236), using the conversion factors given as equation 4-1 and Table 4-1 in Reference 235:

$$Emb = 0.253 + 0.907 \cdot M_d \qquad \text{(Equation 2.5.2-1)}$$

$$Emb = 0.655 + 0.812 \cdot M_L \qquad \text{(Equation 2.5.2-2)}$$

where M_d is duration or coda magnitude and M_L is "local" magnitude.

The EPRI PSHA study expressed maximum magnitude (M_{max}) values in terms of body-wave magnitude (m_b), whereas most modern seismic hazard analyses describe M_{max} in terms of moment magnitude (**M**). To provide a consistent comparison between magnitude scales, this study relates body-wave magnitude to moment magnitude using the arithmetic average of three equations, or their inversions, presented in Atkinson and Boore (Reference 207), Frankel et al. (Reference 240), and EPRI TR-102293 (Reference 230). The conversion relations are very consistent for magnitudes 4.5 and greater and begin to show divergence at lower magnitudes. Table 2.5.2-201 lists m_b and **M** equivalences developed from these relations over the range of interest for this study.

Equation 4-2 of EPRI (Reference 235) indicates that the equation from which EPRI *uniform magnitude* m_b* (referred to as Rmb in Reference 236) is estimated from the best estimate of magnitude $E[m_b]$ or Emb and the standard deviation of m_b, σ_{mb} (referred to as Smb in Reference 236), is:

$$m_b{}^* = E[m_b] + (1/2) \cdot ln(10) \cdot b \cdot \sigma^2{}_{mb} \qquad \text{(Equation 2.5.2-3)}$$

where b = 1.0.

Values for σ_{mb} [Smb] were estimated for the two catalogs following the EPRI evaluations, and m_b* [Rmb] calculated using Equation 2.5.2-3 for each event added to the updated catalog.

The result of the above process was a catalog of 207 earthquakes shown in Table 2.5.2-202 as the update of the EPRI (Reference 235) seismicity catalog recommended for the site region. For the purpose of recurrence analysis, these should be considered independent events (equivalent to EPRI "MAIN" events).

The 207 events in the 30° to 38° N, 77° to 89° W latitude-longitude window, incorporating the 200-mile (320-kilometer) radius site region, from 1985 to August 2006 with m_b* [Rmb] 3.0 or greater or MMI IV or greater have been incorporated into a number of figures, including tectonic features discussed in Subsection 2.5.2.2.

2.5.2.1.3   Reservoir-Induced Seismicity

A concentration of seismicity in the site area is attributed to the filling of the Monticello Reservoir beginning in December 1977. This zone of small, shallow earthquakes concentrated beneath the reservoir is considered reservoir-induced seismicity because it is spatially and temporally associated with the impoundment of water in the reservoir. Factors that are believed to control reservoir-induced seismicity include ambient stress field conditions, availability of fractures, hydromechanical properties of the underlying rocks, geology of the area, and the dimensions and fluctuations of the reservoir (Reference 273). Reservoir-induced seismicity is common throughout the world and has been observed at other reservoirs in South Carolina, such as Lake Jocassee (References 277 and 278).

Given that this type of induced seismicity had been anticipated, SCE&G installed a microseismic monitoring network in 1977 (three months before the impoundment of the reservoir) to record seismic activity in the area of the VCSNS site and the Monticello Reservoir. This network originally consisted of four high gain/high frequency seismometers located around the Monticello Reservoir and the permanent seismic station near Jenkinsville (Station JSC on Figure 2.5.2-201). The Jenkinsville station began operating as part of the USGS state grid network and subsequently was operated and maintained by the University of South Carolina as part of the South Carolina Seismic Network.

Filling of the Monticello Reservoir began on December 3, 1977, and the reservoir level reached a maximum pond elevation on February 8, 1978 (References 221 and 222). Earthquake activity began in and around the reservoir area on December 25, 1977, about three weeks after filling of the reservoir began (Figure 2.5.2-202). Seismic activity reached a peak in 1978 (with over 4,000 events of magnitude $M_L \geq -0.4$) and then began to decay reaching background levels in the early 1990s (Figure 2.5.2-203). The background rate of 40 events per year was established using four years (1973 to 1977) of recorded events from the Station JSC located about 3 miles east-southeast of the Units 2 and 3 site (Reference 221).

Nearly 10,000 small earthquakes have been recorded since the impoundment of the Monticello Reservoir, most of which occurred in 1978 and 1979 (Reference 221). The reservoir-induced seismicity events extend to a depth of 5 kilometers with most confined to within 3 kilometers of the surface. Seismicity in the first two years occurred primarily within three clusters located near the southern, central, and northern portions of the reservoir (Figure 2.5.2-202). The apparent scatter in the locations of reservoir-induced seismicity events demonstrates that the earthquakes are not located on a single major fault, but instead are located along numerous small fractures that pervade the rock (Reference 266).

The largest recorded reservoir-induced seismicity events in the area had a magnitude M_L 2.8 (References 295, 285, and 284). The reservoir-induced seismicity activity is limited to microseismicity and none of these small events are included in the regional earthquake catalogs. Within 5 miles of the Units 2 and 3 site, there are no events in either the EPRI seismicity catalog (through 1984) or the updated seismicity catalog (1985 to 2006), which indicates that no known events of m_b 3 or larger have occurred in the site area.

As discussed in Reference 295, in 1981 and 1982, both the Advisory Committee on Reactor Safeguards and the Atomic Safety and Licensing Board expressed concerns regarding the impact of these small, reservoir-induced earthquakes on plant equipment and components required for shutdown and residual heat removal. Ground motions recorded from the reservoir-induced seismicity events at the Monticello Reservoir displayed high frequency, apparent high peak accelerations, though low energy. Additional concerns were expressed by the Advisory Committee on Reactor Safeguards regarding the impact of the largest postulated earthquake that might occur from reservoir-induced seismicity—expert opinion suggested as high as a magnitude 5.0 event. In 1982, the Atomic Safety and Licensing Board imposed a License Condition that SCE&G successfully complete a confirmatory program on plant equipment and components to demonstrate that satisfactory safety margins exist considering the ground motions from recorded and potential reservoir-induced seismicity events. The SCE&G Seismic Confirmatory Program (References 265 and 264) was implemented and successfully addressed the Atomic Safety and Licensing Board License Condition by the first year of plant operation (1983).

In 1995, NRC noted that SCE&G had demonstrated that reservoir-induced seismicity had decreased to the point that its continued monitoring was not necessary and agreed to delete the requirement for seismic network operation (Reference 287).

A subsequent increase in seismicity began in December 1996, nearly 20 years after impoundment of the reservoir. By the end of 1999, this renewed seismicity had resulted in over 700 earthquakes ranging in magnitude from M_L -0.4 to 2.5 (Reference 221). This renewed seismicity, likely to continue periodically, is still within the acceptable level considered by the earlier studies.

Although the network remained active and there were enough instruments in the network to detect earthquakes in the Monticello Reservoir area up to 2004, after 1999, the earthquake activity around the Monticello Reservoir again dropped to the background level (Figure 2.5.2-203). The network ceased operation in 2004 (Reference 276).

As was discussed above, the maximum size reservoir-induced seismicity events and their high frequency content have already been considered regarding their impact on the Unit 1 site with the implementation of the Seismic Confirmatory Program in 1983. Continuing reservoir-induced seismicity events have occurred at a diminished rate. Reservoir-induced seismicity, therefore, does not pose any risk or safety issue for the Units 2 and 3 site.

2.5.2.2   Geologic Structures and Tectonic Characteristics of the Site and
               Region

As described in Subsection 2.5.1, a comprehensive review of available geological,
seismological, and geophysical data has been conducted for the Units 2 and 3 site
region and adjoining areas. The following sections summarize seismic source
interpretations from the 1989 EPRI PSHA study (Reference 232) and from
relevant post-EPRI seismic source characterization studies and the updated
interpretations of new and existing sources based on more recent data.

Since publication of the EPRI seismic source model, significant new information
has been developed for assessing the earthquake source that produced the 1886
Charleston earthquake. This new information shows that the Charleston seismic
source should be updated according to Regulatory Guides 1.165 and 1.208.
Paleoliquefaction features and other new information published since the 1986
EPRI project (Reference 234) have significant implications regarding the
geometry, M_{max}, and recurrence of M_{max} in the Charleston seismic source.
Results from the 1989 EPRI study also show that the Charleston seismic source is
the most significant contributor to seismic hazard at the Units 2 and 3 site
(References 232 and 233). Thus, an update of the Charleston seismic source has
been developed. Details of the Updated Charleston Seismic Source (UCSS)
model are presented in Subsection 2.5.2.2.2.4.

Sensitivity studies were performed to evaluate the potential significance of the
UCSS model to seismic hazard at the Units 2 and 3 site, as described in detail in
Subsection 2.5.2.4.4. This analysis of the UCSS interpretations for the Charleston
area shows that the Charleston seismic source still dominates the seismic hazard
at the Units 2 and 3 site. These new interpretations of the possible locations,
sizes, and recurrence intervals of large earthquakes in the Charleston area form a
strong basis with which to calculate the seismic ground motion hazard for the site.

2.5.2.2.1   Summary of EPRI Seismic Sources

This section summarizes the seismic sources and parameters used in the 1986
EPRI project (Reference 234). The description of seismic sources is limited to
those sources within 200 miles of the Units 2 and 3 site (*i.e.,* the site region) and
those at distances greater than 200 miles that may affect the hazard at the Units 2
and 3 site.

As part of the 1986 EPRI project on seismic hazard methodology for the CEUS,
six independent Earth Science Teams (ESTs) evaluated geological, geophysical,
and seismological data to develop a model of seismic sources in the CEUS.
These sources were used to model the occurrence of future earthquakes and
evaluate earthquake hazards at nuclear power plant sites across the CEUS.

Throughout this section, the largest assigned values of M_{max} distributions
assigned by the ESTs to seismic sources are presented for both magnitude scales
(m_b and **M**) to give perspective on the maximum earthquakes that were
considered possible in each seismic source. For example, EPRI m_b values of

M_{max} are followed by the equivalent **M** value. See Table 2.5.2-201 for the relationship between m_b and **M**.

The six ESTs involved in the 1986 EPRI project were Bechtel Group, Dames & Moore, Law Engineering, Rondout Associates, Weston Geophysical Corporation, and Woodward-Clyde Consultants. Each team produced a report (Volumes 5 through 10 of EPRI NP-4726) providing detailed descriptions of how they identified and defined seismic sources. The results were implemented into a PSHA study (Reference 231). For the computation of hazard in the 1989 study, a few seismic source parameters were modified or simplified from the original parameters determined by the six ESTs. EPRI NP-6452-D (Reference 231) summarized the parameters used in the final PSHA calculations, and this reference is the primary source for the seismicity parameters. Each EST provides more detailed descriptions of the rationale and methodology used in evaluating tectonic features and establishing the seismic sources (refer to Volumes 5 through 10 of EPRI NP-4726).

The most significant seismic sources (EPRI RP-101-53 1989) developed by each EST are shown in Figures 2.5.2-204 through 2.5.2-209. For the 1989 EPRI seismic hazard calculations, a screening criterion was implemented to identify those sources whose combined hazard exceeded 99% of the total hazard from all sources measures (Reference 233). These sources are identified in the descriptions below as "primary" seismic sources. Other sources, which together contributed less than 1% of the total hazard from all sources, are identified in the descriptions below as "additional" seismic sources. Earthquakes with body-wave magnitude $m_b \geq 3.0$ are also shown in Figures 2.5.2-204 through 2.5.2-209 to show the spatial relationships between seismicity and seismic sources. Earthquake epicenters include both events from the EPRI earthquake catalog and for the period between 1985 and August 2006 as described in Subsection 2.5.2.1.2.

The maximum magnitude, interdependencies, and probability of activity for each EPRI EST's seismic sources are presented in Tables 2.5.2-203 through 2.5.2-208. These tables present the parameters assigned to each source within 200 miles of the Units 2 and 3 site and include primary and additional seismic sources as defined above. The tables also indicate whether new information has been identified that would lead to a revision of the source's geometry, maximum magnitude, or recurrence parameters. The seismicity recurrence parameters (a- and b-values) used in the seismic hazard studies were computed for each 1° latitude and longitude cell that intersects any portion of a seismic source.

The nomenclature used by each EST to describe the various seismic sources in the CEUS varies from team to team. In other words, a number of different names may have been used by the EPRI teams to describe the same or similar tectonic features or sources, or one team may describe seismic sources that another team does not. For example, the Charleston seismic source was modeled by each team but was called the "Charleston Area and Charleston Faults" by the Bechtel Group team; the "Charleston Seismic Zone" by the Dames & Moore, Law, and Weston teams; and "Charleston" by the Rondout and Woodward-Clyde teams. Each

team's source names, data, and rationale are included in its team-specific documentation (Volumes 5 through 10 of EPRI NP-4726).

The following sections describe the most significant EPRI sources (both primary and additional seismic sources) for each EST with respect to the Units 2 and 3 site. Assessment of these and other EPRI sources within the site region shows that the EPRI source parameters (M_{max}, geometry, and recurrence) are sufficient to capture the current understanding of the seismic hazard in the site region.

Except for the Charleston seismic source, no new geological, geophysical, or seismological information in the literature published since the EPRI NP-6395-D source model suggests that these sources should be modified. Each EST's characterization of the Charleston seismic source was replaced by four alternative source geometries. For each source zone geometry, large earthquake occurrences (**M** 6.7 to 7.5) were modeled with a range of mean recurrence rates, and smaller earthquakes (m_b 5 to 6.7) were modeled with an exponential magnitude distribution, with rates and b-values determined from historical seismicity. Also, all surrounding sources for each team were redrawn so that the new Charleston source geometries were accurately represented as a "hole" in the surrounding source, and seismic activity rates and b-values were recalculated for the modified surrounding sources, based on historical seismicity. Further details and the results of sensitivity analyses performed on the modified seismic sources are presented in Subsection 2.5.2.4.

2.5.2.2.1.1   Sources Used for EPRI PSHA – Bechtel Group

Bechtel Group identified and characterized six primary seismic sources. All six of these primary seismic sources are located within the site region (200 miles). They are:

*   Charleston Area (H)

*   Charleston Faults (N3)

*   Atlantic Coastal Region (BZ4)

*   South Appalachians (BZ5)

*   Southeast Appalachians (F)

*   Northwest South Carolina (G)

In addition to these primary sources, the Bechtel Group characterized four additional seismic sources:

*   Eastern Mesozoic Basins (13)

*   Rosman Fault (15)

- Belair Fault (16)

- H-N3 (C07)

Primary and additional seismic sources characterized by the Bechtel Group team within the site region are listed in Table 2.5.2-203. A map showing the locations and geometries of the Bechtel primary seismic sources is provided in Figure 2.5.2-204. The following is a brief discussion of each of the primary seismic sources characterized by the Bechtel Group team.

- Charleston Area (H). The Charleston Area source (H) is located approximately 60 miles from the Units 2 and 3 site. This oblong combination source area is defined based on the historic earthquake pattern (including the Middleton Place-Summerville and Bowman seismic zones), is elongated northwest-southeast, and encompasses all of source zone N3 (described below). Sources H and N3 are interdependent; if N3 is active, it is unlikely that H is active, and vice versa. The largest M_{max} assigned by Bechtel Group to this zone is m_b 7.4 (**M** 7.9), reflecting its assumption that Charleston-type earthquakes are produced within this zone.

- Charleston Faults (N3). The Charleston Faults (N3) source zone is a small area set within the Charleston Area (H) source zone and encompassing a number of identified and postulated faults in the Charleston, South Carolina, area, including the Ashley River, Charleston, and Woodstock faults. Source N3 is located approximately 100 miles from the Units 2 and 3 site. Sources H and N3 are interdependent; if N3 is active, it is unlikely that H is active, and vice versa. According to EPRI NP-4726, this combination was created for computational simplicity. The largest M_{max} assigned by the Bechtel Group team to this zone is m_b 7.4 (**M** 7.9), reflecting its assumption that Charleston-type earthquakes are produced within this zone.

- Atlantic Coastal Region (BZ4). The Atlantic Coastal Region background (BZ4) source zone is located approximately 50 miles from the Units 2 and 3 site. Source BZ4 is a large background zone that extends from offshore New England to Alabama and encompasses portions of the Coastal Plain from Georgia to southern Virginia. The largest M_{max} assigned by the Bechtel Group team to this zone is m_b 7.4 (**M** 7.9), reflecting its assumption that there is a small probability that a Charleston-type earthquake could occur within this region.

- S Appalachians (BZ5). The Units 2 and 3 site is located within the Southern Appalachians background source (BZ5). This source is a large background region that extends from New York to Alabama, including portions of the Southern Appalachians, Piedmont, and Coastal Plain. The largest M_{max} assigned by the Bechtel Group team to this zone is m_b 6.6 (**M** 6.5).

- <u>SE Appalachians (F)</u>. The Units 2 and 3 site is located within the Southeastern Appalachians source (F), a combination source zone that includes parts of Georgia and the Carolinas and flanks the southwest and northeast borders of Zone G (described below). Source Zone F is mutually exclusive with Zone G; if F is active, G is inactive, and vice versa. The largest M_{max} assigned by the Bechtel Group team to this zone is m_b 6.6 (**M** 6.5).

- <u>NW South Carolina (G)</u>. The Units 2 and 3 site is located within the northwestern South Carolina combination source (G). Source Zone G is mutually exclusive with Zone F; if G is active, F is inactive, and vice versa. The largest M_{max} assigned by the Bechtel Group team to this zone is m_b 6.6 (**M** 6.5).

2.5.2.2.1.2   Sources Used for EPRI PSHA – Dames & Moore

Dames & Moore identified and characterized three primary seismic sources. All three of these seismic sources are located within the site region:

- Charleston Seismic Zone (54)

- South Appalachian Mobile Belt (Default Zone) (53)

- South Cratonic Margin (Default Zone) (41)

In addition to these primary sources, Dames & Moore identified four additional seismic sources:

- Jonesboro Basin (49)

- Florence Basin (51)

- Charleston Mesozoic Rift (52)

- Dunbarton Triassic Basin (65)

Primary and additional seismic sources characterized by the Dames & Moore team within the site region are listed in Table 2.5.2-204. A map showing the locations and geometries of the Dames & Moore primary seismic sources is provided in Figure 2.5.2-205. The following is a brief discussion of these primary seismic sources.

- <u>Charleston Seismic Zone (54)</u>. The Charleston Seismic Zone (54) is a northwest-southeast oriented polygon located about 50 miles from the Units 2 and 3 site. This source includes the Ashley River, Woodstock, Helena Banks, and Cooke faults, as well as the Bowman and Middleton Place-Summerville seismic zones. Source 54 was designed to capture the occurrence of Charleston-type earthquakes. The largest M_{max} assigned by the Dames & Moore team to this zone is m_b 7.2 (**M** 7.5).

- <u>S Appalachian Mobile Belt (Default Zone) (53)</u>. The Units 2 and 3 site is located within the Southern Appalachian Mobile Belt (Default Zone) source (53). This default zone comprises crustal rocks that have undergone several periods of extension and compression. The source is bounded on the east by the east coast magnetic anomaly and on the west by the westernmost boundary of the Appalachian gravity gradient. The largest M_{max} assigned by the Dames & Moore team to this zone is m_b 7.2 (**M** 7.5).

- <u>S Cratonic Margin (Default Zone) (41)</u>. The Southern Cratonic Margin (Default Zone) source is located about 25 mi from the Units 2 and 3 site. This large default zone is located between the Appalachian Fold Belt (4) and the Southern Appalachian Mobile Belt (53) sources and includes the region of continental margin deformed during Mesozoic rifting. Located within this default zone are many Triassic basins and border faults. The largest M_{max} assigned by the Dames & Moore team to this zone is m_b 7.2 (**M** 7.5).

2.5.2.2.1.3   Sources Used for EPRI PSHA – Law Engineering

Law Engineering identified and characterized 16 primary seismic sources all within the site region:

- Charleston Seismic Zone (35)

- Eastern Basement (17)

- Reactivated East Seaboard Normal (22)

- Eastern Piedmont (107)

- Brunswick, North Carolina Background (108)

- Mesozoic Basins (8 – Bridged) (C09)

- 8 – 35 (C10)

- 22 – 35 (C11)

- Eight mafic pluton sources (M31 through M34, and M36 through M39)

In addition to these primary sources, Law Engineering characterized six additional seismic sources:

- Eastern Basement Background (217)

- Three mafic pluton sources (M35, M40, and M41)

- 22 – 24 (C12)

- 22 – 24 – 25 (C13)

Primary and additional seismic sources characterized by the Law Engineering team within the site region are listed in Table 2.5.2-205. A map showing the locations and geometries of the Law Engineering primary seismic sources is provided in Figure 2.5.2-206. The following is a brief discussion of Law's primary seismic sources.

- <u>Charleston Seismic Zone (35)</u>. The Charleston Seismic Zone source (35) is a northeast-southwest elongated polygon that includes the Charleston, Ashley River, and Woodstock faults, as well as parts of the offshore Helena Banks fault and most of the more recently discovered liquefaction features identified by Amick (1990) and others. This source was designed to capture the occurrence of Charleston-type earthquakes. This source is located approximately 100 miles from the Units 2 and 3 site and overlaps with the Reactivated East Seaboard Normal (22; described below) and Buried Mesozoic Basins (8; not a 99% contributor) sources. The largest M_{max} assigned by the Law Engineering team to this zone is m_b 6.8 (**M** 6.8).

- <u>Eastern Basement (17)</u>. The Units 2 and 3 site is located 50 miles from the Eastern Basement (17) source. This source was defined as an area containing pre-Cambrian and Cambrian normal faults, developed during the opening of the proto-Atlantic Ocean, in the basement rocks beneath the Appalachian decollement. The Giles County and Eastern Tennessee Zones of seismicity are included in this source. The largest M_{max} assigned by the Law Engineering team to this zone is m_b 6.8 (**M** 6.8).

- <u>Reactivated East Seaboard Normal (22)</u>. The Units 2 and 3 site is located within the Reactivated Eastern Seaboard Normal (22) source. This source was characterized as a region along the eastern seaboard in which Mesozoic normal faults are reactivated as high-angle reverse faults. The Law Engineering team assigned a single M_{max} of m_b 6.8 (**M** 6.8) to this zone.

- <u>Eastern Piedmont (107)</u>. The Units 2 and 3 site is located within the Eastern Piedmont (107) source zone. This source zone was characterized as a region believed to represent a crustal block overlying mafic transitional or mafic crust located east of the relict North American continental margin and possibly underlain by a regional detachment.

- <u>Brunswick, NC Background (108)</u>. The Units 2 and 3 site is located 50 miles from the Brunswick, North Carolina Background source zone (108). This source represents a zone defined by a low-amplitude, long-wavelength magnetic anomaly pattern. The Law Engineering team interpreted this pattern as possibly indicating a zone of Mesozoic extended crust. The largest M_{max} assigned by the Law Engineering team to this zone is m_b 6.8 (**M** 6.8).

- <u>Mesozoic Basins (8 – Bridged) (C09)</u>. The Units 2 and 3 site is located 50 mi from the Mesozoic Basins (C09) source, which comprises eight bridged basins. This source was defined based on northeast-trending sediment-filled troughs in basement rock bounded by normal faults. The largest M_{max} assigned by the Law Engineering team to this zone is m_b 6.8 (**M** 6.8).

- <u>8–35 (C10)</u>. The Units 2 and 3 site is located 60 miles from the 8–35 combination source (C10). The largest M_{max} assigned by the Law Engineering team to this zone is m_b 6.8 (**M** 6.8).

- <u>22–35 (C11)</u>. The Units 2 and 3 site is located within the 22– 5 combination source (C11). The largest M_{max} assigned by the Law Engineering team to this zone is m_b 6.8 (**M** 6.8).

- <u>Eight Mafic Pluton Sources (M31 through M34, and M36 through M39)</u>. The Law Engineering team identified a number of mafic pluton sources, eight of which are located within approximately 125 miles of the Units 2 and 3 site. The Law Engineering team considered pre- and post-metamorphic plutons in the Appalachians to be stress concentrators and, thus, earthquake sources. Law Engineering assigned a single M_{max} of m_b 6.8 (**M** 6.8) to all mafic pluton sources.

2.5.2.2.1.4   Sources Used for EPRI PSHA – Rondout Associates

Rondout Associates characterized two primary seismic sources both within the site region:

- Charleston (24)

- South Carolina (26)

In addition to these primary sources, Rondout Associates identified seven additional seismic sources within the site region:

- Background 49 (C01)

- Background 50 (C02)

- 50 (02) + 12 (C07)

- 49 + 32 (C09)

- Appalachian Basement (49D)

- Grenville Province (50B)

- Grenville Province (50C)

Primary and additional seismic sources characterized by the Rondout Associates team within the site region are listed in Table 2.5.2-206. A map showing the locations and geometries of the Rondout Associates primary seismic sources is provided in Figure 2.5.2-207. Following is a brief discussion of both of these primary seismic sources.

- Charleston (24). The Charleston source is a northwest-southeast-oriented area set within the larger South Carolina (26) source and located about 55 miles from the Units 2 and 3 site. Source 24 includes the Helena Banks, Charleston, Ashley River, and Woodstock faults, as well as the Bowman and Middleton Place-Summerville seismic zones, and was designed to capture the occurrence of Charleston-type earthquakes. The largest M_{max} assigned by the Rondout Associates team to this zone is m_b 7.0 (**M** 7.2).

- South Carolina (26). The Units 2 and 3 site is located within the South Carolina source (26). The South Carolina source (26) is a northwest-southeast elongated area that surrounds, but does not include, Source 24 (described above). Source 26 includes most of South Carolina except the Charleston area. The largest M_{max} assigned by the Rondout Associates team to this zone is m_b 6.8 (**M** 6.8).

2.5.2.2.1.5   Sources Used for EPRI PSHA – Weston Geophysical

Weston Geophysical identified and characterized twelve primary seismic sources, all within the site region:

- Charleston Seismic Zone (25)

- South Carolina (26)

- Southern Coastal Plain (104)

- 103 – 23 – 24 (C19)

- 104 – 22 (C20)

- 104 – 25 (C21)

- 104 – 22 – 26 (C23)

- 104 – 22 – 25 (C24)

- 104 – 28BCDE – 22 (C26)

- 104 – 28BCDE – 22 – 25 (C27)

- 26 – 25 (C33)

- 104 – 28BE – 25 (C35)

In addition to these primary sources, Weston Geophysical characterized ten additional seismic sources within the site region:

- Mesozoic Basin (28D)

- Mesozoic Basin (28E)

- Southern Appalachians (103)

- 28A through E (C01)

- 103 – 23 (C17)

- 103 – 24 (C18)

- 104 – 26 (C22)

- 104 – 28BCDE (C25)

- 104 – 28BCDE – 22 – 26 (C28)

- 104 – 28BE – 26 (C34)

Primary and additional seismic sources characterized by the Weston Geophysical team are listed in Table 2.5.2-207. A map showing the locations and geometries of the Weston Geophysical primary seismic sources is provided in Figure 2.5.2-208. The following is a brief discussion of each of the Weston Geophysical team's primary seismic sources.

- Charleston Seismic Zone (25). The Charleston Seismic Zone source is an irregularly shaped hexagon centered just northeast of Charleston, South Carolina, and located approximately 80 miles from the Units 2 and 3 site. This source includes the Helena Banks, Charleston, Ashley River, and Woodstock faults, but does not include the Bowman Seismic Zone. This source was designed to capture the occurrence of Charleston-type earthquakes. The largest M_{max} assigned by the Weston Geophysical team to this zone is m_b 7.2 (**M** 7.5).

- South Carolina (26). The South Carolina source (26) is a large area covering most of South Carolina and the Units 2 and 3 site. The largest M_{max} assigned by the Weston Geophysical team to this zone is m_b 7.2 (**M** 7.5).

- Southern Coastal Plain (104). The Southern Coastal Plain source (104) extends from New York to Alabama and from the Towaliga-Lowdenville-Kings Mountain fault trends on the west to the offshore east coast magnetic anomaly on the east. Source 104 was designed to include the Central Virginia Seismic Zone, the Charleston Seismic Zone, and a

number of Mesozoic basins. The largest M_{max} assigned by the Weston Geophysical team to this zone is m_b 6.6 (**M** 6.5).

- Nine Combination Zones: (103–23– 24 [C19]; 104–22 [C20]; 104–25 [C21]; 104– 22–26 [C23]; 104–22–25 [C24]; 104–28BCDE–22 [C26]; 104 –28BCDE–22–25 [C27]; 26–25 [C33]; and 104–28BE–25 [C35]). Weston Geophysical specified a number of combination seismic source zones, nine of which are primary sources for the Units 2 and 3 site. The largest M_{max} assigned by the Weston Geophysical team to these combination zones is m_b 6.6 (**M** 6.5).

2.5.2.2.1.6   Sources Used for EPRI PSHA – Woodward-Clyde Consultants

Woodward-Clyde Consultants identified and characterized six primary seismic sources located within the site region:

- South Carolina Gravity Saddle (Extended) (29)

- South Carolina Gravity Saddle No. 2 (Combo C3) (29A)

- South Carolina Gravity Saddle No. 3 (NW Portion) (29B)

- Charleston (includes "none of the above," NOTA) (30)

- Blue Ridge – alternative configuration (31A)

- V. C. Summer Background (B31)

In addition to these primary sources, Woodward-Clyde Consultants identified one additional seismic source:

- Blue Ridge Combination (31)

Primary and additional seismic sources characterized by the Woodward-Clyde team are listed in Table 2.5.2-208. A map showing the locations and geometries of the Woodward-Clyde primary seismic sources is provided in Figure 2.5.2-209. The following is a brief discussion of each of the primary seismic sources identified by the Woodward-Clyde team.

- <u>South Carolina Gravity Saddle (Extended) (29)</u>. The South Carolina Gravity Saddle (Extended) source (29) covers most of South Carolina and parts of Georgia, including the Units 2 and 3 site. The South Carolina Gravity Saddle source (29) is mutually exclusive with Sources 29A, 29B, and 30; if 29 is active, the other three are inactive, and vice versa. The largest M_{max} assigned by the Woodward-Clyde Consultants team to this zone is m_b 7.4 (**M** 7.9), reflecting its assumption that Charleston-type earthquakes can occur in this zone.

- <u>South Carolina Gravity Saddle No. 2 (Combo C3) (29A)</u>. The South Carolina Gravity Saddle No. 2 source (29A) is an irregularly shaped polygon set within the larger area of Source 29 that includes the Units 2 and 3 site. The South Carolina Gravity Saddle No. 2 source (29A) is mutually exclusive with Sources 29, 29B, and 30; if 29A is active, the other three are inactive, and vice versa. The largest M_{max} assigned by the Woodward-Clyde Consultants team to this zone is m_b 7.4 (**M** 7.9), reflecting its assumption that Charleston-type earthquakes can occur in this zone.

- <u>South Carolina Gravity Saddle No. 3 (NW Portion) (29B)</u>. The South Carolina Gravity Saddle No. 3 source (29B) is a polygon set within the larger area of Source 29 and includes the Units 2 and 3 site. The South Carolina Gravity Saddle No. 3 source (29B) is mutually exclusive with Sources 29, 29A, and 30; if 29B is active, the other three are inactive, and vice versa. The largest M_{max} assigned by the Woodward-Clyde Consultants team to this zone is m_b 7.0 (**M** 7.2).

- <u>Charleston (includes NOTA) (30)</u>. The Charleston seismic source (30) is a northeast-southwest-oriented rectangle that includes most of the Charleston earthquake MMI IX and X area and the Charleston, Ashley River, and Woodstock faults. Source 30 is located approximately 100 miles from the Units 2 and 3 site and was designed to capture the occurrence of Charleston-type earthquakes. The Charleston source (30) is mutually exclusive with Sources 29, 29A, and 29B; if 30 is active, the other three are inactive, and vice versa. The largest M_{max} assigned by the Woodward-Clyde Consultants team to this zone is m_b 7.5 (**M** 8.0).

- <u>V. C. Summer Background (B31)</u>. The V.C. Summer Background (B31) source is a large box containing the Units 2 and 3 site and covering most of South Carolina and Georgia as well as parts of adjoining states and extending offshore. This source is a background zone defined as a rectangular area surrounding the Units 2 and 3 site and is not based on any geological, geophysical, or seismological features. The largest M_{max} assigned by the Woodward-Clyde Consultants team to this zone is m_b 6.6 (**M** 6.5).

2.5.2.2.2   Post-EPRI Seismic Source Characterization Studies

Since the EPRI (References 234 and 232) seismic hazard project, three recent studies have been performed to characterize seismic sources within the Units 2 and 3 site region for PSHAs. These studies include the USGS's National Seismic Hazard Mapping Project (References 240 and 241), the SCDOT seismic hazard mapping project (Reference 219), and the NRC's Trial Implementation Project study (Reference 263). These three studies are described below (in Subsections 2.5.2.2.1 through 2.5.2.2.2.3). Based on a review of recent studies, it was determined that an update of the Charleston seismic source for the EPRI (References 234 and 232) seismic hazard project was required. This update is presented in Subsection 2.5.2.2.2.4. In addition, within the Units 2 and 3 site

region is what is now identified as the Eastern Tennessee Seismic Zone. The significance of the Eastern Tennessee Seismic Zone on the V.C. Summer seismic hazard is discussed in Subsection 2.5.2.2.2.5.

2.5.2.2.2.1   U.S. Geological Survey Model

In 2002, the USGS produced updated seismic hazard maps for the continental United States based on new seismological, geophysical, and geological information (Reference 241). The 2002 maps reflect changes to the source model used to construct the previous version of the national seismic hazard maps (Reference 240). The most significant modifications to the CEUS portion of the source model include changes in the recurrence, M_{max}, and geometry of the Charleston and New Madrid sources.

Unlike the EPRI models that incorporate many local sources, the USGS source model in the CEUS includes only five sources: the Extended Margin background, Stable Craton background, Charleston, eastern Tennessee, and New Madrid (Table 2.5.2-209). Except for the Charleston and New Madrid zones, where earthquake recurrence is modeled by paleoliquefaction data, the hazard for the large background or "maximum magnitude" zones is largely based on historical seismicity and the variation of that seismicity. The USGS source model defines the M_{max} distribution for the Extended Margin background source zone as a single magnitude of **M** 7.5 with a weight of 1.0. The EPRI model, however, includes multiple source zones for each of the six ESTs for this region containing the eastern seaboard and the Appalachians. The EPRI M_{max} distributions for these sources capture a wide range of magnitudes and weights, reflecting considerable uncertainty in the assessment of M_{max} for the CEUS. An **M** 7.5 M_{max} is captured in most of the EPRI source zones, although at a lower weight than assigned by the USGS model.

As part of the 2002 update of the National Seismic Hazard Maps, the USGS developed a model of the Charleston source that incorporates available data regarding recurrence, M_{max}, and geometry of the source zone. The USGS model uses two equally weighted source geometries—one an areal source enveloping most of the tectonic features and liquefaction data in the greater Charleston area, and the second a north-northeast-trending elongated areal source enveloping the southern half of the southern segment of the East Coast Fault System (ECFS) (Table 2.5.2-209 and Figure 2.5.2-210). The Frankel et al. (Reference 241) report does not specify why the entire southern segment of the ECFS is not contained in the source geometry. For M_{max}, the study defines a distribution of magnitudes and weights of **M** 6.8 [0.20], 7.1 [0.20], 7.3 [0.45], 7.5 [0.15]. For recurrence, Frankel et al. (Reference 241) adopts a mean paleoliquefaction-based recurrence interval of 550 years and represent the uncertainty with a continuous lognormal distribution.

2.5.2.2.2.2   South Carolina Department of Transportation (SCDOT) Model

Chapman and Talwani (Reference 219) created probabilistic seismic hazard maps for the SCDOT. In the SCDOT model, treatment of the 1886 Charleston, South Carolina earthquake and similar events dominates estimates of hazard statewide.

The SCDOT model employs a combination of line and area sources to characterize Charleston-type earthquakes in three separate geometries and uses a slightly different M_{max} range (**M** 7.1 to 7.5) than the USGS 2002 model (Table 2.5.2-210 and Figure 2.5.2-211). Three equally-weighted source zones defined for this study include:

1.   A source capturing the intersection of the Woodstock and Ashley River faults.

2.   A larger Coastal South Carolina zone that includes most of the paleoliquefaction sites.

3.   A southern East Coast Fault System source zone.

The respective magnitude distributions and weights used for M_{max} are **M** 7.1 [0.20], 7.3 [0.60], 7.5 [0.20]. The mean recurrence interval used in the SCDOT study is 550 years, based on the paleoliquefaction record.

2.5.2.2.2.3   The Trial Implementation Project Study

The purpose of the Lawrence Livermore National Laboratory Trial Implementation Project study (Reference 263) is to "test and implement the guidelines developed by the Senior Seismic Hazard Analysis Committee" (Reference 270). To test the Senior Seismic Hazard Analysis Committee PSHA methodology, the Trial Implementation Project study focuses on seismic zonation and earthquake recurrence models for the Watts Bar site in Tennessee and the Vogtle site in Georgia. The Trial Implementation Project study uses an expert elicitation process to characterize the Charleston seismic source, considering published data through 1996. The study identifies multiple alternative zones for the Charleston source and for the South Carolina–Georgia Seismic Zone, as well as alternative background seismicity zones for the Charleston region. However, the study focuses primarily on implementing the Senior Seismic Hazard Analysis Committee PSHA methodology and was designed to be as much of a test of the methodology as a real estimate of seismic hazard. As a result, its findings are not included.

2.5.2.2.2.4   Updated Charleston Seismic Source Model

It has been nearly 20 years since the six EPRI ESTs evaluated hypotheses for earthquake causes and tectonic features and assessed seismic sources in the CEUS (Reference 234). The EPRI Charleston source zones developed by each EST are shown in Figure 2.5.2-212 and summarized in Table 2.5.2-211. Several studies that post-date the 1986 EPRI EST assessments have demonstrated that the source parameters for geometry, M_{max}, and recurrence of M_{max} in the Charleston seismic source need to be updated to capture a more current understanding for both the 1886 Charleston earthquake and the seismic source that produced this earthquake. In addition, recent PSHA studies of the South Carolina region (References 263 and 219) and the southeastern United States (Reference 241) have developed models of the Charleston seismic source that

differ significantly from the earlier EPRI characterizations. Therefore, the Charleston seismic source was updated.

The UCSS model is summarized below, in Figure 2.5.2-213 and 2.5.2-214 and presented in detail in Reference 209. Methods used to update the Charleston seismic source follow guidelines provided in Regulatory Guides 1.165 and 1.208. A Senior Seismic Hazard Analysis Committee Level 2 study was performed to incorporate current literature and data and the understanding of experts into an update of the Charleston seismic source model. This level of effort is outlined in the Senior Seismic Hazard Analysis Committee report (Reference 270), which provides guidance on incorporating uncertainty and the use of experts in PSHA studies.

The UCSS model incorporates new information to re-characterize geometry, M_{max}, and recurrence for the Charleston seismic source. These components are discussed in the following sections. Paleoliquefaction data indicates that the Charleston earthquake process is defined by repeated, relatively frequent, large earthquakes located in the vicinity of Charleston, indicating that the Charleston source is different from the rest of the eastern seaboard.

2.5.2.2.2.4.1   UCSS Geometry

The UCSS model includes four mutually exclusive source zone geometries (A, B, B', and C) (Figures 2.5.2-213 and 2.5.2-214). The latitude and longitude coordinates that define these four source zones are presented in Table 2.5.2-212. Details for each source geometry are given below. The four geometries of the UCSS are defined based on current understanding of geologic and tectonic features in the 1886 Charleston earthquake epicentral region; the 1886 Charleston earthquake shaking intensity; distribution of seismicity; and geographic distribution, age, and density of liquefaction features associated with both the 1886 and prehistoric earthquakes. These features, shown in Figures 2.5.1-217 through 2.5.1-219, strongly suggest that most evidence for the Charleston source is concentrated in the Charleston area and is not widely distributed throughout South Carolina. Table 2.5.2-213 provides a subset of the Charleston tectonic features differentiated by pre- and post-EPRI information. In addition, pre- and post-1986 instrumental seismicity, $m_b \geq 3$, are shown on Figures 2.5.1-217 through 2.5.1-219. Seismicity continues to be concentrated in the Charleston region in the Middleton Place-Summerville seismic zone, which has been used to define the intersection of the Woodstock and Ashley River faults (References 282 and 248). Notably, two earthquakes in 2002 (m_b 3.5 and 4.4) are located offshore of South Carolina along the Helena Banks Fault Zone in an area previously devoid of seismicity of $m_b > 3$. A compilation of the EPRI EST Charleston source zones is provided in Figure 2.5.2-212 as a comparison to the UCSS geometries shown in Figure 2.5.2-213.

<u>Geometry A – Charleston</u>

Geometry A is an approximately 100 x 50 kilometer, northeast-oriented area centered on the 1886 Charleston meizoseismal area (Figure 2.5.2-213).

Geometry A is intended to represent a localized source area that generally confines the Charleston source to the 1886 meizoseismal area (*i.e.,* a stationary source in time and space). Geometry A completely incorporates the 1886 earthquake MMI X isoseismal (Reference 213), most of the identified Charleston-area tectonic features and inferred fault intersections, and most of the reported 1886 liquefaction features. Geometry A excludes the northern extension of the southern segment of the East Coast Fault System because this system extends well north of the meizoseismal zone and is included in its own source geometry (Geometry C). Geometry A also excludes outlying liquefaction features, because liquefaction occurs as a result of strong ground shaking that may extend well beyond the areal extent of the tectonic source. Geometry A also envelops instrumentally located earthquakes spatially associated with the Middleton Place-Summerville seismic zone (References 282, 281, and 248).

The preponderance of evidence strongly supports the conclusion that the seismic source for the 1886 Charleston earthquake is located in a relatively restricted area defined by Geometry A. Geometry A envelopes:

1.   The meizoseismal area of the 1886 earthquake

2.   The area containing most of the local tectonic features (although many have large uncertainties associated with their existence and activity, as described earlier)

3.   The area of ongoing concentrated seismicity

4.   The area of greatest density of 1886 liquefaction and prehistoric liquefaction

These observations show that future earthquakes having magnitudes comparable to the Charleston earthquake of 1886 most likely will occur within the area defined by Geometry A. A weight of 0.70 is assigned to Geometry A (Figure 2.5.2-214). To confine the rupture dimension to within the source area and to maintain a preferred northeast fault orientation, Geometry A is represented in the model by a series of closely spaced, northeast-trending faults parallel to the long axis of the zone.

Geometries B, B', and C

While the preponderance of evidence supports the assessment that the 1886 Charleston meizoseismal area and Geometry A define the area where future events will most likely be centered, it is possible that the tectonic feature responsible for the 1886 earthquake either extends beyond or lies outside Geometry A. Therefore, the remaining three geometries (B, B', and C) are assessed to capture the uncertainty that future events may not be restricted to Geometry A. The distribution of liquefaction features along the entire coast of South Carolina and observations from the paleoliquefaction record that a few events were localized (moderate earthquakes to the northeast and southwest of Charleston), suggest that the Charleston source could extend well beyond

Charleston proper. Geometries B and B' are assessed to represent a larger source zone, while Geometry C represents the southern segment of the East Coast Fault System as a possible source zone. The combined geometries of B and B' are assigned a weight of 0.20, and Geometry C is assigned a weight of 0.10. Geometry B', a subset of B, formally defines the onshore coastal area as a source (similar to the SCDOT coastal source zone) that would restrict earthquakes to the onshore region. Geometry B, which includes the onshore and offshore regions, and Geometry B' are mutually exclusive and given equal weight in the UCSS model. Therefore, the resulting weight is 0.10 for Geometries B and B'.

Geometry B - Coastal and Offshore Zone

Geometry B is a coast-parallel, approximately 260 x 100-kilometer source area that:

1.   Incorporates all of Geometry A.

2.   Is elongated to the northeast and southwest to capture other, more distant liquefaction features in coastal South Carolina (References 204, 205, 206, and 280).

3.   Extends to the southeast to include the offshore Helena Banks Fault Zone (Reference 210, Figure 2.5.2-213). The elongation and orientation of Geometry B is roughly parallel to the regional structural grain as well as roughly parallel to the elongation of 1886 isoseismals. The northeastern and southwestern extents of Geometry B are controlled by the mapped extent of paleoliquefaction features (References 204, 205, 206, and 280).

The location and timing of paleoliquefaction features in the Georgetown and Bluffton areas to the northeast and southwest of Charleston have suggested to some researchers that the earthquake source may not be restricted to the Charleston area (References 258, 205, 257, and 280). A primary reason for defining Geometry B is to account for the possibility that there may be an elongated source or multiple sources along the South Carolina coast. Paleoliquefaction features in the Georgetown and Bluffton areas may be explained by an earthquake source both northeast and southwest of Charleston, as well as possibly offshore.

Geometry B extends southeast to include an offshore area and the Helena Banks Fault Zone. The Helena Banks Fault Zone is clearly shown by multiple seismic reflection profiles and has demonstrable late Miocene offset (Reference 210). Offshore earthquakes in 2002 (m_b 3.5 and 4.4) suggest a possible spatial association of seismicity with the mapped trace of the Helena Banks fault system (Figure 2.5.2-213). Whereas these two events in the vicinity of the Helena Banks fault system do not provide a positive correlation with seismicity or demonstrate recent fault activity, these small earthquakes are considered new data since the EPRI studies. The EPRI earthquake catalog (Reference 235) was devoid of any events (m_b 3.0) offshore from Charleston. The recent offshore seismicity also

post-dates the development of the USGS and SCDOT source models that exclude any offshore Charleston source geometries.

A low weight of 0.10 is assigned to Geometry B (Figure 2.5.2-214), because the preponderance of evidence indicates that the seismic source that produced the 1886 earthquake lies onshore in the Charleston meizoseismal area and not in the offshore region. To confine the rupture dimension to within the source area and to maintain a preferred northeast fault orientation, Geometry B is represented in the model by a series of closely spaced, northeast-trending faults parallel to the long axis of the zone.

Geometry B' - Coastal Zone

Geometry B' is a coast-parallel, approximately 260 x 50-kilometer source area that incorporates all of Geometry A, as well as most of the reported paleoliquefaction features (References 204, 205, 206, and 280). Unlike Geometry B, however, Geometry B' does not include the offshore Helena Banks Fault Zone (Figure 2.5.2-213).

The Helena Banks fault system is excluded from Geometry B' to recognize that the preponderance of the data and evaluations support the assessment that the fault system is not active and because most evidence strongly suggests that the 1886 Charleston earthquake occurred onshore in the 1886 meizoseismal area and not on an offshore fault. Whereas there is little uncertainty regarding the existence of the Helena Banks fault, there is a lack of evidence that this feature is still active. Isoseismal maps documenting shaking intensity in 1886 indicate an onshore meizoseismal area (the closed bull's-eye centered onshore, north of downtown Charleston Figures 2.5.1-217 and 2.5.1-218). An onshore source for the 1886 earthquake as well as the prehistoric events is supported by the instrumentally recorded seismicity in the Middleton Place-Summerville Seismic Zone and the corresponding high density cluster of 1886 and prehistoric liquefaction features.

Similar to Geometry B above, a weight of 0.10 is assigned to Geometry B' and reflects the assessment that Geometry B' has a much lower probability of being the source zone for Charleston-type earthquakes than Geometry A (Figure 2.5.2-214). To confine the rupture dimension to within the source area and to maintain a preferred northeast fault orientation, Geometry B' is represented in the model by a series of closely spaced, northeast-trending faults parallel to the long axis of the zone.

Geometry C - East Coast Fault System - South

Geometry C is an approximate 200 x 30-kilometer, north-northeast-oriented source area enveloping the southern segment of the proposed East Coast Fault System shown in Figure 3 of Marple and Talwani (Reference 250) (Figures 2.5.2-213 and 2.5.2-215). The USGS hazard model (Reference 241) (Figure 2.5.2-210) incorporates the East Coast Fault System-South as a distinct source geometry (also known as the zone of river anomalies); however, as described earlier, the

USGS model truncates the northeastern extent of the proposed fault segment. The SCDOT hazard model (Reference 219) also incorporates the East Coast Fault System-South as a distinct source geometry; however, this model extends the southern segment of the proposed East Coast Fault System farther to the south than originally postulated by Marple and Talwani (Reference 250) to include, in part, the distribution of liquefaction in southeastern South Carolina (Figure 2.5.2-216).

In this evaluation, the area of Geometry C is restricted to envelope the original depiction of the East Coast Fault System-South by Marple and Talwani (Reference 250). Rationale for the truncation of the zone to the northeast as shown by the 2002 USGS model is not well documented by Frankel et al. (Reference 241). The presence of liquefaction in southeastern South Carolina is best captured in Geometries B and B', rather than extending the Marple and Talwani (Reference 250) depiction of the East Coast Fault System-South farther to the south.

A low weight of 0.10 is assigned to Geometry C to reflect the assessment that Geometries B, B', and C all have equal, but relatively low, likelihood of producing Charleston-type earthquakes (Figure 2.5.2-214). As with the other UCSS geometries, Geometry C is represented as a series of parallel, vertical faults oriented northeast-southwest and parallel to the long axis of the narrow rectangular zone. The faults and extent of earthquake ruptures are confined within the rectangle depicting Geometry C.

UCSS Model Parameters

Based on studies by Bollinger et al. (References 215 and 216) and Bollinger (Reference 214), a 20-kilometer-thick seismogenic crust is assumed for the UCSS. To model the occurrence of earthquakes in the characteristic part of the Charleston distribution (**M**>6.7), the model uses a series of closely-spaced, vertical faults parallel to the long axis of each of the four source zones (A, B, B', and C). Faults and earthquake ruptures are limited to within each respective source zone and are not allowed to extend beyond the zone boundaries, and ruptures are constrained to occur within the depth range of 0 to 20 kilometers. Modeled fault rupture areas are assumed to have a width-to-length aspect ratio of 0.5, conditional on the assumed maximum fault width of 20 kilometers. To obtain M_{max} earthquake rupture lengths from magnitude, the Wells and Coppersmith (Reference 290) empirical relationship between surface rupture length and **M** for earthquakes of all slip types is used.

To maintain as much similarity as possible with the original EPRI model, the UCSS model treats earthquakes in the exponential part of the distribution (**M**<6.7) as point sources uniformly distributed within the source area (full smoothing), with a constant depth fixed at 10 kilometers.

2.5.2.2.2.4.2   UCSS Maximum Magnitude

The six EPRI ESTs developed a distribution of weighted M_{max} values and weights to characterize the largest earthquakes that could occur on Charleston seismic sources. On the low end, the Law Engineering team assessed a single M_{max} of m_b 6.8 to seismic sources it considered capable of producing earthquakes comparable in magnitude to the 1886 Charleston earthquake. On the high end, four teams defined M_{max} upper bounds ranging between m_b 7.2 and 7.5. The m_b magnitude values are converted to moment magnitude (**M**), as described previously. The m_b value and converted moment magnitude value for each team are shown below. The range in **M** for the six ESTs is 6.5 to 8.0.

Team	Charleston M_{max} range
Bechtel Group	m_b 6.8 to 7.4 (**M** 6.8 to 7.9)
Dames & Moore	m_b 6.6 to 7.2 (**M** 6.5 to 7.5)
Law Engineering	m_b 6.8 (**M** 6.8)
Rondout	m_b 6.6 to 7.0 (**M** 6.5 to 7.2)
Weston Geophysical	m_b 6.6 to 7.2 (**M** 6.5 to 7.5)
Woodward-Clyde Consultants	m_b 6.7 to 7.5 (**M** 6.7 to 8.0)

The **M** equivalents of EPRI m_b estimates for Charleston M_{max} earthquakes show that the upper bound values are similar to, and in two cases exceed, the largest modern estimate of **M** 7.3 ±0.26 (Reference 246) for the 1886 earthquake. The upper bound values for five of the six ESTs also exceed the preferred estimate of **M** 6.9 by Bakun and Hopper (Reference 208) for the Charleston event. The EPRI M_{max} estimates are more heavily weighted toward the lower magnitudes, with the upper bound magnitudes given relatively low weights by several ESTs (Tables 2.5.2-203 through 2.5.2-208). Therefore, updating the M_{max} range and weights to reflect the current range of technical interpretations is warranted for the UCSS.

Based on assessment of the currently available data and interpretations regarding the range of modern M_{max} estimates (Table 2.5.2-214), the UCSS model modifies the USGS magnitude distribution (Reference 241) to include a total of five discrete magnitude values, each separated by 0.2 **M** units (Figure 2.5.2-214). The UCSS M_{max} distribution includes a discrete value of **M** 6.9 to represent the Bakun and Hopper (Reference 208) best estimate of the 1886 Charleston earthquake magnitude, as well as a lower value of **M** 6.7 to capture a low probability that the 1886 earthquake was smaller than the Bakun and Hopper mean estimate of **M** 6.9. Bakun and Hopper do not explicitly report a one-sigma range in magnitude estimate of the 1886 earthquake, but do provide a two-sigma range of **M** 6.4 to **M** 7.2.

The UCSS magnitudes and weights are:

M	Weight	
6.7	0.10	
6.9	0.25	Bakun and Hopper (Reference 208) mean
7.1	0.30	
7.3	0.25	Johnston (Reference 246) mean
7.5	0.10	

This results in a weighted M_{max} mean magnitude of **M** 7.1 for the UCSS, which is slightly lower than the mean magnitude of **M** 7.2 in the USGS model (Reference 241).

2.5.2.2.2.4.3   UCSS Recurrence Model

In the 1989 EPRI study (Reference 232), the six EPRI ESTs used an exponential magnitude distribution to represent earthquake sizes for their Charleston sources. Parameters of the exponential magnitude distribution were estimated from historical seismicity in the respective source areas. This resulted in recurrence intervals for M_{max} earthquakes (at the upper end of the exponential distribution) of several thousand years.

The current model for earthquake recurrence is a composite model consisting of two distributions. The first is an exponential magnitude distribution used to estimate recurrence between the lower-bound magnitude used for hazard calculations and m_b 6.7. The parameters of this distribution are estimated from the earthquake catalog, as they were for the 1989 EPRI study. This is the standard procedure for smaller magnitudes and is the model used, for example, by the USGS 2002 national hazard maps (Reference 241). In the second distribution, M_{max} earthquakes (**M**≥6.7) are treated according to a characteristic model, with discrete magnitudes and mean recurrence intervals estimated through analysis of geologic data, including paleoliquefaction studies. In this document, M_{max} is used to describe the range of largest earthquakes in both the characteristic portion of the UCSS recurrence model and the EPRI exponential recurrence model.

This composite model achieves consistency between the occurrence of earthquakes with **M**<6.7 and the earthquake catalog and between the occurrence of large earthquakes (**M**≥6.7) with paleoliquefaction evidence. It is a type of "characteristic earthquake" model in which the recurrence rate of large events is higher than what would be estimated from an exponential distribution inferred from the historical seismic record.

M_{max} Recurrence

This section describes how the UCSS model determines mean recurrence intervals for M_{max} earthquakes. The UCSS model incorporates geologic data to characterize the recurrence intervals for M_{max} earthquakes. As described earlier, identifying and dating paleoliquefaction features provides a basis for estimating the recurrence of large Charleston area earthquakes. Most of the available geologic data pertaining to the recurrence of large earthquakes in the Charleston area were published after 1990 and, therefore, was not available to the six EPRI ESTs. In the absence of geologic data, the six EPRI EST estimates of recurrence for large, Charleston-type earthquakes were based on a truncated exponential model using historical seismicity (References 234 and 232). The truncated exponential model also provided the relative frequency of all earthquakes greater than m_b 5.0 up to M_{max} in the EPRI PSHA. The recurrence of M_{max} earthquakes in the EPRI models was on the order of several thousand years, which is significantly greater than more recently published estimates of about 500 to 600 years, based on paleoliquefaction data (Reference 280).

Paleoliquefaction Data

Strong ground shaking during the 1886 Charleston earthquake produced extensive liquefaction, and liquefaction features from the 1886 event are preserved in geologic deposits at many locations in the region. Documentation of older liquefaction-related features in geologic deposits provides evidence for prior strong ground motions during prehistoric large earthquakes. Estimates of the recurrence of large earthquakes in the UCSS are based on dating paleoliquefaction features. Many potential sources of ambiguity and/or error are associated with dating and interpreting paleoliquefaction features. This assessment does not reevaluate field interpretations and data; rather, it reevaluates criteria used to define individual paleoearthquakes in the published literature. In particular, the UCSS reevaluates the paleoearthquake record interpreted by Talwani and Schaeffer (Reference 280) based on that study's compilation of sites with paleoliquefaction features.

Talwani and Schaeffer (Reference 280) compiled radiocarbon ages from paleoliquefaction features along the coast of South Carolina. This data include ages that provide contemporary, minimum, and maximum limiting ages for liquefaction events. Radiocarbon ages were corrected for past variability in atmospheric ^{14}C using well-established calibration curves and converted to "calibrated" (approximately calendar) ages. From their compilation of calibrated radiocarbon ages from various geographic locations, Talwani and Schaeffer correlated individual earthquake episodes. They identified an individual earthquake episode based on samples with a "contemporary" age constraint that had overlapping calibrated radiocarbon ages at approximately one-sigma confidence interval. The estimated age of each earthquake was "calculated from the weighted averages of overlapping contemporary ages." They defined as many as eight events (named 1886, A, B, C, D, E, F, and G in order of increasing age) from the paleoliquefaction record, and offered two scenarios to explain the distribution and timing of paleoliquefaction features (Table 2.5.2-217).

The two scenario paleoearthquake records proposed by Talwani and Schaeffer (Reference 280) have different interpretations for the size and location of prehistoric events (Table 2.5.2-215). In their Scenario 1, the four prehistoric events that produced widespread liquefaction features similar to the large 1886 Charleston earthquake (A, B, E, and G) are interpreted to be large, 1886 Charleston-type events. Three events—C, D, and F—are defined by paleoliquefaction features that are more limited in geographic extent than other events and are interpreted to be smaller, moderate-magnitude events (approximately **M** 6). Events C and F are defined by features found north of Charleston in the Georgetown region, and Event D is defined by sites south of Charleston in the Bluffton area. In their Scenario 2, all events are interpreted as large, 1886 Charleston-type events. Furthermore, Events C and D are combined into a large Event C'. Talwani and Schaeffer justify the grouping of the two events based on the observation that the calibrated radiocarbon ages that constrain the timing of Events C and D are indistinguishable at the 95% (two-sigma) confidence interval.

The length and completeness of the paleoearthquake record based on paleoliquefaction features is a source of epistemic uncertainty in the UCSS. The paleoliquefaction record along the South Carolina coast extends from 1886 to the mid-Holocene (Reference 280). The consensus of the scientists who have evaluated this data (*e.g.,* Talwani and Schaeffer) is that the paleoliquefaction record of earthquakes is complete only for the most recent about 2,000 years and that it is possible that liquefaction events are missing from the older portions of the record. The suggested incompleteness of the paleoseismic record is based on the argument that past fluctuations in sea level have produced time intervals of low water table conditions (and thus low liquefaction susceptibility), during which large earthquake events may not have been recorded in the paleoliquefaction record (Reference 280). While this assertion may be true, it cannot be ruled out that the paleoliquefaction record may be complete back to the mid-Holocene.

<u>Two-Sigma Analysis of Event Ages</u>

Analysis of the coastal South Carolina paleoliquefaction record is based on the Talwani and Schaeffer data compilation. As described above, Talwani and Schaeffer use calibrated radiocarbon ages with one-sigma error bands to define the timing of past liquefaction episodes in coastal South Carolina. The standard in paleoseismology, however, is to use calibrated ages with two-sigma (95.4% confidence interval) error bands (Reference 242). Likewise, in paleoliquefaction studies, to more accurately reflect the uncertainties in radiocarbon dating, the use of calibrated radiocarbon dates with two-sigma error bands (as opposed to narrower one-sigma error bands) is advisable (Reference 283). The Talwani and Schaeffer use of one-sigma error bands may lead to over-interpretation of the paleoliquefaction record such that more episodes are interpreted than actually occurred. In recognition of this possibility, the conventional radiocarbon ages presented in Talwani and Schaeffer (Reference 280) have been recalibrated and reported with two-sigma error bands. The recalibration of individual radiocarbon samples and estimation of age ranges for paleoliquefaction events show broader

age ranges with two-sigma error bands that are used to obtain broader age ranges for paleoliquefaction events in the Charleston area.

Event ages based on overlapping two-sigma ages of paleoliquefaction features are presented in Table 2.5.2-215. Paleoearthquakes have been distinguished based on grouping paleoliquefaction features that have contemporary radiocarbon samples with overlapping calibrated ages. Event ages have then been defined by selecting the age range common to each of the samples. For example, an event defined by overlapping two-sigma sample ages of 100 to 200 cal yr BP and 50 to 150 cal yr BP would have an event age of 100 to 150 cal yr BP. The UCSS study considers the "trimmed" ages to represent the approximately 95% confidence interval, with a "best estimate" event age as the midpoint of the approximately 95% age range.

The two-sigma analysis identified six distinct paleoearthquakes in the data presented by Talwani and Schaeffer (Reference 280). As noted by that study, Events C and D are indistinguishable at the 95% confidence interval, and in the UCSS, those samples define Event C' (Table 2.5.2-215). Additionally, the UCSS two-sigma analysis suggests that Talwani and Schaeffer Events F and G may have been a single, large event, defined in the UCSS as F'. One important difference between the UCSS result and that of Talwani and Schaeffer is that the three—Events C, D, and F—in their Scenario 1, which are inferred to be smaller, moderate-magnitude events, are grouped into more regionally extensive Events C' and F' (Table 2.5.2-215). Therefore, in the UCSS, all earthquakes in the two-sigma analysis have been interpreted to represent large, Charleston-type events. The incorporation of large Events C' and F' into the UCSS model is, in effect, a conservative approach. In the effort to estimate the recurrence of M_{max} events (**M** 6.7 to 7.5), moderate-magnitude (about **M** 6) earthquakes C and D would be eliminated from the record of large (M_{max}) earthquakes in the UCSS model, thereby increasing the calculated M_{max} recurrence interval and lowering the hazard without sufficient justification. For these reasons, the UCSS model uses a single, large Event C' (instead of separate, smaller Events C and D) and a single, large Event F' (instead of separate, smaller Events F and G). Analysis suggests that there have been four large earthquakes in the most recent, about 2000-year portion of the record (1886 and Events A, B, and C'). In the entire 5000-year paleoliquefaction record, there is evidence for six large, Charleston-type earthquakes (1886, A, B, C', E, F') (Table 2.5.2-215). Figure 2.5.2-216 shows the geographic distribution of liquefaction features associated with each event in the UCSS model. The distributions of paleoliquefaction sites for Events A, B, C', E, and F' are all very similar to the coastal extent of the liquefaction features from the 1886 earthquake.

Recurrence intervals developed from the earthquakes recorded by paleoliquefaction features are based on an assumption that these features were produced by large M_{max} events and that both the 2000-year and 5000-year records are complete. However, the UCSS report (Reference 209) mentions at least two concerns regarding the use of the paleoliquefaction record to characterize the recurrence of past M_{max} events. First, it is possible that the paleoliquefaction features associated with one or more of these pre-1886 events

were produced by multiple moderate-sized events closely spaced in time. If this were the case, then the calculated recurrence interval would yield artificially short recurrence for M_{max}, because it was calculated using repeat times of both large (M_{max}) events and smaller earthquakes. Limitations of radiocarbon dating and limitations in the stratigraphic record often preclude identifying individual events in the paleoseismologic record that are closely spaced in time (*i.e.,* separated by only a few years to a few decades). Several seismic sources have demonstrated tightly clustered earthquake activity in space and time that are indistinguishable in the radiocarbon and paleoseismic record:

• New Madrid (1811, 1811, 1812)

• North Anatolian Fault (1999 and 1999)

• San Andreas Fault (1812 and 1857)

The distinct possibility that M_{max} occurs less frequently than what is calculated from the paleoliquefaction record is discussed in the UCSS report Reference 209.

A second concern is that the recurrence behavior of the M_{max} event may be highly variable through time. For example, the UCSS considers it unlikely that **M** 6.7 to **M** 7.5 events have occurred on a Charleston source at an average repeat time of about 500 to 600 years (Reference 280) throughout the Holocene Epoch. Such a moment release rate would likely produce tectonic landforms with clear geomorphic expression, such as are present in regions of the world with comparably high rates of moderate to large earthquakes (for example, faults in the eastern California shear zone with submillimeter-per-year slip rates and recurrence intervals on the order of about 5000 years have clear geomorphic expression (Reference 261). Perhaps it is more likely that the Charleston source has a recurrence behavior that is highly variable through time, such that a sequence of events spaced approximately 500 years apart is followed by quiescent intervals of thousands of years or longer. This sort of variability in inter-event time may be represented by the entire mid-Holocene record, in which both short inter-event times (*e.g.,* about 400 years between Events A and B) are included in a record with long inter-event times (*e.g.,* about 1900 years between Events C' and E).

<u>Recurrence Rates</u>

The UCSS model includes a calculation of two average recurrence intervals covering two different time intervals that are used as two recurrence branches on the logic tree (Figure 2.5.2-214). The first average recurrence interval is based on the four events that occurred within the past approximate 2000 years. This time period is considered to represent a complete portion of the paleoseismic record (Reference 280). These events include 1886, A, B, and C' (Table 2.5.2-215). The average recurrence interval calculated for the most recent portion of the paleoliquefaction record (four events over the past approximately 2000 years) is given 0.80 weight on the logic tree (Figure 2.5.2-214).

The second average recurrence interval is based on events that occurred within the past approximate 5,000 years. This time period represents the entire paleoseismic record based on paleoliquefaction data (Reference 280). These events include 1886, A, B, C', E, and F' as listed in Table 2.5.2-215. As mentioned previously, published papers and researchers suggest that the older part of the record (older than about 2000 years ago) may be incomplete. Whereas this assertion may be true, it is also possible that the older record, which exhibits longer inter-event times, is complete. The average recurrence interval calculated for the 5000-year record (six events) is given 0.20 weight on the logic tree (Figure 2.5.2-214). The 0.80 and 0.20 weighting of the 2000-year and 5000-year paleoliquefaction records, respectively, reflects incomplete knowledge of both the current short-term recurrence behavior and the long-term recurrence behavior of the Charleston source.

The mean recurrence intervals for the most recent 2000-year and past 5000-year records represent the average time interval between earthquakes attributed to the Charleston seismic source. The mean recurrence intervals and their parametric uncertainties were calculated according to the methods outlined by Savage (Reference 262) and Cramer (Reference 227). The methods provide a description of mean recurrence interval, with a best estimate mean T_{ave} and an uncertainty described as a lognormal distribution with median $T_{0.5}$ and parametric lognormal shape factor $\sigma_{0.5}$.

The lognormal distribution is one of several distributions, including the Weibull, Double Exponential, and Gaussian, among others, used to characterize earthquake recurrence (Reference 228). Ellsworth et al. (Reference 228) and Matthews et al. (Reference 253) propose a Brownian-passage time model to represent earthquake recurrence, arguing that it more closely simulates the physical process of strain buildup and release. This Brownian-passage time model is currently used to calculate earthquake probabilities in the greater San Francisco Bay region (Reference 294). Analyses show that the lognormal distribution is very similar to the Brownian-passage time model of earthquake recurrence for cases where the time elapsed since the most recent earthquake is less than the mean recurrence interval (References 226 and 228). This is the case for Charleston, where 120 years have elapsed since the 1886 earthquake and the mean recurrence interval determined over the past 2000 years is approximately 548 years. The UCSS study calculates an average recurrence interval using a lognormal distribution because its statistics are well known (Reference 256) and it has been used in numerous studies (References 262, 293, and 227).

The average interval between earthquakes is expressed as two continuous lognormal distributions. The average recurrence interval for the 2,000-year record, based on the three most recent inter-event times (1886-A, A-B, B-C'), has a best estimate mean value of 548 years and an uncertainty distribution described by a median value of 531 years and a lognormal shape factor of 0.25. The average recurrence interval for the 5,000-year record, based on five inter-event times (1886-A, A-B, B-C', C'-E, E-F'), has a best estimate mean value of 958 years and an uncertainty distribution described by a median value of 841 years and a lognormal shape factor of 0.51. At one standard deviation, the average recurrence

interval for the 2,000-year record is between 409 and 690 years; for the 5,000-year record, it is between 452 and 1,564 years. Combining these mean values of 548 and 958 years with their respective logic tree weights of 0.8 and 0.2 results in a weighted mean of 630 years for Charleston M_{max} recurrence.

The mean recurrence interval values used in the UCSS model are similar to those determined by earlier studies. Talwani and Schaeffer (Reference 280) consider two possible scenarios to explain the distribution in time and space of paleoliquefaction features. In their Scenario 1, large earthquakes have occurred with an average recurrence of 454 ±21 years over about the past 2000 years; in their Scenario 2, large earthquakes have occurred with an average recurrence of 523 ±100 years over the past 2,000 years. Talwani and Schaeffer state that, "In anticipation of additional data we suggest a recurrence rate between 500 and 600 years for **M** 7+ earthquakes at Charleston." For the 2000-year record, the one-standard-deviation range of 409 to 690 years completely encompasses the range of average recurrence interval reported by Talwani and Schaeffer. The best-estimate mean recurrence interval value of 548 years is comparable to the midpoint of the Talwani and Schaeffer best-estimate range of 500 to 600 years. The best estimate mean recurrence interval value from the 5000-year paleoseismic record of 958 years is outside the age ranges reported by Talwani and Schaeffer, although they did not determine an average recurrence interval based on the longer record.

In the updated seismic hazard maps for the conterminous United States, Frankel et al. (Reference 241) use a mean recurrence value of 550 years for characteristic earthquakes in the Charleston region. This value is based on the above-quoted 500 to 600 year estimate from Talwani and Schaeffer. Frankel et al. do not incorporate uncertainty in mean recurrence interval in their calculations.

For computation of seismic hazard, discrete values of activity rate (inverse of recurrence interval) are required as input to the PSHA code (Reference 225). To evaluate PSHA based on mean hazard, the mean recurrence interval and its uncertainty distribution should be converted to mean activity rate with associated uncertainty. The final discretized activity rates used to model the UCSS in the PSHA reflect a mean recurrence of 548 years and 958 years for the 2000-year and 5000-year branches of the logic tree, respectively. Lognormal uncertainty distributions in activity rate are obtained by the following steps:

1. Invert the mean recurrence intervals to get mean activity rates.

2. Calculate median activity rates using the mean rates and lognormal shape factors of 0.25 and 0.51 established for the 2000-year and 5000-year records, respectively.

3. Determine the lognormal distributions based on the calculated median rate and shape factors.

The lognormal distributions of activity rate can then be discretized to obtain individual activity rates with corresponding weights.

2.5.2.2.2.5   Eastern Tennessee Seismic Zone

The Eastern Tennessee Seismic Zone is one of the most active seismic zones in eastern North America. This region of seismicity in the southern Appalachians is described in detail in Subsection 2.5.1. Despite its high rate of activity, the largest known earthquake in the Eastern Tennessee Seismic Zone is magnitude 4.6 (magnitude scale unspecified) (Reference 220). No evidence for larger prehistoric earthquakes, such as paleoliquefaction features has been discovered (References 220 and 292). While the lack of large earthquakes in the relatively short historical record cannot preclude the future occurrence of large events, there is a much higher degree of uncertainty associated with the assignment of M_{max} for the Eastern Tennessee Seismic Zone than other CEUS seismic source zones, such as New Madrid and Charleston, where large historical earthquakes are known to have occurred.

The EPRI source model (Reference 234) includes various source geometries and parameters to represent the seismicity of the Eastern Tennessee Seismic Zone. All but one of the EPRI ESTs modeled local source zones to capture this area of seismicity and some of the teams included more than one zone. The Law Engineering team did not include a specific, local source for the Eastern Tennessee Seismic Zone; however, the Eastern Tennessee Seismic Zone and Giles County Seismic Zones were included in a larger seismic source zone called the Eastern Basement (17). A wide range of M_{max} values and associated probabilities were assigned to these sources to reflect the uncertainty of multiple experts from each EST. The moment magnitude (**M**) equivalents of body-wave magnitude (m_b) M_{max} values assigned by the ESTs range from **M** 4.8 to 7.5. The Dames & Moore sources for the Eastern Tennessee Seismic Zone included the largest upper-bound M_{max} value of **M** 7.5. Sources from the Woodward-Clyde and Rondout teams assigned large upper-bound M_{max} values of **M** 7.2.

Subsequent hazard studies have used M_{max} values within the range of maximum magnitudes used by the six EPRI models. Collectively, upper-bound maximum values of M_{max} used by the EPRI teams ranged from **M** 6.3 to 7.5. Using three different methods specific to the eastern Tennessee seismic source, Bollinger (Reference 214) estimated an M_{max} of **M** 6.3. The Bollinger model also included the possibility that the Eastern Tennessee Seismic Zone was capable of generating a larger magnitude event and included an **M** 7.8 (m_b 7.37) with a low probability of 5% in the M_{max} distribution. The 5% weighted **M** 7.8 by Bollinger slightly exceeds the ERPI range, but the **M** 6.3 value was given nearly the entire weight (95%) in his characterization of the Eastern Tennessee Seismic Zone. This smaller magnitude is much closer to the mean magnitude (approximately **M** 6.2) of the EPRI study. The Trial Implementation Project study (Reference 263) also provided a broad M_{max} distribution for the Eastern Tennessee Seismic Zone. This study developed magnitude distributions for all Eastern Tennessee Seismic Zone source zone representations that ranged from as low as **M** 4.5 to as high as **M** 7.5, with a mode of about **M** 6.5 for almost each distribution (Reference 263). The broad distribution of the Trial Implementation Project study magnitude distribution for the Eastern Tennessee Seismic Zone source zones is very similar to the EPRI distribution of **M** 4.8 to **M** 7.5. The USGS source model assigns a single M_{max}

value of **M** 7.5 for the Eastern Tennessee Seismic Zone (Reference 241). The most recent characterizations of the Eastern Tennessee Seismic Zone M_{max} by the USGS and Trial Implementation Project study consider **M** 7.5 as the largest magnitude in the distribution and this magnitude is captured by the range of M_{max} values used in EPRI (Reference 234). Therefore, it is concluded that no new information has been developed since 1986 that would require a significant revision to the EPRI seismic source model.

The ground motion hazard at the Units 2 and 3 site is dominated by the Charleston seismic source, and the inclusion of new recurrence values for Charleston based on paleoliquefaction serves to increase the relative contribution of Charleston with respect to any distant source, such as the Eastern Tennessee Seismic Zone. No modifications to the EPRI parameters for Eastern Tennessee Seismic Zone source zones were made.

2.5.2.3   Correlation of Earthquake Activity with Seismic Sources

The final part of the review and update of the 1989 EPRI seismic source model was a correlation of updated seismicity with the 1989 model source. The EPRI seismicity catalog covers earthquakes in the CEUS through 1984, as described in Subsection 2.5.2.1. Figures 2.5.2-204 through 2.5.2-209 show the distribution of earthquake epicenters from both the EPRI (pre-1985) and updated (post-1984 through August 2006) earthquake catalogs in comparison to the seismic sources identified by each of the EPRI ESTs.

Comparison of the additional events of the updated earthquake catalog to the EPRI earthquake catalog shows:

*   There are no new earthquakes within the site region that can be associated with a known geologic structure.

*   There are no unique clusters of seismicity that suggest a new seismic source not captured by the EPRI seismic source model.

*   The updated catalog does not show a pattern of seismicity that requires significant revision to the geometry of any of the EPRI seismic sources.

*   The updated catalog neither shows nor suggests any increase in M_{max} for any of the EPRI seismic sources.

The updated catalog does not imply a significant change in seismicity parameters (rate of activity, b-value) for any of the EPRI seismic sources (Subsection 2.5.2.4.2).

2.5.2.4   Probabilistic Seismic Hazard Analysis and Controlling Earthquakes

This section describes the PSHA conducted for the VCSNS site. Following the procedures outlined in Regulatory Guides 1.165 and 1.208, Subsection 2.5.2.4.1 contains a description of the basis for the PSHA, which is the 1989 EPRI study

(Reference 232). Subsection 2.5.2.4.2 presents sensitivity studies using an updated earthquake catalog that includes an analysis of historical seismicity through August 2006. The significance of new information on maximum magnitudes and on seismic source characterization is discussed in Subsections 2.5.2.4.3 and 2.5.2.4.4, respectively. The effects of recent models to characterize earthquake ground motions in the CEUS are presented in Subsection 2.5.2.4.5. Subsection 2.5.2.4.6 presents the results of these revisions to the PSHA in the form of uniform hazard response spectra (UHRS). Finally, Subsection 2.5.2.4.7 develops vertical ground motions in the form of vertical UHRS that are consistent with the horizontal UHRS, to present a complete representation of earthquake shaking.

2.5.2.4.1   1989 EPRI Seismic Hazard Study

The 1989 EPRI study (Reference 232) was the starting point for probabilistic seismic hazard calculations. This follows the recommendation of Regulatory Guide 1.165. An underlying principle of this study was that expert opinion on alternative, competing models of earthquake occurrence (size, location, and rates of occurrence) and of ground motion amplitude and its variability should be used to weight alternative hypotheses. The result is a family of weighted seismic hazard curves from which mean and fractile seismic hazard can be derived.

The first task was to calculate seismic hazard using the assumptions on seismic sources and ground motion equations developed in the 1989 EPRI study to ensure that seismic sources were modeled correctly and that the software being used (Risk Engineering, Inc.'s FRISK88[a] software) could accurately reproduce the 1989 study results. Table 2.5.2-216 compares the mean annual frequencies of exceedance calculated for the Units 2 and 3 site to published annual frequencies of exceedance from the 1989 EPRI study for this site. All results are for hard rock conditions. The "% diff" column shows the percent difference of hazard calculated for current calculations at the Units 2 and 3 site compared to the 1989 result. Comparisons are shown for peak ground acceleration hazard for the mean, median, and 85th fractile hazard curves. For the mean hazard curves, the current calculation indicates slightly higher hazard, with up to +6.1% difference at 1g. For ground motions associated with typical seismic design levels (peak ground acceleration <0.5g), the differences are 3.5% or less. Differences in hazard are also small for the median hazard, except at large ground motions (peak ground acceleration ≥0.7g), where differences of +20% and +30% are seen. For the 85th fractile hazard, differences are both positive and negative, but are less than 6.4% (absolute value) for peak ground acceleration ≤0.5g.

The comparisons shown in Table 2.5.2-216 are considered to be within acceptable agreement, given that independent software is used and that the recommendations for seismic spectra are made using the mean hazard. Differences in seismic hazard of +6% will correspond to differences in ground motions of about +2%, for a given hazard level.

---

a.   FRISK88 is a proprietary software of Risk Engineering, Inc.

Several types of new information on the sources of earthquakes may require changes in inputs to PSHA, resulting in changes in the level of seismic hazard at the Units 2 and 3 site compared to what would be calculated based on the EPRI (Reference 232) evaluation. Seismic source characterization data and information that could affect the calculated level of seismic hazard include:

- Effects caused by an updated earthquake catalog and resulting changes in the characterization of the rate of earthquake occurrence as a function of magnitude for one or more seismic sources.

- Identification of possible new seismic sources in the site region.

- Changes in the characterization of the maximum magnitude for seismic sources.

- Changes to models used to estimate strong ground shaking and its variability in the CEUS.

Possible changes to seismic hazard caused by changes in these areas are addressed in the following sections.

2.5.2.4.2   Effect of Updated Earthquake Catalog

Subsection 2.5.2.1.2 describes the development of an updated earthquake catalog. This updated catalog includes modifications to the EPRI evaluation by subsequent researchers, the addition of earthquakes that have occurred after completion of the EPRI evaluation development (post-March 1985), and identification of additional earthquakes in the time period covered by the EPRI evaluation (1627 to 1984). The impact of the new catalog information is assessed by evaluating the effect of the new data on earthquake magnitude estimates and on earthquake recurrence estimates within the 200-mile region around the Units 2 and 3 site.

The effect of the updated earthquake catalog on earthquake occurrence rates is assessed by computing earthquake recurrence parameters for three test areas shown in Figure 2.5.2-219. These consist of a rectangular area encompassing seismicity in the vicinity of the site, a polygon encompassing seismicity in the region of eastern Tennessee, and a square area encompassing seismicity in the Charleston, South Carolina region. The truncated exponential recurrence model is fit to the seismicity data using the EPRI EQPARAM program, which uses the maximum likelihood technique. Earthquake recurrence parameters are computed first using the original EPRI catalog and periods of completeness, and then using the updated catalog and extending the periods of completeness to 2005, assuming that the probability of detection for all magnitudes is unity for the time period 1985 to 2005. The resulting earthquake recurrence rates are compared in Figures 2.5.2-220 through 2.5.2-222 for the three test areas. The comparison for all three areas shows that the extended earthquake catalog results in lower estimated earthquake occurrence rates.

On the basis of the comparisons shown in Figures 2.5.2-220 through 2.5.2-222, it is concluded that the earthquake occurrence rate parameters developed in the EPRI (Reference 232) evaluation adequately and conservatively represent seismicity rates in the vicinity of the Units 2 and 3 site.

As discussed in Subsection 2.5.2.2.2.4.3 paleoliquefaction studies also have been conducted in the region of the 1886 Charleston, South Carolina, earthquake. The results of these studies have led to estimated repeat times for large earthquakes in the Charleston region of approximately 550 years. This repeat time represents higher occurrence rates than obtained from the EPRI seismic hazard model. As a result, the Charleston seismic source model of each EPRI team is modified as discussed in Subsection 2.5.2.4.4.

2.5.2.4.3   New Maximum Magnitude Information

As discussed in Subsection 2.5.2.2.1, no new scientific information has been published that would lead to a change in the EPRI seismic source characterization or parameters, including the assessment of maximum magnitude. The only exceptions are for the Charleston, South Carolina and New Madrid, Missouri regions, which are addressed in the next subsection. As a result, the maximum magnitude distributions assigned to the 1989 EPRI sources are not modified for the calculation of seismic hazard.

2.5.2.4.4   New Seismic Source Characterization

Subsections 2.5.1 and 2.5.2.2.2 contain a review of new geological, geophysical, and seismological information related to seismic source characterization models developed for post-EPRI seismic hazard analyses. Subsection 2.5.2.1.2 describes the updated earthquake catalog that was developed to augment the EPRI 1989 (References 234, 235, and 236) earthquake catalog. Based on these evaluations, no additional specific seismic sources have been identified. Figures 2.5.2-204 through 2.5.2-209 show the range of seismic source geometries defined by the EPRI teams in the vicinity of the Units 2 and 3 site.

Seismic sources defined by the EPRI ESTs to represent possible locations for a recurrence of the 1886 Charleston earthquake were included in the EPRI (References 232 and 233) hazard calculation for the vicinity of the Units 2 and 3 site. These sources were updated as described in Subsection 2.5.2.2.2.4 because more recent data regarding the location and recurrence of large magnitude earthquakes in the vicinity of Charleston, South Carolina, suggest alternative source configurations and more frequent occurrence of these events than were modeled by the EPRI teams. These new interpretations are considered as follows.

The new UCSS model reflects updated estimates of the possible geometries of seismic sources in the Charleston region. The UCSS model also updates the characteristic earthquake magnitudes that might occur and the possible mean recurrence rates associated with those characteristic magnitudes. The following four geometries and weights are used:

- Geometry A, weight 0.7

- Geometry B, weight 0.1

- Geometry BP, weight 0.1

- Geometry C, weight 0.1.

As described in Subsection 2.5.2.2.2.4.2, the distribution of characteristic magnitudes is represented with five discrete values and associated weights: **M**=6.7 (0.1), 6.9 (0.25), 7.1 (0.3), 7.3 (0.25), and 7.5 (0.1). The distribution of the mean recurrence interval is described in Subsection 2.5.2.2.2.4.3 and is based on two data periods for paleoliquefaction events. For each data period, a separate mean recurrence interval and uncertainty are estimated, and a five-point discrete distribution (with weights) is used to quantify each distribution. This results in a total of 10 estimates of mean recurrence interval, each with an associated weight.

The four geometries described above are shown in Figure 2.5.2-223. For seismic hazard calculations, these geometries were represented with parallel faults spaced 10 kilometers apart, and the activity rate estimated for the Charleston source was distributed equally among the parallel faults. A general rupture length equation (Reference 290) is used to model a finite rupture length for each earthquake. The distance between the Units 2 and 3 site and the Charleston sources, and the general northeast-southwest trend of the UCSS geometries (resulting in the fault ruptures being generally perpendicular to a line drawn between the site and the Charleston faults) means that the seismic hazard at the Units 2 and 3 site is not very sensitive to the details of the faults or rupture length equation.

In addition to the UCSS fault model, four area sources for the Charleston region were included in the seismic hazard calculation, to represent small magnitude, exponentially distributed earthquakes. Because large-magnitude earthquakes were modeled with the UCSS, the exponential distribution Charleston sources were modeled with magnitude distributions up to m_b 6.5. The rates of occurrence and b-values for these four area sources were calculated with the EPRI EQPARAM software using the EPRI earthquake catalog through 1984.

Seismicity in the Charleston area was modeled by the EPRI ESTs. In order not to double-count seismicity and seismic hazard, these EPRI team Charleston sources were removed from the seismic hazard analysis. Other EPRI team sources surrounding the Charleston area are modified to have sources that fully surrounded the UCSS geometries, without any areas that leave a gap in seismicity. As examples, Figures 2.5.2-224 through 2.5.2-227 show Rondout source 26 with UCSS geometries A, B, BP (equivalent to B'), and C as holes, so that there are no gaps in seismicity. The seismicity parameters for these modified EPRI team sources were recalculated using the EPRI EQPARAM software and using the same seismicity parameter assumptions specified by each team for that source, for the 1989 EPRI study. For consistency, the EPRI earthquake catalog

(through 1984) was used for these calculations. Other assumptions about these sources (specifically the maximum magnitude distributions) were not modified.

The source logic of the EPRI ESTs was also modified to reflect the new source logic of the UCSS and to reflect the weights (given above) of the UCSS geometries. The probabilities of activity of other EPRI team sources in the eastern United States were not modified.

An updated New Madrid Seismic Zone source model is also included in the PSHA. The New Madrid Seismic Zone extends from southeastern Missouri to southwestern Tennessee and is located more than 700 kilometers west of VCSNS (Figure 2.5.2-217). The original EPRI Seismicity Owners Group study did not consider the New Madrid source because it is more than 500 kilometers from the VCSNS site (Reference 232). Analysis based on the updated New Madrid source model indicates a minimal contribution to the low frequency hazard at the VCSNS site as described below.

Subsection 2.5.1.1.3.2.3 presents a detailed discussion of the New Madrid Seismic Zone. The New Madrid Seismic Zone produced a series of historical, large-magnitude earthquakes between December 1811 and February 1812 (Reference 245). Several studies that post-date the 1986 EPRI EST assessments demonstrate that the source parameters for geometry, M_{max}, and recurrence of M_{max} in the New Madrid region need to be updated to capture a more current understanding of this seismic source (References 241, 246, 208, 227, 245, and 283).

The updated New Madrid seismic source model described in Reference 238 forms the basis for determining the potential contribution from the New Madrid Seismic Zone to seismic hazard at the VCSNS (Figures 2.5.2-217 and 2.5.2-218). This model accounts for new information on recurrence intervals for large earthquakes in the New Madrid area, for recent estimates of possible earthquake sizes on each of the active faults, and for the possibility of multiple earthquake occurrences within a short period of time (earthquake clusters).

Three sources are identified in the New Madrid Seismic Zone, each with two alternative fault geometries:

Seismic Source	Fault Geometry
Southern New Madrid	Blytheville Arch/Bootheel Lineament
	Blytheville Arch/Blytheville Fault Zone
Northern New Madrid	New Madrid North
	New Madrid North Plus Extension
Reelfoot Fault	Reelfoot Central Section
	Reelfoot Full Length

Earthquakes are treated as characteristic events in terms of magnitudes. Table 2.5.2-221 presents the magnitudes that represent the centers of characteristic magnitude ranges that extend ±0.25 magnitude units above and below the indicated magnitude.

Seismic hazard is calculated considering the possibility of clustered earthquake occurrences. The modeling of earthquake clusters in the New Madrid Seismic Zone has undergone considerable study. A model is adopted in which all three sources rupture during each "event," and the hazard is computed using this simplified model. This model results in slightly higher ground motion hazard than if the possibility of two source ruptures is considered, or if a smaller-magnitude earthquake is considered for one of the three ruptures. The occurrence rate of earthquake clusters is developed using two models—a Poisson model and a lognormal renewal model with a range of coefficients of variation (Reference 238). Consistent with Reference 238, all faults are assumed to be vertical and to extend from the surface to a 20-kilometer depth. A finite rupture model is used to represent an extended rupture on all sources. Because of the great distance between the New Madrid Seismic Zone and the VCSNS site, the details of the geometrical representation of each fault are not critical to the seismic hazard calculations.

2.5.2.4.5   New Ground Motion Models

Since the 1989 EPRI (Reference 232) study, ground motion models for the CEUS have evolved. An EPRI project was conducted to summarize knowledge about CEUS ground motions, and results were published in EPRI (Reference 229). These updated equations estimate median spectral acceleration and its uncertainty as a function of earthquake magnitude and distance. Epistemic uncertainty is modeled using multiple ground motion equations with weights, and using multiple estimates of aleatory uncertainty, also with weights. Different sets of equations are recommended for seismic sources that represent rifted versus non-rifted regions of the earth's crust. Equations are available for hard rock site for spectral frequencies of 100 Hz (which is equivalent to PGA), 25 Hz, 10 Hz, 5 Hz, 2.5 Hz, 1 Hz, and 0.5 Hz.

Abrahamson and Bommer (Reference 201) reexamined the aleatory uncertainties published by EPRI (Reference 229) because it was thought that the aleatory uncertainties were probably too large, resulting in overestimates of seismic hazard. The Abrahamson and Bommer study recommended a revised set of aleatory uncertainties and weights that can be used to replace the original aleatory uncertainties.

To correctly model the damageability of small magnitude earthquakes to engineered facilities, the cumulative absolute velocity model of Hardy et al. (Reference 244) is used. The cumulative absolute velocity model in effect filters out the fraction of small magnitude earthquakes that do not cause damage to engineered structures, and includes in the hazard calculations only those ground motions with a cumulative absolute velocity value greater than 0.16g-sec. The filter that is used is based on empirical ground motion records and depends on

ground motion amplitude, duration of motion (which depends on earthquake magnitude), and shear-wave velocity in the top 30 meters at the site. The ground motions for frequencies other than 100 Hz are assumed to be correlated with the ground motions at 100 Hz, so that the filtering is consistent from frequency to frequency.

In summary, the ground motion model used in the seismic hazard calculations consists of the median equations from EPRI (Reference 229) combined with the updated aleatory uncertainties of the Abrahamson and Bommer (Reference 201) study. The cumulative absolute velocity filter is applied to account for the lack of damage of small magnitude earthquake ground motions.

2.5.2.4.6   Updated Probabilistic Seismic Hazard Analysis and Deaggregation

The seismic hazard at the Units 2 and 3 site is recalculated with the previously described changes to the Charleston and New Madrid source models, to the surrounding EPRI EST sources, and to the ground motion model for the CEUS. This calculation is for hard rock conditions, which is consistent with conditions at the Units 2 and 3 site and with the EPRI (Reference 229) ground motion model.

A PSHA consists of calculating annual frequencies of exceeding various ground motion amplitudes for all possible earthquakes that are hypothesized in a region. The seismic sources specify the rates of occurrence of earthquakes as a function of magnitude and location, and the ground motion model estimates the distribution of ground motions at the site for each event. Multiple weighted hypotheses on seismic sources, earthquake rates of occurrence, and ground motions (characterized by the median ground motion amplitude and its uncertainty) result in multiple weighted seismic hazard curves, and from these the mean and fractile seismic hazard can be determined. The calculation is made separately for each of the six EPRI teams, and the seismic hazard distribution for the teams is combined, weighting each team equally. This combination gives the overall mean and distribution of seismic hazard at the site.

Figures 2.5.2-228 through 2.5.2-234 show mean and fractile (15th, median, and 85th) seismic hazard curves from this calculation for the seven spectral frequencies that are available from the EPRI (Reference 229) ground motion model. Figure 2.5.2-235 shows mean and median UHRS for 10^{-4} and 10^{-5} annual frequencies of exceedance. The mean UHRS values are also documented in Table 2.5.2-217 for annual frequencies of exceedance of 10^{-4}, 10^{-5}, and 10^{-6}.

The seismic hazard was deaggregated following the guidelines of Regulatory Guide 1.165. Specifically, the mean contributions to seismic hazard for 1 Hz and 2.5 Hz were deaggregated by magnitude and distance for the mean 10^{-4} ground motions at 1 Hz and 2.5 Hz, and these deaggregations were combined. Figure 2.5.2-236 shows this combined deaggregation. Similar deaggregations of the mean hazard were performed for 5 and 10 Hz spectral accelerations (Figure 2.5.2-237). Deaggregations of the mean hazard for 10^{-5} and 10^{-6} ground motions are shown in Figures 2.5.2-238 through 2.5.2-241. Deaggregation of the mean seismic hazard is recommended in Regulatory Guide 1.206. Table 2.5.2-218

summarizes the mean magnitudes and distances resulting from these deaggregations for all contributions to hazard and for contributions with distances exceeding 100 kilometers.

Figures 2.5.2-236 through 2.5.2-241 include the contribution to hazard for the number of logarithmic standard deviations that the applicable ground motion (10^{-4}, 10^{-5}, or 10^{-6}) is above the logarithmic mean. These figures indicate that the largest contribution to hazard for 10^{-4} and 10^{-5} ground motions comes from values between 0 and 2 standard deviations above the mean, which is a common result.

The deaggregation plots in Figures 2.5.2-236 through 2.5.2-239 for 10^{-4} and 10^{-5} ground motions indicate that the Charleston seismic source has a major contribution to seismic hazard at the Units 2 and 3 site. For 10^{-4} annual frequency of exceedance, this source is the largest contributor to seismic hazard for both 5 and 10 Hz (Figure 2.5.2-237) and 1 and 2.5 Hz (Figure 2.5.2-236). For an annual frequency of 10^{-5}, the contribution is smaller particularly for high frequencies (see Figures 2.5.2-238 and 2.5.2-239). For an annual frequency of 10^{-6}, virtually all the hazard at high frequencies comes from local sources (Figure 2.5.2-241), while low frequencies have about equal contributions from the Charleston seismic source and from local sources (Figure 2.5.2-240).

Table 2.5.2-218 indicates mean magnitudes and distances calculated from the deaggregations, both for all distances and for R>100 kilometers.   For the 1 and 2.5 Hz results, contributions from events with R>100-kilometer exceed 5% of the total hazard. As a result, following the guidance of Regulatory Guide 1.165, the controlling earthquake for low-frequency ground motions was selected from the R>100-kilometer calculation, and the controlling earthquake for high-frequency ground motions was selected from the overall calculation. The values of **M** and R selected in this way are shown in shaded cells in Table 2.5.2-218.

Smooth UHRS in Table 2.5.2-220 were developed from the UHRS amplitudes in Table 2.5.2-217, using controlling earthquake **M** and R values shown in Table 2.5.2-218 and using the hard rock spectral shapes for CEUS earthquake ground motions recommended in NUREG/CR-6728 (Reference 260). Separate spectral shapes were developed for high frequencies and low frequencies. To reflect accurately the UHRS values calculated by the PSHA as shown in Table 2.5.2-217, the high-frequency spectral shape was anchored to the UHRS values from Table 2.5.2-217 at 100 Hz, 25 Hz, 10 Hz, and 5 Hz. In between these frequencies, the spectrum was interpolated using shapes anchored to the next higher and lower frequency and using weights on the two shape equal to the inverse logarithmic difference between the intermediate frequency and the next higher or lower frequency. Below 5 Hz, the high-frequency shape was extrapolated from 5 Hz. For the low-frequency spectral shape, a similar procedure was used except that the low-frequency spectral shape was anchored to the UHRS values at 2.5 Hz, 1 Hz, and 0.5 Hz. Below 0.5 Hz and above 2.5 Hz, the low-frequency shape was extrapolated from those frequencies.

Figures 2.5.2-242 and 2.5.2-243 show the horizontal high-frequency and low-frequency spectra calculated in this way for 10^{-4} and 10^{-5} annual frequencies of

exceedance, respectively. For each annual frequency of exceedance, the envelope of the high-frequency and low-frequency spectra gives the rock UHRS for that annual frequency. As mentioned previously, these spectra accurately reflect the UHRS amplitudes in Table 2.5.2-217 that were calculated for the seven spectral frequencies at which PSHA calculations were done.

2.5.2.4.7   Vertical Ground Motions

Vertical spectra were scaled from the horizontal spectra using scaling factors for hard rock published by Risk Engineering, Inc. (Reference 260). These scaling factors (V/H ratios) depend on the peak ground acceleration of the horizontal motion and are different for the 10^{-4} UHRS and the 10^{-5} UHRS. (Categories of V/H ratios in Reference 260 are for peak ground acceleration less than 0.2g, between 0.2g and 0.5g, and greater than 0.5g.) Figure 2.5.2-244 shows the V/H ratios as a function of structural frequency that apply to the 10^{-4} horizontal UHRS (peak ground acceleration less than 0.2g) and to the 10^{-5} horizontal UHRS (peak ground acceleration between 0.2g and 0.5g).

Figure 2.5.2-245 shows the resulting estimated vertical UHRS for 10^{-4}, calculated by multiplying the envelope of the 10^{-4} high-frequency and low-frequency spectra from Figure 2.5.2-242 by the V/H ratio shown in Figure 2.5.2-244 for peak ground acceleration <0.2g. Similarly, Figure 2.5.2-245 shows the resulting estimated vertical UHRS for 10^{-5}, calculated by multiplying the envelope of the 10^{-5} high-frequency and low-frequency spectra from Figure 2.5.2-243 by the V/H ratio shown in Figure 2.5.2-244 for peak ground acceleration between 0.2g and 0.5g.

2.5.2.5   Seismic Wave Transmission Characteristics of the Site

The geotechnical conditions at the Units 2 and 3 site are described in Subsection 2.5.4.1. The description in this subsection indicates that the Units 2 and 3 site is underlain by weathered and unweathered bedrock with a high shear wave velocity (greater than 8,500 ft/sec) (see Figure 2.5.4-226). Safety-related structures are founded on fresh, hard bedrock.

The requirement of conducting a site response analysis to assess seismic wave transmission characteristics at the site is contingent on the ground motion conditions implied by the ground motion attenuation model used in the PSHA. As stated in Reference 229, the ground model used for the PSHA presented in Subsection 2.5.2.4 *"The ground motion model will be applicable to hard-rock conditions in the CEUS. For this application hard rock conditions are defined as shear-wave velocities (V_S) greater than 2.8 km/s,"* or 9,200 ft/s. While the 2004 EPRI study (Reference 229) does not specify an applicable range for this minimum shear-wave velocity, this study and the various ground motion models used in development of the 2004 EPRI ground motion model commonly refer to an earlier 1993 EPRI study (Reference 230) for the basis of the shear-wave velocity, which is that at the top of a shallow crustal model used in ground motion modelling. The 1993 EPRI study, in addressing the variation in several crustal models considered for the CEUS, as well as uncertainty in Poisson's Ratio—used for converting the original compressional-wave velocity-based crustal models to

shear-wave velocity models—suggests at least an uncertainty of several hundred feet/sec in the specification of the best estimate of 9,200 ft/s. Further, the 1993 EPRI study concluded that this variability in shear-wave velocity was not significant in ground motion modelling compared to other modeling factors.

Therefore, the site-specific ground motions are developed for a surface outcrop of the hard bedrock. Given that the shear-wave velocity of this material within several hundred feet/sec is consistent with the hard rock site classification used for the EPRI (Reference 229) ground motion model, the PSHA results and uniform hazard spectra developed in Subsection 2.5.2.4 are considered representative of surface motions on this outcropping material without modification. Under this condition, the rock motions shown in Figures 2.5.2-242 and 2.5.2-243 do not have to be modified to account for the effects of local soft rock or soil profiles on seismic wave propagation.

VCS COL 2.5-3

2.5.2.6 Ground Motion Response Spectrum

The horizontal GMRS was developed from the horizontal UHRS using the approach described in ASCE/SEI Standard 43-05 (Reference 203) and Regulatory Guide 1.208. The vertical GMRS was developed from the vertical UHRS described in Subsection 2.5.2.4.7.

The ASCE/SEI Standard 43-05 (Reference 203) approach defines the GMRS using the site-specific UHRS, which is defined for Seismic Design Category SDC-5 at a mean 10^{-4} annual frequency of exceedance. The procedure for computing the GMRS is as follows.

For each spectral frequency at which the UHRS is defined, a slope factor A_R is determined from:

$$A_R = SA(10^{-5})/SA(10^{-4})$$ (Equation 2.5.2-4)

where $SA(10^{-4})$ is the spectral acceleration SA at a mean UHRS exceedance frequency of 10^{-4}/year (and similarly for $SA(10^{-5})$). A design factor is defined based on A_R, which reflects the slope of the mean hazard curve between 10^{-4} and 10^{-5} mean annual frequencies of exceedance. The design factor at each spectral frequency is given by:

$$\text{design factor} = 0.6(A_R)^{0.80}$$ (Equation 2.5.2-5)

and

$$GMRS = \max[SA(10^{-4}) \times \max(1, \text{design factor}), 0.45 \times SA(10^{-5})]$$ (Equation 2.5.2-6)

The derivation of design factor is described in detail in the Commentary to ASCE/SEI Standard 43-05 and in Regulatory Guide 1.208. Table 2.5.2-219 shows the

values of A_R and DF calculated at each structural frequency and the resulting GMRS. The horizontal GMRS is plotted in Figure 2.5.2-246.

The vertical GMRS was calculated in an identical way, using the 10^{-4} and 10^{-5} vertical UHRS as shown in Figure 2.5.2-245. Table 2.5.2-220 shows V/H ratios at each frequency, the 10^{-4} and 10^{-5} vertical UHRS, the values of A_R and design factor, and the vertical GMRS. The vertical GMRS is plotted in Figure 2.5.2-246.

A comparison of the site-specific GMRS to the hard rock high frequency spectra (HRHFS) is provided in Figures 2.0-201 and 2.0-202. The HRHFS are also shown in DCD Figures 3I.1-1 and 3I.1-2, where they are compared to the Certified Seismic Design Response Spectra (CSDRS).

Section 2.5.2 References

201. Abrahamson, N. A. and Bommer, J., *Program on Technology Innovation: Truncation of the Lognormal Distribution and Value of the Standard Deviation for Ground Motion Models in the Central and Eastern United States,* Electric Power Research Institute, Palo Alto, California, Technical Report 1014381, August 2006.

202. Advanced National Seismic System 2006. ANSS/CNSS Worldwide Earthquake Catalog file (catalog_search2_pl_ext_SEARCH_081606.htm) was downloaded August 16, 2006. Available at http://www.ncedc.org/anss/catalog-search.html.

203. American Society of Civil Engineers, *Seismic Design Criteria for Structures, Systems, and Components in Nuclear Facilities*, Report ASCE/SEI 43-05, 2005.

204. Amick, D., *Paleoliquefaction Investigations Along the Atlantic Seaboard With Emphasis on the Prehistoric Earthquake Chronology of Coastal South Carolina*: unpub. Ph.D. dissertation, University of South Carolina, 1990.

205. Amick, D., Gelinas, R., Maurath, G., Cannon, R., Moore, D., Billington, E., and Kemppinen, H., *Paleoliquefaction Features Along the Atlantic Seaboard,* U.S. NRC Report, NUREG/CR-5613, 147p., 1990.

206. Amick, D., Maurath, G., and Gelinas, R., *Characteristics of Seismically Induced Liquefaction Sites and Features Located In the Vicinity of the 1886 Charleston, South Carolina Earthquake:* Seismological Research Letters, Volume 61, no. 2, p. 117-130, 1990.

207. Atkinson, G. M. and Boore, D. M., *Ground-Motion Relations for Eastern North America:* Bulletin of the Seismological Society of America, Volume 85, no. 1, 17-30, 1995.

208. Bakun, W. H. and Hopper, M. G., *Magnitudes and Locations of the 1811-1812 New Madrid, Missouri, and the 1886 Charleston, South Carolina, Earthquakes:* Bulletin of the Seismological Society of America, Volume 94, no. 1, p. 64-75, 2004.

209. Bechtel, *Update of Charleston Seismic Source and Integration with EPRI Source Models:* Bechtel Engineering Study, Report 25144-006-V14-CY06-00006, Revision 002, 2006.

210. Behrendt, J. C. and Yuan, A., *The Helena Banks Strike-slip (?) Fault Zone in the Charleston, South Carolina, Earthquake Area: Results From a Marine, High-resolution, Multichannel, Seismic-reflection Survey:* Geological Society of America Bulletin, Volume 98, p. 591-601, 1987.

211. Behrendt, J. C., Hamilton, R. M., Ackermann, H. D., and Henry, V. J., *Cenozoic Faulting in the Vicinity of the Charleston, South Carolina, 1886 Earthquake:* Geology, Volume 9, no. 3, p. 117-122, 1981.

212. Behrendt, J. C., Hamilton, R. M., Ackermann, H. D., Henry, V. J., and Bayer, K. C., *Marine Multichannel Seismic-reflection Evidence for Cenozoic Faulting and Deep Crustal Structure Near Charleston, South Carolina,* U.S. Geological Survey Professional Paper 1313-J, p. J1-J29, 1983.

213. Bollinger, G. A., *Reinterpretation of the Intensity Data for the 1886 Charleston, South Carolina, Earthquake: in Studies Related to the Charleston, South Carolina, Earthquake of 1886 - A Preliminary Report* (D. W. Rankin, ed.), U.S. Geological Survey Professional Paper 1028, p. 17-32, 1977.

214. Bollinger, G. A. *Specification of Source Zones, Recurrence Rates, Focal Depths, and Maximum Magnitudes for Earthquakes Affecting the Savannah River Site in South Carolina,* U.S. Geological Survey Bulletin 2017, 1992.

215. Bollinger, G. A., Chapman, M. C., Sibol, M. S., and Costain, J. K., *An Analysis of Earthquake Focal Depths in the Southeastern U.S.,* Geophysical Research Letters, Volume 12, no. 11, p. 785-788, 1985.

216. Bollinger, G. A., Johnston, A. C., Talwani, P., Long, L. T., Shedlock, K. M., Sibol, M. S., and Chapman, M. C., *Seismicity of the Southeastern United States; 1698-1986: in Neotectonics of North America, Decade Map Volume to Accompany the Neotectonic Maps* (D. B. Slemmons, E. R. Engdahl, M. D. Zoback, D. B. Blackwell, eds.), p. 291-308, 1991.

217. Bronk Ramsey, C., *Radiocarbon Calibration and Analysis of Stratigraphy: the OxCal Program:* Radiocarbon, Volume 37, no. 2, p. 425-430, 1995.

218. Bronk Ramsey, C., *Development of the Radiocarbon Program OxCal:* Radiocarbon, Volume 43, no. 2A, p. 355-363, 2001.

219. Chapman, M. C. and Talwani, P., *Seismic Hazard Mapping for Bridge and Highway Design in South Carolina,* South Carolina Department of Transportation Report, 2002.

220. Chapman, M. C., Munsey, J. W., Powell, C. A., Whisner, S. C., and Whisner J., *The Eastern Tennessee Seismic Zone - Summary after 20 Years of Network Monitoring,* Seismological Research Letters, Volume 73, no. 2, p. 245, 2002.

221. Chen, L. and Talwani, P., *Renewed Seismicity near Monticello Reservoir, South Carolina, 1996-1999,* Bulletin of the Seismological Society of America, Volume 91, no. 1, p. 94-101, February 2001.

222.   Chen, L. and Talwani, P., *Mechanism of Initial Seismicity Following Impoundment of the Monticello Reservoir, South Carolina,* Bulletin of the Seismological Society of America, Volume 91, no. 6, p. 1582-1594, December 2001.

223.   Cook, F. A., Albaugh, D. S., Brown, L. D., Kaufman, S., Oliver, J. E., and Hatcher, R. D. Jr., *Thin-skinned Tectonics in the Crystalline Southern Appalachians: COCORP Seismic Reflection Profiling of the Blue Ridge and Piedmont:* Geology, Volume 7, p. 563-567, 1979.

224.   Cook, F. A., Brown, L. D., Kaufman, S., Oliver, J. E., and Petersen, T. A., *COCORP Seismic Profiling of the Appalachian Orogen Beneath the Coastal Plain of Georgia,* Geological Society of America Bulletin, Volume 92, no. 10, p. 738-748, 1981.

225.   Cornell, C. A., *Engineering Seismic Risk Analysis*: Bulletin of the Seismological Society of America, Volume 58, no. 5, p. 1583-1606, 1968.

226.   Cornell, C. A. and Winterstein, S. R., *Temporal and Magnitude Dependence in Earthquake Recurrence Models,* Bulletin of the Seismological Society of America, Volume 79, p. 1522-1537, 1988.

227.   Cramer, C. H., *A Seismic Hazard Uncertainty Analysis for the New Madrid Seismic Zone:* Engineering Geology, Volume 62, p. 251-266, 2001.

228.   Ellsworth, W. L., Matthews, M. V., Nadeau, R. M., Nishenko, S. P., Reasenberg, P. A., and Simpson, R. W., *A Physically-Based Earthquake Recurrence Model for Estimation of Long-Term Earthquake Probabilities,* U.S. Geological Survey Open-File Report 99-522, 22p., 1999.

229.   EPRI, *CEUS Ground Motion Project Final Report*, Technical Report 1009684, December 2004.

230.   EPRI, *Guidelines for Determining Design Basis Ground Motions, Volume 5 Quantification of Seismic Source Effects*, EPRI Report TR-102293, Project 3302, Final Report, Palo Alto, California, November 1993.

231.   EPRI, *EQHAZARD Primer:* Prepared by Risk Engineering for Seismicity Owners Group and EPRI, EPRI Report NP-6452-D, Palo Alto, California, June 1989.

232.   EPRI, *Probabilistic Seismic Hazard Evaluation at Nuclear Plant Sites in the Central and Eastern United States, Resolution of the Charleston Earthquake Issue,* EPRI Report 6395-D, Palo Alto, California, April 1989.

233.   EPRI, *Probabilistic Seismic Hazard Evaluation for Virgil C. Summer Nuclear Station*, Project Report RP 101-53, Palo Alto, California, April 1989.

234. EPRI, *Seismic Hazard Methodology for the Central and Eastern United States, Tectonic Interpretations*, Volumes 5–10 EPRI Report NP-4726, Palo Alto, California, July 1986.

235. EPRI, S*eismic Hazard Methodology for the Central and Eastern United States*, Volume 1, Part 2: Methodology (Revision 1). EPRI Report NP-4726-A, Rev. 1, Palo Alto, California, November 1988.

236. EPRI, S*eismic Hazard Methodology for Central and Eastern United States*, Volume 3: User's Manual (Revision 1). EPRI Report NP-4726-CCML-A, Palo Alto, California, February 1989.

237. EPRI, *The Earthquakes of Stable Continental Regions*, TR-102261, Electric Power Research Institute, Palo Alto, California, 1994.

238. Exelon, Exelon Generation Company, LLC, *Site Safety Analysis Report for the Clinton ESP Site*, Rev. 4, April 2006.

239. Fletcher, J. B., Sbar, M. L., and Sykes, L. R., *Seismic Trends and Travel-time Residuals in Eastern North America and Their Tectonic Implications.* Gaol. So. Am. Bull., v. 89, p. 1656-1676, 1978.

240. Frankel, A., Barnhard, T., Perkins, D., Leyendecker, E. V., Dickman, N., Hanson, S., and Hopper, M., *National Seismic-Hazard Maps,* Documentation: U.S. Geological Survey Open-File Report 96-532, 1996.

241. Frankel, A. D., Petersen, M. D., Mueller, C. S., Haller, K. M., Wheeler, R. L., Leyendecker, E. V., Wesson, R. L., Harmsen, S. C., Cramer, C. H., Perkins, D. M., and Rukstales, K. S., *Documentation for the 2002 Update of the National Seismic Hazard Maps,* U.S. Geological Survey Open-File Report 02-420, 2002.

242. Grant, L. B. and Sieh, K., *Paleoseismic Evidence of Clustered Earthquakes on the San Andreas Fault in the Carrizo Plain, California,* Journal of Geophysical Research, Volume 99, no. B4, p. 6819-6841, 1994.

243. Hamilton, R. M., Behrendt, J. C., and Ackermann, H. D., Land *Multichannel Seismic-Reflection Evidence for Tectonic Features near Charleston, South Carolina,* Studies Related to the Charleston, South Carolina, Earthquake of 1886-Tectonics and Seismicity: U.S. Geologic Survey Professional Paper 1313-I, p. I1-I18, 1983.

244. Hardy, G., Merz, K., Abrahamson, N. A., and Watson-Lamprey, J., *Program on Technology Innovation: Use of Cumulative Absolute Velocity (CAV) in Determining Effects of Small Magnitude Earthquakes on Seismic Hazard Analyses*, EPRI, Technical Report 1014099, August 2006.

245. Hough, S. E., Armbruster, J. G., Seeber, L., and Hough, J. S., *On the Modified Mercalli Intensities and Magnitudes of the 1811-1812 New*

Madrid Earthquakes, Journal of Geophysical Research, Volume 105, no. B10, p. 23839-23864, 2000.

246.   Johnston, A. C., *Seismic Moment Assessment of Earthquake in Stable Continental Regions — III. New Madrid 1811-1812, Charleston 1886 and Lisbon 1755,* Geophysical Journal International, Volume 126, p.314-344, 1996.

247.   Lennon, G., *Identification of a Northwest Trending Seismogenic Graben Near Charleston, South Carolina,* U.S. Nuclear Regulatory Commission Report, NUREG/CR-4075, 43p., 1986.

248.   Madabhushi, S. and Talwani, P., *Fault Plane Solutions and Relocations of Recent Earthquakes in Middleton Place-Summerville Seismic Zone near Charleston, South Carolina*: Bulletin of the Seismological Society of America, Volume 83, no. 5, p. 1442-1466, 1993.

249.   Marple, R. T. and Talwani, P., *Evidence for Possible Tectonic Upwarping along the South Carolina Coastal Plain from an Examination of River Morphology and Elevation Data:* Geology, Volume 21, p. 651-654, 1993.

250.   Marple, R. T. and Talwani, P., *Evidence for a Buried Fault System in the Coastal Plain of the Carolinas and Virginia - Implications for Neotectonics in the Southeastern United Sates,* Geological Society of America Bulletin, Volume 112, no. 2, p. 200-220, 2000.

251.   Marple, R. T. and Talwani, P., *Proposed Shenandoah Fault and East Coast-Stafford Fault System and Their Implications for Eastern U.S. Tectonics:* Southeastern Geology, Volume 43, no. 2, p. 57-80, 2004.

252.   Martin, J. R. and Clough, G. W., *Seismic Parameters from Liquefaction Evidence,* Journal of Geotechnical Engineering, Volume 120, no. 8, p. 1345-1361, 1994.

253.   Matthews, M. V., Ellsworth, W. L., and Reasenberg, P. A., *A Brownian Model for Recurrent Earthquakes,* Bulletin of the Seismological Society of America, Volume 92, p. 2233-2250, 2002.

254.   McGuire, R. K., Silva, W. J., and Constantino, C. J., *Technical Basis for Revision of Regulatory Guidance on Design Ground Motions: Development of Hazard- and Risk-Consistent Seismic Spectra for Two Sites*. NUREG/CR-6769. U.S. Nuclear Regulatory Commission, 2002.

255.   McGuire, R. K., Silva, W. J., and Constantino, C. J., *Technical Basis for Revision of Regulatory Guidance on Design Ground Motions: Hazard- and Risk-Consistent Ground Motion Spectra Guidelines*. NUREG/CR-6728. U.S. Nuclear Regulatory Commission, 2001.

256.   NIST/SEMATECH, e-Handbook of Statistical Methods. Available at http://www.itl.nist.gov/div898/handbook/. Accessed January 11, 2006.

257.   Obermeier, S., *Liquefaction-Induced Features:* in Paleoseismology, J. McCalpin (ed.), Academic Press, San Diego, p. 331-396, 1996.

258.   Obermeier, S. F., Weems, R. E., Jacobson, R. B., and Gohn, G. S., *Liquefaction Evidence for Repeated Holocene Earthquakes in the Coastal Region of South Carolina:* Annals of the New York Academy of Sciences, Volume 558, p. 183-195, 1989.

259.   Rajendran, K. and Talwani, P., *The Role of Elastic, Undrained, and Drained Responses in Triggering Earthquakes at Monticello Reservoir, South Carolina,* Bulletin of the Seismological Society of America, Volume 82, no. 4, p. 1867-1888, 1992.

260.   Risk Engineering, Inc., *Technical Basis for Revision of Regulatory Guidance on Design Ground Motions: Hazard- and Risk-Consistent Ground Motion Spectra Guidelines*, U.S. Nuclear Regulatory Commission Report NUREG/CR-6728, October 2001.

261.   Rockwell, T. K., Lindvall, S., Herzberg, M., Murbach, D., Dawson, T., and Berger, G., *Paleoseismology of the Johnson Valley, Kickapoo, and Homestead Valley Faults: Clustering of Earthquakes in the Eastern California Shear Zone*: Bulletin of the Seismological Society of America, Volume 90, no. 5, p. 1200-1236, 2000.

262.   Savage, J. C., *Criticism of Some Forecasts of the National Earthquake Evaluation Council,* Bulletin of the Seismological Society of America, Volume 81, no. 3, p. 862-881, 1991.

263.   Savy, J. B., Foxall, W., Abrahamson, N., and Bernreuter, D., *Guidance for Performing Probabilistic Seismic Hazard Analysis for a Nuclear Plant Site: Example Application to the Southeastern United States,* U.S. Nuclear Regulatory Commission, NUREG/CR-6607, 2002.

264.   SCE&G, *Seismic Confirmatory Program – Equipment Margin Study*, Virgil C. Summer Nuclear Station, November 1983.

265.   SCE&G, *Seismic Confirmatory Program*, Virgil C. Summer Nuclear Station, February 1983.

266.   Secor, D. T., Jr., Peck, L. S., Pitcher, D. M., Prowell, D. C., Simpson, D. H., Smith, W. A., and Snoke, A. W., *Geology of the Area of Induced Seismic Activity at Monticello Reservoir, South Carolina*, Journal of Geophysical Research, 87, 6945-6957, 1982.

267. Seeber, L. and Armbruster, J. G., *The 1886 Charleston, South Carolina Earthquake and the Appalachian Detachment*, Journal of Geophysical Research, Volume 86, no. B9, p. 7874-7894, 1981.

268. Southeastern United States Seismic Network, *SEUSSN Bulletin, Number 39: January 1, 2004 – December 31, 2004*, Virginia Polytechnic Institute and State University, Seismological Observatory, June 2006.

269. Smith, W. A. and Talwani, P., *Preliminary Interpretation of a Detailed Gravity Survey in the Bowman and Charleston, S.C. Seismogenic Zones: Abstracts with Programs,* Geological Society of America Southeastern Section, Volume 17, no. 2, p. 137, 1985.

270. Senior Seismic Hazards Analysis Committee, *Recommendations for Probabilistic Seismic Hazard Analysis: Guidance on Uncertainty and Use of Experts*, Prepared by Senior Seismic Hazard Analysis Committee (SSHAC), NUREG/CR-6372, 1997.

271. Sykes, L. R., *Intraplate Seismicity, Reactivation of Preexisting Zones of Weakness, Alkaline Magmatism, and Other Tectonism Post-Dating Continental Fragmentation:* Review of Geophysics and Space Physics, Volume 15, p. 621-688, 1978.

272. Talwani, P., *An Internally Consistent Pattern of Seismicity Near Charleston, South Carolina,* Geology, Volume 10, 655–658, 1982.

273. Talwani, P., *On the Nature of Reservoir-Induced Seismicity:* Pure and Applied Geophysics, Volume 150, p. 473-492, 1997.

274. Talwani, P., *Fault Geometry and Earthquakes in Continental Interiors:* Tectonophysics, Volume 305, p. 371-379, 1999.

275. Talwani, P., *Macroscopic Effects of the 1886 Charleston Earthquake, A Compendium of Field Trips of South Carolina Geology,* South Carolina Geological Survey, p. 1-6, 2000.

276. Talwani, P., Personal Communication, 2007.

277. Talwani, P. and Acree, S., *Pore Pressure Diffusion and the Mechanism of Reservoir-Induced Seismicity:* Pure and Applied Geophysics, Volume 122, 1984–1985.

278. Talwani, P., Cobb, J. S., and Schaeffer, M. F., *In Situ Measurements of Hydraulic Properties of a Shear Zone in Northwestern South Carolina,* Journal of Geophysical Research, Volume 104, no. B7. p. 14,993-15,003, 1999.

279. Talwani, P. and Katuna M., *Macroseismic Effects of the 1886 Charleston Earthquake,* Carolina Geological Society Field Trip Guidebook, p. 18, 2004.

280. Talwani, P. and Schaeffer, W. T., *Recurrence Rates of Large Earthquakes in the South Carolina Coastal Plain Based on Paleoliquefaction Data,* Journal of Geophysical Research, Volume 106, no. B4, p. 6621-6642, 2001.

281. Tarr, A. C. and Rhea, S., *Seismicity Near Charleston, South Carolina, March 1973 to December 1979* in Studies Related to the Charleston, South Carolina Earthquake of 1886: Tectonics and Seismicity, G. S. Gohn (ed.), U.S. Geological Survey Professional Paper 1313, R1-R17, 1983.

282. Tarr, A. C., Talwani, P., Rhea, S., Carver, D., and Amick, D., *Results of Recent South Carolina Seismological Studies,* Bulletin of the Seismological Society of America, Volume 71, no. 6, p. 1883-1902, 1981.

283. Tuttle, M. P., *The Use of Liquefaction Features in Paleoseismology: Lessons Learned in the New Madrid Seismic Zone*, Central United States: Journal of Seismology, Volume 5, p. 361-380, 2001.

284. U.S. Nuclear Regulatory Commission, *Safety Evaluation Report Related to the Operation of the Virgil C. Summer Nuclear Station Unit No. 1,* Docket No. 50-395, NUREG-0717, February 1981.

285. U.S. NRC, *South Carolina Electric & Gas Company Virgil C. Summer Nuclear Station Unit 1, Applicants' Proposed Findings of Fact and Conclusions of Law - Before the Atomic Safety and Licensing Board,* Docket No. 50-395 OL, 171p., February 16, 1982.

286. U.S. NRC, *Safety Evaluation Report Related to the Operation of the Virgil C. Summer Nuclear Station Unit No. 1,* Docket No. 50-395, NUREG-0717, Supplement No. 4, August 1982.

287. U.S. NRC, *Safety Evaluation by the Office of Nuclear Reactor Regulation, related to Amendment No. 124 to Facility Operating License No. NPF-12, SCE&G, South Carolina Public Services Authority, Virgil C. Summer Nuclear Station, Unit No. 1*, Docket No. 50-395, 1995.

288. Weems, R. E. and Lewis, W. C., *Structural and Tectonic Setting of the Charleston, South Carolina, Region; Evidence from the Tertiary Stratigraphic Record*: Geological Society of America Bulletin, Volume 114, no. 1, p. 24-42, 2002.

289. Weems, R. E., Lemon, E. M. Jr., and Nelson, M. S., *Geology of the Pringletown, Ridgeville, Summerville, and Summerville Northwest 7.5-Minute Quadrangles, Berkeley, Charleston, and Dorchester Counties,*

South Carolina, Miscellaneous Investigations Series - U.S. Geological Survey, 1997.

290. Wells, D. L. and Coppersmith, K. J., *New Empirical Relationships Among Magnitude, Rupture Length, Rupture Width, Rupture Area, and Surface Displacement,* Bulletin Seismological Society of America, Volume 84, no. 4, p. 974-1002, 1994.

291. Wentworth, C. M. and Mergner-Keefer, M., *Regenerate Faults of the Southeastern United States, in Studies Related to the Charleston, South Carolina, Earthquake of 1886: Tectonics and Seismicity*, Gohn, G. S. (ed., U.S. Geological Survey Professional Paper 1313, p. S1-S20, 1983.

292. Wheeler, R. L., *Known or Suggested Quaternary Tectonic Faulting, Central and Eastern United States- New and Updated Assessments for 2005,* U.S. Geological Survey Open-File Report 2005-1336, 2005.

293. Working Group on California Earthquake Probabilities, *Seismic Hazards in Southern California: Probable Earthquakes, 1994 to 2024:* Bulletin of the Seismological Society of America, Volume 85, p. 379-439, 1995.

294. Working Group on California Earthquake Probabilities, *Earthquake Probabilities in the San Francisco Bay Region: 2002-2031,* U.S. Geological Survey Open-File Report 03-2134, 2003.

295. Whorton, R. B., *High Frequency, High Amplitude, and Low Energy Earthquake Study at V. C. Summer Nuclear Station:* Nuclear Engineering and Design, Volume 107, p. 109-125, 1988.

296. Zoback, M. D. and Hickman, S., *In Situ Study of the Physical Mechanisms Controlling Induced Seismicity at Monticello Reservoir, South Carolina,* Journal of Geophysical Research, Volume 87, no. B8, p. 6959-6974, 1982.

Table 2.5.2-201
Conversion Between Body-Wave (m_b) and Moment (M) Magnitudes[a]

Convert m_b	To M	Convert M	To m_b
4.00	3.77	4.00	4.28
4.10	3.84	4.10	4.41
4.20	3.92	4.20	4.54
4.30	4.00	4.30	4.66
4.40	4.08	4.40	4.78
4.50	4.16	4.50	4.90
4.60	4.24	4.60	5.01
4.70	4.33	4.70	5.12
4.80	4.42	4.80	5.23
4.90	4.50	4.90	5.33
5.00	4.59	5.00	5.43
5.10	4.69	5.10	5.52
5.20	4.78	5.20	5.61
5.30	4.88	5.30	5.70
5.40	4.97	5.40	5.78
5.50	5.08	5.50	5.87
5.60	5.19	5.60	5.95
5.70	5.31	5.70	6.03
5.80	5.42	5.80	6.11
5.90	5.54	5.90	6.18
6.00	5.66	6.00	6.26
6.10	5.79	6.10	6.33
6.20	5.92	6.20	6.40
6.30	6.06	6.30	6.47
6.40	6.20	6.40	6.53
6.50	6.34	6.50	6.60
6.60	6.49	6.60	6.66
6.70	6.65	6.70	6.73
6.80	6.82	6.80	6.79
6.90	6.98	6.90	6.85
7.00	7.16	7.00	6.91
7.10	7.33	7.10	6.97
7.20	7.51	7.20	7.03
7.30	7.69	7.30	7.09
7.40	7.87	7.40	7.15
7.50	8.04	7.50	7.20
		7.60	7.26
		7.70	7.32
		7.80	7.37
		7.90	7.43
		8.00	7.49

a) Average of relations given by Atkinson and Boore (Reference 207), Frankel et al. (Reference 240), and EPRI TR-102293 (Reference 230)

Table 2.5.2-202 (Sheet 1 of 5)
Earthquakes 1985–August 2006, Update to the EPRI Seismicity Catalog with Rmb≥3.0[a] or MMI≥4

Year	Month	Day	Hour	Minute	Second	Lat.	Long.	Depth	MMI	Emb	Smb	Rmb
1985	3	12	8	57	43.30	35.294	−84.482	11.3	4	1.61	0.27	1.70
1985	5	1	1	16	27.80	37.780	−87.610	10		3.01	0.41	3.20
1985	6	10	12	22	38.30	37.248	−80.485	11.1		3.30	0.10	3.31
1985	7	12	18	20	28.30	35.202	−85.148	19.6		2.97	0.30	3.08
1985	12	22	0	56	5.00	35.701	−83.720	13.4		3.25	0.30	3.35
1986	1	7	1	26	43.30	35.610	−84.761	23.1		3.06	0.30	3.17
1986	2	3	0	53	6.80	35.928	−83.634	19.1	4	1.43	0.27	1.52
1986	2	13	11	35	45.55	34.755	−82.943	5		3.50	0.10	3.51
1986	3	13	2	29	31.40	33.229	−83.226	5		3.30	0.25	3.37
1986	3	26	16	36	23.90	37.245	−80.494	11.9		3.30	0.25	3.37
1986	4	19	7	40	53.00	35.187	−85.510	27.3		2.97	0.30	3.08
1986	5	7	2	27	0.46	33.233	−87.361	1		4.50	0.10	4.51
1986	5	13	14	30	36.00	35.539	−84.176	14.3	5	1.70	0.27	1.79
1986	5	18	2	18	5.20	35.508	−83.642	15.7	6	1.07	0.27	1.15
1986	6	21	0	40	2.30	35.374	−85.144	16.6	4	1.79	0.27	1.88
1986	7	11	14	26	14.80	34.937	−84.987	13		3.80	0.10	3.81
1986	7	25	12	43	55.10	35.635	−84.253	14.2	4	1.61	0.27	1.70
1986	9	17	9	33	49.50	32.931	−80.159	6.7		3.30	0.25	3.37
1986	10	26	8	19	33.30	35.903	−83.917	18.9	4	1.34	0.27	1.43
1986	11	15	12	7	56.20	35.885	−83.826	13.9	4	2.16	0.27	2.24
1986	12	3	9	44	21.20	37.580	−77.458	1.6		3.30	0.25	3.37
1986	12	10	11	30	6.10	37.585	−77.468	1.2		3.50	0.10	3.51
1986	12	24	17	58	38.30	37.583	−77.458	1		3.30	0.25	3.37
1987	1	13	14	50	40.90	37.584	−77.465	2.5		3.30	0.25	3.37
1987	3	16	13	9	26.80	34.560	−80.948	3		3.06	0.30	3.17
1987	3	27	7	29	30.50	35.565	−84.230	18.5		4.20	0.10	4.21
1987	5	5	2	3	30.60	36.398	−84.079	19	4	1.34	0.27	1.43
1987	5	10	19	47	41.90	37.793	−83.393	0.7		2.97	0.30	3.08
1987	5	12	12	17	59.60	35.988	−83.998	13.3	5	1.16	0.27	1.24
1987	6	4	17	19	23.40	37.939	−85.800	7.6		3.06	0.30	3.17
1987	7	4	10	47	25.00	35.540	−84.445	16.1	4	1.07	0.27	1.15
1987	7	11	0	4	29.50	36.105	−83.816	25.1		3.79	0.10	3.80
1987	7	11	2	48	5.90	36.103	−83.819	23.8		3.43	0.10	3.44
1987	9	1	23	2	49.40	35.515	−84.396	21.1		3.06	0.30	3.17
1987	9	22	17	23	50.10	35.623	−84.312	19.4	3	3.50	0.10	3.51
1987	10	14	15	49	40.10	37.050	−88.780	2		3.74	0.41	3.93
1987	10	20	22	49	55.90	35.841	−84.444	12.8	5	2.34	0.27	2.42
1987	11	27	18	58	29.30	36.852	−83.110	26.8		3.50	0.10	3.51
1987	11	29	2	10	51.40	36.862	−83.107	8.6	5	2.07	0.27	2.15
1987	11	30	7	2	44.10	36.095	−83.805	20.8	6	0.98	0.27	1.06
1987	12	12	3	53	28.79	34.244	-82.628	5		3.00	0.10	3.01
1988	1	9	1	7	40.60	35.279	−84.199	12.2		3.30	0.25	3.37
1988	1	23	1	57	16.40	32.935	−80.157	7.4		3.50	0.25	3.57
1988	2	16	15	26	54.80	36.595	−82.274	4		3.30	0.10	3.31
1988	2	18	0	37	45.40	35.346	−83.837	2.4		3.50	0.10	3.51
1988	2	27	17	36	32.60	35.266	−84.622	19.3	4	0.62	0.27	0.70

Table 2.5.2-202 (Sheet 2 of 5)
Earthquakes 1985–August 2006, Update to the EPRI Seismicity Catalog with
Rmb$\geq$3.0[(a)] or MMI$\geq$4

Year	Month	Day	Hour	Minute	Second	Lat.	Long.	Depth	MMI	Emb	Smb	Rmb
1988	3	10	21	24	9.50	37.750	−88.830	4.4		3.09	0.41	3.28
1988	6	15	14	46	16.60	34.630	−82.529	1.4	4	1.52	0.27	1.61
1988	7	3	11	28	8.30	35.686	−84.302	17.7	4	0.98	0.27	1.06
1988	8	27	16	52	29.50	37.718	−77.775	14.3	5	3.30	0.25	3.37
1988	9	18	16	16	1.00	37.310	−87.210	12.6		2.85	0.41	3.04
1988	11	1	13	7	40.70	35.743	−84.087	11.2	4	1.70	0.27	1.79
1989	1	21	23	50	8.90	33.391	−80.688	4.3	4	1.70	0.27	1.79
1989	2	28	17	31	50.84	33.643	−87.092	0		3.50	0.10	3.51
1989	6	2	5	4	34.00	32.934	−80.166	5.8		3.30	0.25	3.37
1989	6	28	9	35	0.20	37.810	−88.950	12.7		3.01	0.41	3.20
1989	7	15	18	58	28.00	34.373	−87.323	13.9		3.16	0.10	3.17
1989	8	13	20	16	2.90	33.632	−87.086	0		3.40	0.10	3.41
1989	8	20	0	3	18.30	34.803	−87.596	6.7	6	4.00	0.10	4.01
1990	5	30	9	12	54.50	35.246	−84.359	6.1	5	0.34	0.27	0.43
1990	6	23	20	44	2.10	33.720	−87.946	6.4		3.06	0.30	3.17
1990	6	30	16	38	32.80	33.734	−88.063	2	5	2.25	0.27	2.33
1990	8	17	21	1	15.90	36.934	−83.384	0.6		4.00	0.10	4.01
1990	9	2	4	35	40.20	33.758	−87.928	0.9		3.16	0.30	3.26
1990	11	8	10	8	25.40	37.108	−83.031	0.4		3.16	0.30	3.26
1990	11	13	15	22	13.00	32.947	−80.136	3.4		3.50	0.10	3.51
1991	1	11	21	1	59.00	37.510	−78.190	9.6	5	2.07	0.27	2.15
1991	1	23	9	25	23.20	37.940	−88.873	0.8		3.17	0.41	3.37
1991	1	28	11	43	55.70	37.349	−87.324	1.2		2.93	0.41	3.12
1991	3	15	6	54	8.30	37.746	−77.909	15.5		3.80	0.10	3.81
1991	4	22	1	1	20.20	37.942	−80.205	14.8		3.50	0.10	3.51
1991	5	10	19	40	36.60	34.865	−85.201	11.2	5	2.25	0.27	2.33
1991	6	2	6	5	34.90	32.980	−80.214	5		3.50	0.25	3.57
1991	9	24	7	21	7.00	35.701	−84.117	13.3		3.30	0.10	3.31
1991	10	9	1	29	23.30	34.895	−85.327	6.5	4	0.62	0.27	0.70
1991	10	28	10	46	20.90	35.615	−84.712	11.5	4	1.70	0.27	1.79
1991	10	30	14	54	12.60	34.904	−84.713	8.1		3.06	0.30	3.17
1992	1	3	4	21	23.90	33.981	−82.421	3.3		3.50	0.25	3.57
1992	2	1	5	6	30.30	33.991	−82.425	4.8	5	2.16	0.27	2.24
1992	8	21	16	31	56.10	32.985	−80.163	6.5	1	4.10	0.10	4.11
1992	9	6	11	15	51.80	32.945	−80.130	5.8	6	0.98	0.27	1.06
1992	9	11	16	34	11.70	33.171	−87.501	6.5		2.97	0.30	3.08
1992	11	10	17	16	46.80	35.644	−84.132	10.2	1	2.97	0.27	3.06
1993	1	1	5	8	5.20	35.878	−82.086	2.3		2.97	0.30	3.08
1993	1	15	2	2	50.90	35.039	−85.025	8.1		3.30	0.10	3.31
1993	4	15	6	34	56.40	35.867	−83.620	16.5	5	1.43	0.27	1.52
1993	5	19	10	31	18.20	35.505	−84.890	22.7	4	2.34	0.27	2.42
1993	7	1	21	24	34.00	35.972	−82.519	2.4	4	2.34	0.27	2.42
1993	7	12	4	48	20.80	36.035	−79.823	5		3.30	0.10	3.31
1993	7	16	10	54	32.86	31.747	−88.341	5		3.70	0.10	3.71
1993	8	8	9	24	32.40	33.597	−81.591	8.5		3.50	0.10	3.51
1994	1	31	14	33	8.90	35.756	−84.599	10.2	4	2.34	0.27	2.42
1994	2	12	2	40	24.50	36.800	−82.000	5		3.42	0.41	3.61
1994	2	27	22	36	42.90	37.279	−80.760	2.1	5	1.25	0.27	1.33

Table 2.5.2-202 (Sheet 3 of 5)
Earthquakes 1985–August 2006, Update to the EPRI Seismicity Catalog with
Rmb≥3.0[a] or MMI≥4

Year	Month	Day	Hour	Minute	Second	Lat.	Long.	Depth	MMI	Emb	Smb	Rmb
1994	4	5	22	22	0.40	34.969	−85.491	24.3		3.50	0.10	3.51
1994	4	16	20	10	12.20	35.752	−83.968	1.8		3.50	0.25	3.57
1994	4	30	1	56	16.80	32.835	−80.187	3.4	5	0.80	0.27	0.88
1994	5	4	9	12	3.40	34.222	−87.195	19.3		3.25	0.10	3.26
1994	9	26	14	23	22.84	36.960	−88.920	12.7		3.42	0.41	3.61
1995	3	2	0	2	18.10	32.962	−80.165	4.6	4	0.89	0.27	0.97
1995	3	11	8	15	52.32	36.959	−83.133	1		3.80	0.10	3.81
1995	3	11	9	50	4.44	36.990	−83.180	1		3.30	0.10	3.31
1995	3	18	22	6	20.80	35.422	−84.941	26	4	3.25	0.27	3.33
1995	4	17	13	46	0.00	32.997	−80.171	8.4		3.90	0.10	3.91
1995	5	28	15	28	37.00	33.191	−87.827	1	F	3.40	0.10	3.41
1995	6	26	0	36	17.10	36.752	−81.481	1.8	3	3.40	0.10	3.41
1995	7	5	14	16	44.70	35.334	−84.163	10	6	3.70	0.10	3.71
1995	7	7	21	1	3.00	36.493	−81.833	10		3.06	0.10	3.08
1995	7	15	1	3	28.40	33.478	−87.665	1		3.30	0.10	3.31
1995	8	18	20	11	23.20	32.932	−80.143	3.6	4	0.43	0.27	0.52
1995	8	19	3	59	8.80	32.979	−80.188	7.3	4	0.25	0.27	0.34
1995	9	16	12	53	50.70	32.979	−80.157	3.9	5	2.34	0.27	2.42
1996	3	25	14	15	50.55	32.131	−88.671	5		3.50	0.41	3.69
1996	4	19	8	50	14.01	36.981	−83.018	0		3.90	0.10	3.91
1997	3	29	10	16	57.10	37.088	−81.906	4.4	4	2.34	0.27	2.42
1997	5	4	3	39	12.80	30.934	−87.494	0		3.10	0.10	3.11
1997	5	19	19	45	35.80	34.622	−85.353	2.7		3.06	0.10	3.08
1997	7	19	17	6	34.40	34.953	−84.811	2.8		3.61	0.10	3.62
1997	7	30	12	29	25.30	36.512	−83.547	23		3.80	0.10	3.81
1997	9	14	7	24	54.50	34.533	−85.693	8.2	4	0.98	0.27	1.06
1997	9	14	7	53	37.90	34.505	−85.628	10.7	4	0.80	0.27	0.88
1997	10	19	18	39	55.10	35.286	−84.753	15.1	6	2.43	0.27	2.51
1997	10	24	8	35	17.90	31.118	−87.339	10		4.90	0.10	4.91
1997	10	26	23	27	12.00	31.118	−87.339	10		3.70	0.10	3.71
1997	10	28	9	0	11.00	31.100	−87.300	10	6	3.00	0.10	3.01
1997	10	28	10	36	46.56	37.162	−82.025	1		3.42	0.41	3.61
1997	12	12	8	42	20.25	33.466	−87.306	1		3.90	0.41	4.10
1997	12	24	1	35	49.40	35.493	−85.125	6.5	4	1.70	0.27	1.79
1997	12	27	3	36	46.20	34.126	−87.263	0	5	1.98	0.27	2.06
1997	12	27	7	44	46.70	37.985	−79.953	0	4	2.25	0.27	2.33
1998	4	13	9	56	15.60	34.471	−80.603	6.6		3.90	0.10	3.91
1998	6	5	2	31	3.90	35.554	−80.785	9.4	5	3.34	0.10	3.35
1998	6	17	8	0	23.90	35.944	−84.392	11.3		3.60	0.10	3.61
1998	6	24	15	20	4.70	32.760	−87.759	2.7		3.40	0.10	3.41
1998	7	24	13	56	26.60	37.245	−87.219	9.7	5	2.34	0.27	2.42
1998	10	21	5	56	46.90	37.422	−78.439	12.6		3.80	0.10	3.81
1999	1	17	18	38	5.10	36.893	−83.799	1		3.06	0.30	3.17
1999	1	18	7	0	53.47	33.405	−87.255	1		4.80	0.10	4.81
1999	3	29	14	49	37.80	33.064	−80.140	10.7		2.97	0.30	3.08
1999	11	28	11	0	9.30	33.416	−87.253	1		3.74	0.41	3.93
2000	1	18	22	19	32.20	32.920	−83.465	19.2		3.50	0.10	3.51
2000	4	10	12	48	15.50	35.458	−84.175	10.3	4	1.89	0.27	1.97

Table 2.5.2-202 (Sheet 4 of 5)
Earthquakes 1985–August 2006, Update to the EPRI Seismicity Catalog with
Rmb≥3.0[a] or MMI≥4

Year	Month	Day	Hour	Minute	Second	Lat.	Long.	Depth	MMI	Emb	Smb	Rmb
2000	4	28	23	36	26.00	37.690	−88.460	5		3.01	0.41	3.20
2000	5	28	11	32	6.30	33.708	−87.811	0		3.00	0.10	3.01
2000	6	27	6	2	57.00	37.130	−88.870	4.1		3.01	0.41	3.20
2000	8	10	23	54	13.00	33.016	−80.179	7.1	5	1.70	0.27	1.79
2000	12	7	14	8	49.40	37.973	−87.660	5		3.90	0.10	3.91
2001	3	7	17	12	23.80	35.552	−84.850	6.8	3	3.20	0.10	3.21
2001	3	21	23	35	34.90	34.847	−85.438	0	3	3.16	0.27	3.24
2001	3	30	22	1	12.30	35.508	−84.481	18.1	5	1.89	0.27	1.97
2001	4	13	16	36	20.70	36.526	−83.342	0		2.97	0.30	3.08
2001	6	11	18	27	54.25	30.226	−79.885	10		3.33	0.41	3.53
2001	7	26	5	26	46.00	35.971	−83.552	14.3		3.25	0.10	3.26
2001	9	22	16	1	20.60	38.026	−78.396	0.4		3.20	0.10	3.21
2001	12	4	21	15	13.90	37.726	−80.752	8.5		3.10	0.10	3.11
2001	12	8	1	8	22.40	34.710	−86.231	0		3.90	0.10	3.91
2002	5	21	20	35	31.90	32.456	−88.221	27.4		2.97	0.30	3.08
2002	6	18	17	37	15.17	37.987	−87.780	5		5.00	0.10	5.01
2002	7	26	21	7	3.00	33.060	−80.195	10		2.97	0.30	3.08
2002	11	8	13	29	3.19	32.422	−79.950	3.9		3.50	0.41	3.69
2002	11	11	23	39	29.72	32.404	−79.936	2.4		4.23	0.41	4.42
2003	1	3	16	17	7.00	37.830	−88.090	5		3.01	0.41	3.20
2003	3	15	9	2	24.40	32.918	−80.160	5.8	5	1.07	0.27	1.15
2003	3	18	6	4	24.21	33.689	−82.888	5		3.50	0.41	3.69
2003	4	29	8	59	38.10	34.445	−85.620	9.1		4.70	0.10	4.71
2003	4	29	9	45	45.00	34.440	−85.640	3.1		3.01	0.41	3.20
2003	5	2	8	10	13.00	37.960	−88.650	0.6		3.25	0.41	3.45
2003	5	2	10	48	44.00	34.490	−85.610	14.5		3.17	0.41	3.37
2003	5	5	10	53	49.90	33.055	−80.190	11.4		3.06	0.30	3.17
2003	5	5	16	32	33.90	37.655	−78.055	2.8		3.90	0.10	3.91
2003	5	8	11	33	6.00	33.989	−81.053	0.9	6	1.61	0.27	1.70
2003	6	6	12	29	34.00	36.870	−88.980	2.6		3.90	0.41	4.10
2003	7	13	20	15	16.96	32.335	−82.144	5		3.58	0.41	3.77
2003	8	26	2	26	58.00	37.100	−88.680	1.9		3.17	0.41	3.37
2003	9	30	2	28	4.50	31.022	−87.462	12.5		2.97	0.30	3.08
2003	12	9	20	59	18.70	37.774	−78.100	10		4.50	0.10	4.51
2003	12	22	23	50	26.00	32.924	−80.157	5.6	6	2.97	0.27	3.06
2004	3	20	10	40	34.80	33.267	−86.955	0		2.97	0.30	3.08
2004	5	7	22	43	24.80	35.240	−84.297	8.4	5	1.61	0.27	1.70
2004	5	9	8	56	10.40	33.231	−86.960	5		3.30	0.10	3.31
2004	7	20	9	13	14.40	32.972	−80.248	10.3		3.06	0.30	3.17
2004	8	19	23	51	49.40	33.203	−86.968	5		3.50	0.10	3.51
2004	9	17	15	21	43.60	36.933	−84.004	1.3		3.70	0.10	3.71
2004	11	7	11	20	25.70	32.976	−87.913	11.4		4.43	0.30	4.53
2004	11	30	23	59	34.20	36.936	−83.893	10		2.97	0.30	3.08
2004	12	23	6	54	20.70	35.429	−84.204	7.7		2.97	0.30	3.08
2005	2	8	11	42	53.00	37.220	−81.930	9.4		2.85	0.41	3.04

Table 2.5.2-202 (Sheet 5 of 5)
Earthquakes 1985–August 2006, Update to the EPRI Seismicity Catalog with
Rmb≥3.0[(a)] or MMI≥4

Year	Month	Day	Hour	Minute	Second	Lat.	Long.	Depth	MMI	Emb	Smb	Rmb
2005	2	15	2	36	55.00	37.190	−81.920	11.2		2.93	0.41	3.12
2005	2	18	14	21	54.00	34.050	−81.110	5		3.17	0.41	3.37
2005	3	18	1	2	16.00	35.720	−84.160	9.1		2.85	0.41	3.04
2005	3	22	8	11	50.51	31.836	−88.060	5		3.33	0.41	3.53
2005	4	5	20	37	43.00	36.150	−83.690	10		3.01	0.41	3.20
2005	4	14	15	38	16.00	35.470	−84.090	15.4		2.93	0.41	3.12
2005	6	7	16	33	36.71	33.531	−87.304	5		2.93	0.41	3.12
2005	6	20	2	0	32.00	36.930	−88.990	9.8		2.85	0.41	3.04
2005	6	20	12	21	42.00	36.920	−89.000	18.7		3.58	0.41	3.77
2005	8	25	3	9	42.00	35.880	−82.800	7.9		3.66	0.41	3.85
2005	10	12	6	27	30.00	35.510	−84.540	8.2		3.58	0.41	3.77
2005	12	7	19	29	45.83	35.862	−82.380	5		2.93	0.41	3.12
2006	1	2	21	48	57.00	37.840	−88.420	10.7		3.58	0.41	3.77
2006	3	1	17	42	42.00	37.500	−88.980	6.2		3.09	0.41	3.28
2006	3	7	10	28	2.00	35.910	−82.340	3.7		2.93	0.41	3.12
2006	3	11	2	37	20.00	35.200	−88.010	1.7		2.85	0.41	3.04
2006	4	11	3	29	21.00	35.360	−84.480	19.6		3.33	0.41	3.53
2006	5	10	12	17	29.00	35.530	−84.400	24.6		3.25	0.41	3.45
2006	6	16	0	57	27.00	35.510	−83.200	1.4		3.42	0.41	3.61
2006	8	7	8	44	28.00	34.940	−85.460	14.2		3.01	0.41	3.20

(a) Within a 30° to 38° N, 77° to 89° W Latitude-Longitude Window, Incorporating the 200-mile (320-kilometer) Radius Site Region

Lat. – Latitude
Long. – Longitude

Table 2.5.2-203 (Sheet 1 of 2)
Summary of EPRI Seismic Sources — Bechtel

Source	Description	Pa	M_{max} (m_b) and Weights[a]	Smoothing Options and Weights[b]	Interdependencies[c]	New Data to Suggest Change in Source?		
						Geom.[d]	M_{max}[e]	RI[f]
Primary sources that contribute to 99% of hazard								
F	Southeast Appalachians	0.35	5.4 [0.10] 5.7 [0.40] 6.0 [0.40] 6.6 [0.10]	1 [0.33] 2 [0.34] 4 [0.33]	ME with G, 13, 15, 16, 17	No	No	No
G	Northwest South Carolina	0.35	5.4 [0.10] 5.7 [0.40] 6.0 [0.40] 6.6 [0.10]	1 [0.33] 2 [0.34] 4 [0.33]	ME with F, 13, 15, 16, 17	No	No	No
H	**Charleston Area**	0.50	6.8 [0.20] 7.1 [0.40] 7.4 [0.20]	1 [0.33] 2 [0.34] 4 [0.33]	P(H|N3)=0.15	**Yes**[g]	**Yes**[g]	**Yes**[g]
N3	**Charleston Faults**	0.53	6.8 [0.20] 7.1 [0.40] 7.4 [0.20]	1 [0.33] 2 [0.34] 4 [0.33]	P(N3|H)=0.16	**Yes**[g]	**Yes**[g]	**Yes**[g]
BZ4	Atlantic Coastal Region	1.00	6.6 [0.10] 6.8 [0.40] 7.1 [0.40] 7.4 [0.10]	1 [0.33] 2 [0.34] 3 [0.33]	Background; P_B=1.00	No	No	No
BZ5	South Appalachians	1.00	5.7 [0.10] 6.0 [0.40] 6.3 [0.40] 6.6 [0.10]	1 [0.33] 2 [0.34] 3 [0.33]	Background; P_B=1.00	No	No	No

Table 2.5.2-203 (Sheet 2 of 2)
Summary of EPRI Seismic Sources — Bechtel

Source	Description	Pa	M_{max} (m_b) and Weights[a]	Smoothing Options and Weights[b]	Interdependencies[c]	New Data to Suggest Change in Source?		
						Geom.[d]	M_{max}[e]	RI[f]
Additional sources that do not contribute to 99% of hazard								
13	Eastern Mesozoic Basins	0.10	5.4 [0.10] 5.7 [0.40] 6.0 [0.40] 6.6 [0.10]	1 [0.33] 2 [0.34] 4 [0.33]	No overlap with H or N3; ME with all sources in BZ5	No	No	No
15	Rosman Fault	0.05	5.4 [0.10] 5.7 [0.40] 6.0 [0.40] 6.6 [0.10]	1 [0.33] 2 [0.34] 4 [0.33]	ME with all other sources	No	No	No
16	Belair Fault	0.05	5.4 [0.10] 5.7 [0.40] 6.0 [0.40] 6.6 [0.10]	1 [0.33] 2 [0.34] 4 [0.33]	ME with all other sources	No	No	No
C07	H–N3	NA	6.8 [0.20] 7.1 [0.40] 7.4 [0.40]	1 [0.33] 2 [0.34] 4 [0.33]	NA	No	No	No

Pa – probability of activity (from EPRI NP-6452-D 1989, Reference 231).
a) Maximum Magnitude (M_{max}) and weights (from EPRI NP-6452-D 1989).
b) Smoothing options are defined as follows (from EPRI NP-6452-D 1989):
    1 = constant a, constant b (no prior b).
    2 = low smoothing on a, high smoothing on b (no prior b).
    3 = low smoothing on a, low smoothing on b (no prior b).
    4 = low smoothing on a, low smoothing on b (weak prior of 1.05).
    Weights on magnitude intervals are [1.0, 1.0, 1.0, 1.0, 1.0, 1.0, 1.0].
c) ME – mutually exclusive; PD – perfectly dependent.
d) No, unless (1) new geometry proposed in literature or (2) new seismicity pattern.
e) No, unless (1) new data suggest M_{max} exceeds or differs significantly from the EPRI M_{max} distribution or (2) exceeded by historical seismicity.
f) RI – recurrence interval; assumed no change if no new paleoseismic data or rate of seismicity has not significantly changed.
g) Replace this source with the Updated Charleston Seismic Source Model - original Charleston sources shown in bold.

**Table 2.5.2-204
Summary of EPRI Seismic Sources — Dames & Moore**

Source	Description	Pa	M_{max} (m_b) and Weights[a]	Smoothing Options and Weights[b]	Interdependencies[c]	New Data to Suggest Change in Source?		
						Geom.[d]	M_{max}[e]	RI[f]
Primary sources that contribute to 99% of hazard								
41	S. Cratonic Margin (default Zone)	0.12	6.1 [0.80] 7.2 [0.20]	1 [0.75] 2 [0.25]	Default for 42, 43, 46	No	No	No
53	So. Appal. Mobile Belt (default zone)	0.26	5.6 [0.80] 7.2 [0.20]	1 [0.75] 2 [0.25]	Default for 47 through 52, 65	No	No	No
54	**Charleston Seismic Zone**	1.00	6.6 [0.75] 7.2 [0.25]	1 [0.22] 2 [0.08] 3 [0.52] 4 [0.18]	None	**Yes[g]**	**Yes[g]**	**Yes[g]**
Additional sources that do not contribute to 99% of hazard								
49	Jonesboro B.	0.28	6.0 [0.75] 7.2 [0.25]	3 [0.75] 4 [0.25]	PD with 47, 48, 50, 51, 65; ME with 52	No	No	No
51	Florence B.	0.28	6.0 [0.75] 7.2 [0.25]	3 [0.75] 4 [0.25]	PD with 47 through 50, 65; ME with 52	No	No	No
52	Charleston Mes. Rift	0.46	4.7 [0.75] 7.2 [0.25]	3 [0.75] 4 [0.25]	ME with 47 through 51, 65	No	No	No
65	Dunbarton Tr. Basin	0.28	5.9 [0.75] 7.2 [0.25]	3 [0.75] 4 [0.25]	PD with 47 tthrough51; ME with 52	No	No	No

Pa – probability of activity (from EPRI NP-6452-D 1989, Reference 231).
(a) Maximum Magnitude (M_{max}) and weights (from EPRI NP-6452-D 1989).
(b) Smoothing options are defined as follows (from EPRI NP-6452-D 1989):
    1 = No smoothing on a, no smoothing on b (strong prior of 1.04).
    2 = No smoothing on a, no smoothing on b (weak prior of 1.04).
    3 = Constant a, constant b (strong prior of 1.04.
    4 = Constant a, constant b (weak prior of 1.04).
    Weights on magnitude intervals are [0.1, 0.2, 0.4, 1.0, 1.0, 1.0, 1.0].
(c) ME – mutually exclusive; PD – perfectly dependent.
(d) No, unless (1) new geometry proposed in literature or (2) new seismicity pattern.
(e) No, unless (1) new data suggest M_{max} exceeds or differs significantly from the EPRI M_{max} distribution or (2) exceeded by historical seismicity.
(f) RI – recurrence interval; assumed no change if no new paleoseismic data or rate of seismicity has not significantly changed.
(g) Replace this source with the Updated Charleston Seismic Source Model - original Charleston sources shown in bold.

Table 2.5.2-205 (Sheet 1 of 2)
Summary of EPRI Seismic Sources — Law Engineering

Source	Description	Pa	M_{max} (m_b) and Weights[a]	Smoothing Options and Weights[b]	Interdependencies[c]	New Data to Suggest Change in Source? Geom.[d]	M_{max}[e]	RI[f]
Primary sources that contribute to 99% of hazard								
17	Eastern Basement	0.62	5.7 [0.20] 6.8 [0.80]	1b [1.00]	none	No	No	No
22	Reactivated E. Seaboard	0.27	6.8 [1.00]	2a [1.00]	ME with 8, 21; overlaps 24, 35, 39	No	No	No
35	**Charleston Seismic Zone**	0.45	6.8 [1.00]	2a [1.00]	Overlaps 8 and 22	**Yes[g]**	**Yes[g]**	**Yes[g]**
107	Eastern Piedmont	1.00	4.9 [0.30] 5.5 [0.40] 5.7 [0.30]	1a [1.00]	Background; P_B=0.42	No	No	No
108	Brunswick, NC Background	1.00	4.9 [0.50] 5.5 [0.30] 6.8 [0.20]	2a [1.00]	Background; P_B=0.42	No	No	No
C09	Mesozoic Basins (8 - Bridged)	NA	6.8 [1.00]	2a [1.00]	NA	No	No	No
C10	8 - 35	NA	6.8 [1.00]	2a [1.00]	NA	No	No	No
C11	22 - 35	NA	6.8 [1.00]	2a [1.00]	NA	No	No	No
M31	Mafic Pluton	0.43	6.8 [1.00]	5 [1.00]	none	No	No	No
M32	Mafic Pluton	0.43	6.8 [1.00]	5 [1.00]	none	No	No	No
M33	Mafic Pluton	0.43	6.8 [1.00]	5 [1.00]	none	No	No	No
M34	Mafic Pluton	0.43	6.8 [1.00]	5 [1.00]	none	No	No	No
M36	Mafic Pluton	0.43	6.8 [1.00]	5 [1.00]	none	No	No	No
M37	Mafic Pluton	0.43	6.8 [1.00]	5 [1.00]	none	No	No	No
M38	Mafic Pluton	0.43	6.8 [1.00]	5 [1.00]	none	No	No	No
M39	Mafic Pluton	0.43	6.8 [1.00]	5 [1.00]	none	No	No	No

Table 2.5.2-205 (Sheet 2 of 2)
Summary of EPRI Seismic Sources — Law Engineering

Source	Description	Pa	M_{max} (m_b) and Weights[a]	Smoothing Options and Weights[b]	Interdependencies[c]	New Data to Suggest Change in Source? Geom.[d]	M_{max}[e]	RI[f]
Additional sources that do not contribute to 99% of hazard								
217	Eastern Basement Background	1.00	4.9 [0.50] 5.7 [0.50]	1b [1.00]	Background; P_B = 0.29	No	No	No
M35	Mafic Pluton	0.43	6.8 [1.00]	5 [1.00]	none	No	No	No
M40	Mafic Pluton	0.43	6.8 [1.00]	5 [1.00]	none	No	No	No
M41	Mafic Pluton	0.43	6.8 [1.00]	5 [1.00]	none	No	No	No
C12	22 – 24	NA	6.8 [1.00]	2a [1.00]	none	No	No	No
C13	22 – 24 - 25	NA	6.8 [1.00]	2a [1.00]	none	No	No	No

Pa – probability of activity (from EPRI NP-6452-D 1989, Reference 231).

(a) Maximum Magnitude (M_{max}) and weights (from EPRI NP-6452-D 1989).

(b) Smoothing options are defined as follows (from EPRI NP-6452-D 1989):

    1a = High smoothing on a, constant b (strong prior of 1.05).
    1b = High smoothing on b, constant b (strong prior of 1.00).
    1c = High smoothing on a, constant b (strong prior of 0.95).
    1d = High smoothing on a, constant b (strong prior of 0.90).
    1e = High smoothing on a, constant b (strong prior of 0.70).
    2a = Constant a, constant b (strong prior of 1.05).
    2c = Constant a, constant b (strong prior of 0.95).
    2d = Constant a, constant b (strong prior of 0.90).
    Weights on magnitude intervals are all 1.0 for above options (1a through 2d).
    3a = High smoothing on a, constant b (strong prior of 1.05).
    Weights on magnitude intervals are [0.0, 1.0, 1.0, 1.0, 1.0, 1.0, 1.0] for option 3a.

(c) ME – mutually exclusive; PD – perfectly dependent.

(d) No, unless (1) new geometry proposed in literature or (2) new seismicity pattern.

(e) No, unless (1) new data suggest M_{max} exceeds or differs significantly from the EPRI M_{max} distribution or (2) exceeded by historical seismicity.

(f) RI – recurrence interval; assumed no change if no new paleoseismic data or rate of seismicity has not significantly changed.

(g) Replace this source with the Updated Charleston Seismic Source Model - original Charleston sources shown in bold. Source (35) was not included in EPRI NP-6452-D 1989 calculations; however this should be considered a significant source to the VCSNS site.

Table 2.5.2-206 (Sheet 1 of 2)
Summary of EPRI Seismic Sources — Rondout Associates

Source	Description	Pa	M$_{max}$ (m$_b$) and Weights[a]	Smoothing Options and Weights[b]	Interdependencies[c]	New Data to Suggest Change in Source?		
						Geom.[d]	M$_{max}$[e]	RI[f]
Primary sources that contribute to 99% of hazard								
24	**Charleston**	1.00	6.6 [0.20] 6.8 [0.60] 7.0 [0.20]	1 [1.00] (a=-0.710, b=1.020)	none	**Yes[g]**	**Yes[g]**	**Yes[g]**
26	South Carolina	1.00	5.8 [0.15] 6.5 [0.60] 6.8 [0.35]	1 [1.00] (a=-1.390, b=0.970)	none	No	No	No
Additional sources that do not contribute to 99% of hazard								
49D	Appalachian Basement	1.00	4.8 [0.20] 5.5 [0.60] 5.8 [0.20]	2 [1.00]	Background; P$_B$=1.00	No	No	No
50B	Grenville Province	1.00	4.8 [0.20] 5.5 [0.60] 5.8 [0.20]	2 [1.00]	Background; P$_B$=1.00	No	No	No
50C	Grenville Province	1.00	4.8 [0.20] 5.5 [0.60] 5.8 [0.20]	2 [1.00]	Background; P$_B$=1.00			
C01	Background 49	NA	4.8 [0.20] 5.5 [0.60] 5.8 [0.20]	3 [1.00]	none	No	No	No
C02	Background 50	NA	4.8 [0.20] 5.5 [0.60] 5.8 [0.20]	3 [1.00]	none	No	No	No
C07	50 (02) + 12	NA	4.8 [0.20] 5.5 [0.60] 5.8 [0.20]	3 [1.00]	none	No	No	No

Table 2.5.2-206 (Sheet 2 of 2)
Summary of EPRI Seismic Sources — Rondout Associates

Source	Description	Pa	M$_{max}$ (m$_b$) and Weights[a]	Smoothing Options and Weights[b]	Interdependencies[c]	New Data to Suggest Change in Source?		
						Geom.[d]	M$_{max}$[e]	RI[f]
Additional sources that do not contribute to 99% of hazard (continued)								
C09	49+32	NA	4.8 [0.20] 5.5 [0.60] 5.8 [0.20]	3 [1.00]	none	No	No	No

Pa – probability of activity (from EPRI NP-6452-D 1989, Reference 231).

a) Maximum Magnitude (M$_{max}$) and weights (from EPRI NP-6452-D 1989).

b) Smoothing options are defined as follows (from EPRI NP-6452-D 1989):
    1, 6, 7, 8 = a, b values as listed above, with weights shown.
    3 = Low smoothing on a, constant b (strong prior of 1.0).
    5 = a, b values as listed above, with weights shown.

c) ME – mutually exclusive; PD – perfectly dependent.

d) No, unless (1) new geometry proposed in literature or (2) new seismicity pattern.

e) No, unless (1) new data suggest M$_{max}$ exceeds or differs significantly from the EPRI M$_{max}$ distribution or (2) exceeded by historical seismicity.

f) RI = recurrence interval; assumed no change if no new paleoseismic data or rate of seismicity has not significantly changed.

g) Replace this source with the Updated Charleston Seismic Source (UCSS) Model - original Charleston sources shown in bold.

Table 2.5.2-207 (Sheet 1 of 3)
Summary of EPRI Seismic Sources — Weston Geophysical

Source	Description	Pa	M_{max} (m_b) and Weights[a]	Smoothing Options and Weights[b]	Interdependencies[c]	New Data to Suggest Change in Source?		
						Geom.[d]	M_{max}[e]	RI[f]
Primary sources that contribute to 99% of hazard								
25	**Charleston, SC**	0.99	6.6 [0.90] 7.2 [0.10]	1b [1.00]	none	**Yes**[g]	**Yes**[g]	**Yes**[g]
26	S. Carolina	0.86	6.0 [0.67] 6.6 [0.27] 7.2 [0.06]	1b [1.00]	none	No	No	No
104	S. Coastal Plain	1.00	5.4 [0.24] 6.0 [0.61] 6.6 [0.15]	1a [0.20] 2a [0.80]	Background; P_B=1.00	No	No	No
C19	103-23-24	NA	5.4 [0.26] 6.0 [0.58] 6.6 [0.16]	1a [1.00]	NA	No	No	No
C20	104-22	NA	6.0 [0.85] 6.6 [0.15]	1a [0.30] 2a [0.70]	NA	No	No	No
C21	104-25	NA	5.4 [0.24] 6.0 [0.61] 6.6 [0.15]	1a [0.30] 2a [0.70]	NA	No	No	No
C23	104-22-26	NA	5.4 [0.80] 6.0 [0.14] 6.6 [0.06]	1a [0.50] 2a [0.50]	NA	No	No	No
C24	104-22-25	NA	5.4 [0.80] 6.0 [0.14] 6.6 [0.06]	1a [0.50] 2a [0.50]	NA	No	No	No
C26	104-28BCDE-22	NA	5.4 [0.24] 6.0 [0.61] 6.6 [0.15]	1a [0.30] 2a [0.70]	NA	No	No	No

Table 2.5.2-207 (Sheet 2 of 3)
Summary of EPRI Seismic Sources — Weston Geophysical

Source	Description	Pa	M_{max} (m_b) and Weights[a]	Smoothing Options and Weights[b]	Interdependencies[c]	New Data to Suggest Change in Source?		
						Geom.[d]	M_{max}[e]	RI[f]
Primary sources that contribute to 99% of hazard (continued)								
C27	104-28BCDE-22-25	NA	5.4 [0.30] 6.0 [0.70]	1a [0.70] 2a [0.30]	NA	No	No	No
C33	26-25	NA	6.6 [0.90] 7.2 [0.10]	1b [1.00]	NA	No	No	No
C35	104-28BE-25	NA	5.4 [0.24] 6.0 [0.61] 6.6 [0.15]	1a [0.20] 1b [0.80]	NA	No	No	No
Additional sources that do not contribute to 99% of hazard								
28D	Mesozoic Basin	0.26	5.4 [0.65] 6.0 [0.25] 6.6 [0.20]	1b [1.00]	PD with 28B, 28C, 28E	No	No	No
28E	Mesozoic Basin	0.26	5.4 [0.65] 6.0 [0.25] 6.6 [0.20]	1b [1.00]	PD with 28B, 28C, 28D	No	No	No
103	S. Appalachians	1.00	5.4 [0.26] 6.0 [0.58] 6.6 [0.16]	1a [0.20] 2a [0.80]	Background; P_B=1.00	No	No	No
C01	28A through E	NA	5.4 [0.65] 6.0 [0.25] 6.6 [0.10]	1b [1.00]	NA	No	No	No
C17	103-23	NA	5.4 [0.26] 6.0 [0.58] 6.6 [0.16]	1a [0.70] 2a [0.30]	NA	No	No	No
C18	103-24	NA	5.4 [0.26] 6.0 [0.58] 6.6 [0.16]	1a [0.70] 1b [0.30]	NA	No	No	No

Table 2.5.2-207 (Sheet 3 of 3)
Summary of EPRI Seismic Sources — Weston Geophysical

Source	Description	Pa	M_{max} (m_b) and Weights[a]	Smoothing Options and Weights[b]	Interdependencies[c]	New Data to Suggest Change in Source?		
						Geom.[d]	M_{max}[e]	RI[f]
Additional sources that do not contribute to 99% of hazard (continued)								
C22	104-26	NA	5.4 [0.24] 6.0 [0.61] 6.6 [0.15]	1a [0.30] 1b [0.70]	NA	No	No	No
C25	104-28BCDE	NA	5.4 [0.26] 6.0 [0.58] 6.6 [0.16]	1a [0.30] 2a [0.70]	NA	No	No	No
C28	104-28BCDE-22-26	NA	5.4 [0.30] 6.0 [0.70]	1a [0.70] 2a [0.30]	NA	No	No	No
C34	104-28BE-26	NA	5.4 [0.24] 6.0 [0.61] 6.6 [0.15]	1a [0.20] 1b [0.80]	NA	No	No	No

Pa – probability of activity (from EPRI NP-6452-D 1989, Reference 231).
a) Maximum Magnitude (M_{max}) and weights (from EPRI NP-6452-D 1989).
b) Smoothing options are defined as follows (from EPRI NP-6452-D 1989):
    1a = Constant a, constant b (medium prior of 1.0).
    1b = Constant a, constant b (medium prior of 0.9).
    1c = Constant a, constant b (medium prior of 0.7.)
    2a = Medium smoothing on a, medium smoothing on b (medium prior of 1.0).
    2b = Medium smoothing on a, medium smoothing on b (medium prior of 0.9).
    2c = Medium smoothing on a, medium smoothing on b (medium prior of 0.7).
c) ME – mutually exclusive; PD – perfectly dependent.
d) No, unless (1) new geometry proposed in literature or (2) new seismicity pattern.
e) No, unless (1) new data suggest M_{max} exceeds or differs significantly from the EPRI M_{max} distribution or (2) exceeded by historical seismicity.
f) RI = recurrence interval; assumed no change if no new paleoseismic data or rate of seismicity has not significantly changed.
g) Replace this source with the Updated Charleston Seismic Source Model - original Charleston sources shown in bold.

Table 2.5.2-208 (Sheet 1 of 2)
Summary of EPRI Seismic Sources — Woodward-Clyde Consultants

Source	Description	Pa	M_{max} (m_b) and Weights[a]	Smoothing Options and Weights[b]	Interdependencies[c]	New Data to Suggest Change in Source?		
						Geom.[d]	M_{max}[e]	RI[f]
Primary sources that contribute to 99% of hazard								
29	**S. Carolina Gravity Saddle (Extended)**	0.122	6.7 [0.33] 7.0 [0.34] 7.4 [0.33]	2 [0.25] 3 [0.25] 4 [0.25] 5 [0.25]	ME with 29A, 29B, 30	**Yes[g]**	**Yes[g]**	**Yes[g]**
29A	**SC Gravity Saddle No. 2 (Combo C3)**	0.305	6.7 [0.33] 7.0 [0.34] 7.4 [0.33]	2 [0.25] 3 [0.25] 4 [0.25] 5 [0.25]	ME with 29, 29B, 30	**Yes[g]**	**Yes[g]**	**Yes[g]**
29B	SC Gravity Saddle No. 3 (NW portion)	0.183	5.4 [0.33] 6.0 [0.34] 7.0 [0.33]	2 [0.25] 3 [0.25] 4 [0.25] 5 [0.25]	ME with 29, 29A	No	No	No
30	**Charleston (includes NOTA)**	0.573	6.8 [0.33] 7.3 [0.34] 7.5 [0.33]	2 [0.25] 3 [0.25] 4 [0.25] 5 [0.25]	ME with 29, 29A	**Yes[g]**	**Yes[g]**	**Yes[g]**
31A	Blue Ridge - Alternate Configuration	0.211	5.9 [0.33] 6.3 [0.34] 7.0 [0.33]	2 [0.10] 3 [0.10] 4 [0.10] 5 [0.10] 9 [0.60] (a=-1.005, b=0.852)	ME with 31	No	No	No
BG-VCSNS	V. C. Summer Background	NA	5.8 [0.33] 6.2 [0.34] 6.6 [0.33]	1 [0.25] 6 [0.25] 7 [0.25] 8 [0.25]	NA	No	No	No

Table 2.5.2-208 (Sheet 2 of 2)
Summary of EPRI Seismic Sources — Woodward-Clyde Consultants

Source	Description	Pa	M$_{max}$ (m$_b$) and Weights[a]	Smoothing Options and Weights[b]	Interdependencies[c]	New Data to Suggest Change in Source? Geom.[d]	New Data to Suggest Change in Source? M$_{max}$[e]	New Data to Suggest Change in Source? RI[f]
Additional sources that do not contribute to 99% of hazard								
31	Blue Ridge Combo.	0.024	5.9 [0.33] 6.3 [0.34] 7.0 [0.33]	2 [0.25] 3 [0.25] 4 [0.25] 5 [0.25]	ME with 31A	No	No	No

Pa – probability of activity (from EPRI NP-6452-D 1989, Reference 231).

(a) Maximum Magnitude (M$_{max}$) and weights (from EPRI NP-6452-D 1989).

(b) Smoothing options are defined as follows (from EPRI NP-6452-D 1989):
   1 = Low smoothing on a, high smoothing on b (no prior).
   2 = High smoothing on a, high smoothing on b (no prior).
   3 = High smoothing on a, high smoothing on b (moderate prior of 1.0).
   4 = High smoothing on a, high smoothing on b (moderate prior of 0.9).
   5 = High smoothing on a, high smoothing on b (moderate prior of 0.8).
   6 = Low smoothing on a, high smoothing on b (moderate prior of 1.0).
   7 = Low smoothing on a, high smoothing on b (moderate prior of 0.9).
   8 = Low smoothing on a, high smoothing on b (moderate prior of 0.8)
   Weights on magnitude intervals are all 1.0.
   9 = a and b values as listed.

(c   ME – mutually exclusive; PD – perfectly dependent.

(d) No, unless (1) new geometry proposed in literature or (2) new seismicity pattern.

(e) No, unless (1) new data suggest M$_{max}$ exceeds or differs significantly from the EPRI M$_{max}$ distribution or (2) exceeded by historical seismicity.

(f)   RI = recurrence interval; assumed no change if no new paleoseismic data or rate of seismicity has not significantly changed.

(g) Replace this source with the Updated Charleston Seismic Source Model - original Charleston sources shown in bold.

Table 2.5.2-209
Summary of USGS Seismic Sources (Frankel et al. 2002)

Source	M_{max} (M) and Wts.	Largest M_{max} Value Considered by USGS	
		M	m_b[a]
Sources within 200 mi (320 km)			
Extended Margin Background	7.5 [1.00]	7.5	7.2
Charleston	6.8 [0.20] 7.1 [0.20] 7.3 [0.45] 7.5 [0.15]	7.5	7.2
Eastern Tennessee	7.5 [1.00]	7.5	7.2
Selected Sources Beyond 200 mi (320km)			
New Madrid	7.3 [0.15] 7.5 [0.20] 7.7 [0.50] 8.0 [0.15]	8.0	7.5
Stable Craton Background	7.0 [1.00]	7.0	6.9

(a) m_b converted from **M** using average of Atkinson and Boore (Reference 207), Frankel et al. (Reference 240), and EPRI (Reference 230) relations

Wts. – Weights

Table 2.5.2-210
Chapman and Talwani (2002) Seismic Source Zone Parameters

Charleston Characteristic Sources	Mean Recurrence	M_{max}[b]	
		m_{blg}	M
Charleston Area Source	550 years	—	7.1 [.2]
			7.3 [.6]
			7.5 [.2]
ZRA Fault Source	550 years	—	7.1 [.2]
(Zone of River Anomalies)			7.3 [.6]
			7.5 [.2]
Ashley River-Woodstock Fault Source	550 years	—	7.1 [.2]
(modeled as 3 parallel faults)			7.3 [.6]
			7.5 [.2]

Non-Characteristic Background Sources	a[a]	b[a]	m_{blg}	M
1. Zone1	0.242	0.84	6.84	7.00
2. Zone2	−0.270	0.84	6.84	7.00
3. Central Virginia	1.184	0.64	6.84	7.00
4. Zone4	0.319	0.84	6.84	7.00
5. Zone5	0.596	0.84	6.84	7.00
6. Piedmont and Coastal Plain	1.537	0.84	6.84	7.00
6a. Pied&CP NE	0.604	0.84	6.84	7.00
6b. Pied&CP SW	1.312	0.84	6.84	7.00
7. South Carolina Piedmont	2.220	0.84	6.84	7.00
8. Middleton Place	1.690	0.77	6.84	7.00
9. Florida and continental margin	1.371	0.84	6.84	7.00
10. Alabama	1.800	0.84	6.84	7.00
11. Eastern Tennessee	2.720	0.90	6.84	7.00
12. Southern Appalachian	2.420	0.84	6.84	7.00
12a. Southern Appalachian North	2.185	0.84	6.84	7.00
13. Giles County, VA	1.070	0.84	6.84	7.00
14. Central Appalachians	1.630	0.84	6.84	7.00
15. Western Tennessee	2.431	1.00	6.84	7.00
16. Central Tennessee	2.273	1.00	6.84	7.00
17. Ohio-Kentucky	2.726	1.00	6.84	7.00
18. West VA-Pennsylvania	2.491	1.00	6.84	7.00
19. USGS (1996) gridded seismicity rates and b value	—	0.95	6.84	7.00

(a) a and b values in terms of m_{blg} magnitude, reported in Chapman and Talwani (Reference 219).

(b) M_{max} range for characteristic events was designed to "represent the range of magnitude estimates of the 1886 Charleston shock proposed by Johnston (Reference 246)" (Reference 219, p. 12). Square brackets indicate weights assigned to characteristic magnitudes. For non-characteristic background events, a truncated form of the exponential probability density function was used (Chapman and Talwani, p. 6-7, Reference 219).

— = not reported

Table 2.5.2-211
Comparison of EPRI Characterizations of the Charleston Seismic Zone

EST	Source	Description	Pa	M_{max} (m_b) and Wts.[a]	M_{max} (M) and Wts.	Upper Bound M_{max}		Weighted Mean M_{max}	
						m_b	$M^{[b]}$	m_b	$M^{[a]}$
Bechtel	H	Charleston Area	0.50	6.8 [0.20] 7.1 [0.40] 7.4 [0.40]	6.82 [0.20] 7.33 [0.40] 7.87 [0.40]	7.4	7.9	7.2	7.4
	N3	Charleston Faults	0.53	6.8 [0.20] 7.1 [0.40] 7.4 [0.40]	6.82 [0.20] 7.33 [0.40] 7.87 [0.40]	7.4	7.9	7.2	7.4
	BZ4	Atlantic Coastal Region	1.00	6.6 [0.10] 6.8 [0.40] 7.1 [0.40] 7.4 [0.10]	6.49 [0.10] 6.82 [0.40] 7.33 [0.40] 7.87 [0.10]	7.4	7.9	7.0	7.1
Dames & Moore	54	Charleston Seismic Zone	1.00	6.6 [0.75] 7.2 [0.25]	6.49 [0.75] 7.51 [0.25]	7.2	7.5	6.8	6.7
Law Engineering	35	Charleston Seismic Zone	0.45	6.8 [1.00]	6.82 [1.00]	6.8	6.8	6.8	6.8
Rondout Associates	24	Charleston	1.00	6.6 [0.20] 6.8 [0.60] 7.0 [0.20]	6.49 [0.20] 6.82 [0.60] 7.16 [0.20]	7.0	7.2	6.8	6.8
Weston Geophysical	25	Charleston Seismic Zone	0.99	6.6 [0.90] 7.2 [0.10]	6.49 [0.90] 7.51 [0.10]	7.2	7.5	6.7	6.6
Woodward-Clyde Consultants	29	S. Carolina Gravity Saddle (Extended)	0.122	6.7 [0.33] 7.0 [0.34] 7.4 [0.33]	6.65 [0.33] 7.16 [0.34] 7.87 [0.33]	7.4	7.9	7.0	7.2
	29A	SC Gravity Saddle No. 2 (Combo C3)	0.305	6.7 [0.33] 7.0 [0.34] 7.4 [0.33]	6.65 [0.33] 7.16 [0.34] 7.87 [0.33]	7.4	7.9	7.0	7.2
	30	Charleston (includes NOTA)	0.573	6.8 [0.33] 7.3 [0.34] 7.5 [0.33]	6.82 [0.33] 7.69 [0.34] 8.04 [0.33]	7.5	8.0	7.2	7.5
Composite Range of M_{max} Values for all EPRI ESTs =						m_b 6.6 - 7.5 (**M** 6.5 - 8.0)			

(a) Maximum Magnitude (M_{max}) and weights (wts.) from EPRI NP 6452-D 1989.

(b) Moment magnitude (**M**) converted from body wave magnitude (m_b) using average of Atkinson and Boore (Reference 207), Frankel et al. (Reference 240), and EPRI (Reference 230) relations.

Table 2.5.2-212
Geographic Coordinates (Latitude and Longitude) of Corner Points of UCSS Geometries

Source Geometry	Longitude (decimal degrees)	Latitude (decimal degrees)
A	−80.707	32.811
A	−79.840	33.354
A	−79.527	32.997
A	−80.392	32.455
B	−81.216	32.485
B	−78.965	33.891
B	−78.3432	33.168
B	−80.587	31.775
B'	−78.965	33.891
B'	−78.654	33.531
B'	−80.900	32.131
B'	−81.216	32.485
C	−80.397	32.687
C	−79.776	34.425
C	−79.483	34.351
C	−80.109	32.614

Table 2.5.2-213
Local Charleston-Area Tectonic Features

Name of Feature	Evidence	Key References
Adams Run fault	**subsurface stratigraphy**	**Weems and Lewis (Reference 288)**
Ashley River fault	microseismicity	Talwani (References 272 and 275) Weems and Lewis (Reference 288)
Appalachian detachment (decollement)	gravity & magnetic data seismic reflection & refraction	Cook et al. (References 223 and 224) Behrendt et al. (References 211 and 212) Seeber and Armbruster (Reference 267)
Blake Spur fracture zone	oceanic transform postulated to extend westward to Charleston area	Seeber and Armbruster (Reference 267) Talwani (Reference 275) Sykes (Reference 271) Fletcher et al. (Reference 239)
Bowman seismic zone	microseismicity	Smith and Talwani (Reference 269)
Charleston fault	subsurface stratigraphy	Lennon (Reference 247) Talwani (Reference 275) Weems and Lewis (Reference 288)
Cooke fault	seismic reflection	Behrendt et al. (References 211 and 212) Hamilton et al. (Reference 243) Wentworth and Mergner-Keefer (Reference 291) Behrendt and Yuan (Reference 210
Drayton fault	seismic reflection	Hamilton et al. (Reference 243) Behrendt et al. (Reference 212) Behrendt and Yuan (Reference 210)
East Coast fault system/ Zone of river anomalies (ZRA)	**geomorphology seismic reflection microseismicity**	**Marple and Talwani (References 249, 250, and 251)**
Gants fault	seismic reflection	Hamilton et al. (Reference 243) Behrendt and Yuan (Reference 210)
Helena Banks fault zone	seismic reflection	Behrendt et al. (References 211 and 212) Behrendt and Yuan (Reference 210)
Middleton Place- Summerville seismic zone	microseismicity	Tarr et al. (Reference 282) Madabhushi and Talwani (Reference 248)
Sawmill Branch fault	**microseismicity**	**Talwani and Katuna (Reference 279)**
Summerville fault	**microseismicity**	**Weems et al. (Reference 289)**
Woodstock fault	geomorphology microseismicity	Talwani (References 272, 274, and 275) Marple and Talwani (Reference 250)

Those tectonic features identified following publication of the EPRI teams' reports (post-1986) are highlighted by bold-face type.

Table 2.5.2-214

Comparison of Post-EPRI NP-6395-D 1989 Magnitude Estimates for the 1886 Charleston Earthquake

Study	Magnitude Estimation Method	Reported Magnitude Estimate	Assigned Weights	Mean Magnitude (M)
EPRI (1994) (Reference 237)	Worldwide survey of passive-margin, extended-crust earthquakes	**M** 7.56 ± 0.35[a]	—	7.56
Martin and Clough (Reference 252)	Geotechnical assessment of 1886 liquefaction data	**M** 7 - 7.5	—	7.25
Johnston (Reference 246)	Isoseismal area regression, accounting for eastern North America anelastic attenuation	**M** 7.3 ± 0.26	—	7.3
Chapman and Talwani (Reference 219) (SCDOT)	Consideration of available magnitude estimates	**M** 7.1 **M** 7.3 **M** 7.5	0.2 0.6 0.2	7.3
Frankel et al. (Reference 241) (USGS National seismic hazard mapping project)	Consideration of available magnitude estimates	**M** 6.8 **M** 7.1 **M** 7.3 **M** 7.5	0.20 0.20 0.45 0.15	7.2
Bakun and Hopper (Reference 208)	Isoseismal area regression, including empirical site corrections	MI 6.4 - 7.2[b]	—	6.9[c]

(a) Estimate from EPRI (1994, chapter 3). (Reference 237)
(b) 95% confidence interval estimate; MI (magnitude based on intensity) is considered equivalent to **M** (Bakun and Hopper [Reference 208]).
(c) Bakun and Hopper's (Reference 208) preferred estimate.

Table 2.5.2-215
Comparison of Talwani and Schaeffer (2001) and UCSS Age Constraints on Charleston-Area Paleoliquefaction Events

| Liquefaction Event | Event Age (YBP)[b] | Talwani and Schaeffer (2001) [a] | | | | (this study) |
| | | scenario 1 | | scenario 2 | | |
		Source	M	Source	M	Event Age (YBP) [b], [c]
1886 A.D.	64	Charleston	7.3	Charleston	7.3	64
A	546 ±17	Charleston	7+	Charleston	7+	600 ±70
B	1,021 ±30	Charleston	7+	Charleston	7+	1,025 ±25
C	1,648 ±74	Northern	6+	—	—	—
C'	1,683 ±70	—		Charleston	7+	1,695 ±175
D	1,966 ±212	Southern	6+	—	—	—
E	3,548 ±66	Charleston	7+	Charleston	7+	3,585 ±115
F	5,038 ±166	Northern	6+	Charleston	7+	—
F'	—	—	—	—	—	5,075 ±215
G	5,800 ±500	Charleston	7+	Charleston	7+	—

(a) Modified after Talwani and Schaeffer's (Reference 280) Table 2
(b) Years before present, relative to 1950 A.D.
(c) Event ages based upon recalibration of radiocarbon (to 2-sigma using OxCal 3.8 (Bronk Ramsey, References 217 and 218) data presented in Talwani and Schaeffer's (Reference 280) Table 2

Table 2.5.2-216
Comparison of EPRI (1989) and Current Hazard Using
EPRI (1989) Assumptions

PGA amp, cm/sec^2	EPRI (1989) Hazard	Current Hazard	% Diff
Mean hazard comparison			
50	9.15E-04	9.32E-04	1.81%
100	2.69E-04	2.74E-04	1.82%
250	3.65E-05	3.74E-05	2.47%
500	5.19E-06	5.37E-06	3.45%
700	1.73E-06	1.81E-06	4.39%
1000	4.79E-07	5.08E-07	6.10%
Median hazard comparison			
50	6.05E-04	6.17E-04	1.92%
100	1.80E-04	1.84E-04	2.28%
250	2.26E-05	2.32E-05	2.52%
500	3.22E-06	3.24E-06	0.50%
700	8.27E-07	1.00E-06	20.92%
1000	1.68E-07	2.19E-07	30.24%
85% hazard comparison			
50	1.73E-03	1.62E-03	–6.24%
100	5.10E-04	5.01E-04	–1.73%
250	6.81E-05	7.24E-05	6.37%
500	9.99E-06	9.77E-06	–2.18%
700	3.32E-06	3.02E-06	–9.04%
1000	8.16E-07	8.71E-07	6.74%

Table 2.5.2-217
Mean Rock Uniform Hazard Response Spectral Accelerations (g)

UHS results, g			
Ground Motion Frequency	10^{-4} Mean	10^{-5} Mean	10^{-6} Mean
0.5 Hz	0.0366	0.136	0.295
1 Hz	0.0687	0.192	0.381
2.5 Hz	0.152	0.390	0.797
5 Hz	0.230	0.618	1.40
10 Hz	0.295	0.890	2.25
25 Hz	0.373	1.40	4.01
PGA	0.150	0.493	1.38

Table 2.5.2-218
Mean Magnitudes and Distances from Deaggregation

Struct. Frequency	Annual Freq. Exceed.	Overall Hazard		Hazard from R>100 km	
		M	R, km	M	R, km
1 & 2.5 Hz	1E-4	7.1	220	7.3	250
5 & 10 Hz	1E-4	6.8	160	7.2	210
1 & 2.5 Hz	1E-5	7.1	210	7.3	260
5 & 10 Hz	1E-5	6.1	70	7.2	190
1 & 2.5 Hz	1E-6	6.9	160	7.3	265
5 & 10 Hz	1E-6	5.8	26	7.2	180

Shaded cells indicate values used to construct UHRS.
Horiz. – Horizontal

Table 2.5.2-219
Horizontal 10⁻⁴ and 10⁻⁵ UHRS (in g) and calculation of GMRS (in g)

Frequency	Horizontal 10^{-4}	Horizontal 10^{-5}	AR	DF	Horizontal GMRS
100	0.150	0.493	3.287	1.554	0.233
90	0.164	0.547	3.329	1.570	0.258
80	0.189	0.637	3.376	1.588	0.300
70	0.226	0.774	3.427	1.607	0.363
60	0.273	0.952	3.486	1.629	0.445
50	0.320	1.135	3.552	1.654	0.529
45	0.339	1.215	3.589	1.668	0.565
40	0.353	1.282	3.629	1.682	0.595
35	0.364	1.336	3.670	1.698	0.618
30	0.371	1.376	3.713	1.714	0.635
25	0.373	1.400	3.753	1.729	0.645
20	0.362	1.303	3.600	1.672	0.605
15	0.339	1.144	3.375	1.588	0.538
12.5	0.321	1.032	3.218	1.528	0.490
10	0.295	0.890	3.017	1.451	0.428
9	0.286	0.849	2.967	1.432	0.410
8	0.275	0.802	2.910	1.410	0.388
7	0.263	0.748	2.845	1.385	0.364
6	0.248	0.687	2.771	1.356	0.336
5	0.230	0.618	2.687	1.323	0.304
4	0.204	0.528	2.594	1.286	0.262
3	0.171	0.434	2.541	1.265	0.216
2.5	0.152	0.390	2.566	1.275	0.194
2	0.131	0.345	2.624	1.298	0.171
1.5	0.1042	0.281	2.696	1.326	0.138
1.25	0.0875	0.240	2.740	1.344	0.118
1	0.0687	0.192	2.795	1.365	0.0938
0.9	0.0630	0.187	2.963	1.431	0.0902
0.8	0.0569	0.179	3.137	1.498	0.0852
0.7	0.0504	0.167	3.319	1.567	0.0790
0.6	0.0437	0.153	3.511	1.639	0.0715
0.5	0.0366	0.136	3.716	1.715	0.0628
0.4	0.0275	0.1021	3.716	1.715	0.0471
0.3	0.0188	0.0697	3.717	1.715	0.0322
0.2	0.01058	0.0394	3.720	1.716	0.0182
0.15	0.00680	0.0253	3.722	1.717	0.0117
0.125	0.00504	0.0188	3.724	1.718	0.00865
0.1	0.00341	0.01270	3.726	1.718	0.00586

Table 2.5.2-220
Vertical 10^{-4} and 10^{-5} UHRS (in g) and Calculation of GMRS (in g)

Frequency	V/H for PGA≤0.2g	Vert. 1E-4	V/H for 0.2<PGA<0.5g	Vert. 1E-5	AR	DF	Vert. GMRS
100	0.78	0.117	1.00	0.493	4.214	1.896	0.222
90	0.82	0.135	1.04	0.567	4.192	1.888	0.256
80	0.87	0.163	1.09	0.694	4.249	1.909	0.312
70	0.89	0.202	1.13	0.873	4.324	1.936	0.393
60	0.89	0.244	1.14	1.082	4.440	1.977	0.487
50	0.86	0.275	1.12	1.276	4.639	2.048	0.574
45	0.85	0.287	1.10	1.339	4.674	2.060	0.603
40	0.83	0.293	1.04	1.336	4.566	2.022	0.601
35	0.79	0.289	0.98	1.311	4.530	2.009	0.590
30	0.77	0.284	0.94	1.291	4.550	2.016	0.581
25	0.75	0.280	0.88	1.232	4.404	1.964	0.554
20	0.71	0.258	0.83	1.076	4.176	1.883	0.485
15	0.69	0.234	0.79	0.902	3.859	1.767	0.413
12.5	0.68	0.218	0.77	0.795	3.644	1.688	0.368
10	0.67	0.198	0.75	0.668	3.377	1.589	0.314
9	0.67	0.192	0.75	0.637	3.321	1.567	0.300
8	0.67	0.185	0.75	0.601	3.257	1.543	0.285
7	0.67	0.176	0.75	0.561	3.185	1.516	0.267
6	0.67	0.166	0.75	0.515	3.102	1.484	0.247
5	0.67	0.154	0.75	0.464	3.008	1.448	0.223
4	0.67	0.136	0.75	0.396	2.903	1.408	0.192
3	0.67	0.114	0.75	0.326	2.845	1.385	0.159
2.5	0.67	0.1018	0.75	0.293	2.872	1.395	0.142
2	0.67	0.0880	0.75	0.258	2.937	1.421	0.125
1.5	0.67	0.0698	0.75	0.211	3.018	1.452	0.1014
1.25	0.67	0.0586	0.75	0.180	3.068	1.471	0.0862
1	0.67	0.0460	0.75	0.144	3.128	1.494	0.0688
0.9	0.67	0.0422	0.75	0.140	3.317	1.566	0.0661
0.8	0.67	0.0381	0.75	0.134	3.512	1.639	0.0625
0.7	0.67	0.0338	0.75	0.126	3.715	1.715	0.0580
0.6	0.67	0.0293	0.75	0.1150	3.930	1.793	0.0525
0.5	0.67	0.0245	0.75	0.1020	4.160	1.877	0.0460
0.4	0.67	0.0184	0.75	0.0766	4.160	1.877	0.0345
0.3	0.67	0.0126	0.75	0.0523	4.161	1.877	0.0236
0.2	0.67	0.00709	0.75	0.0295	4.164	1.878	0.0133
0.15	0.67	0.00456	0.75	0.0190	4.166	1.879	0.00856
0.125	0.67	0.00338	0.75	0.0141	4.168	1.880	0.00635
0.1	0.67	0.00228	0.75	0.00953	4.171	1.881	0.00430

Vert. – vertical

Table 2.5.2-221
Magnitudes and Weights for New Madrid Source Faults From the Clinton ESP
Model (Reference 238)

Southern	Reelfoot	Northern	Weight
7.3	7.5	7.0	0.1667
7.2	7.4	7.0	0.1667
7.2	7.4	7.2	0.0833
7.6	7.8	7.5	0.25
7.9	7.8	7.6	0.1667
7.8	7.7	7.5	0.1667
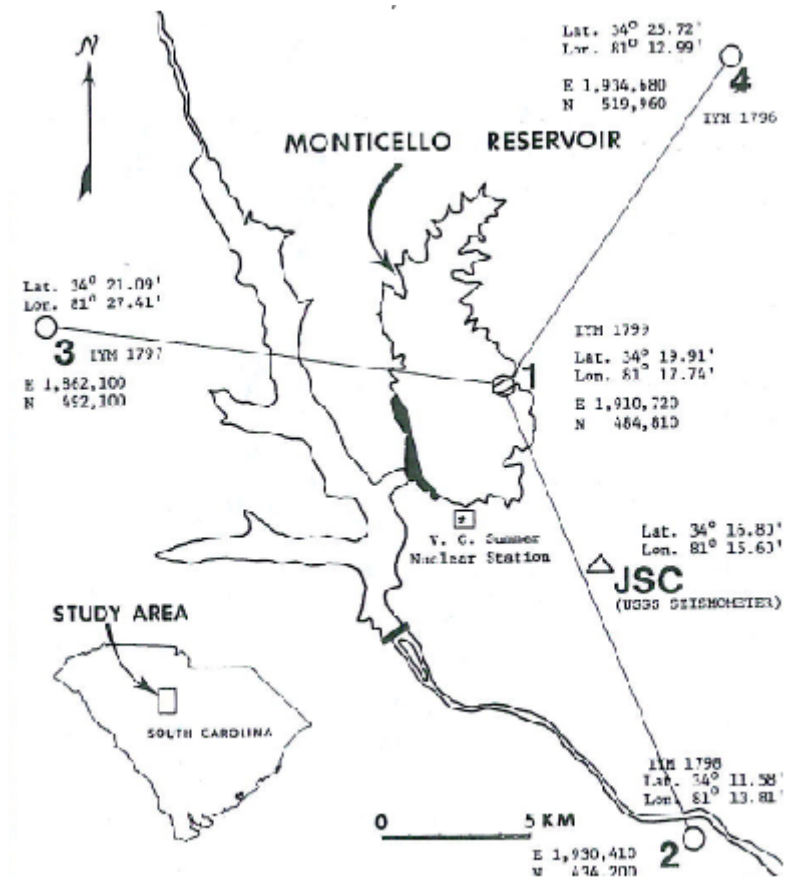
Figure 2.5.2-201. SCE&G 4-Station Microseismic Network and location of Jenkinsville Station (from Whorton 1988, **Reference 295**)
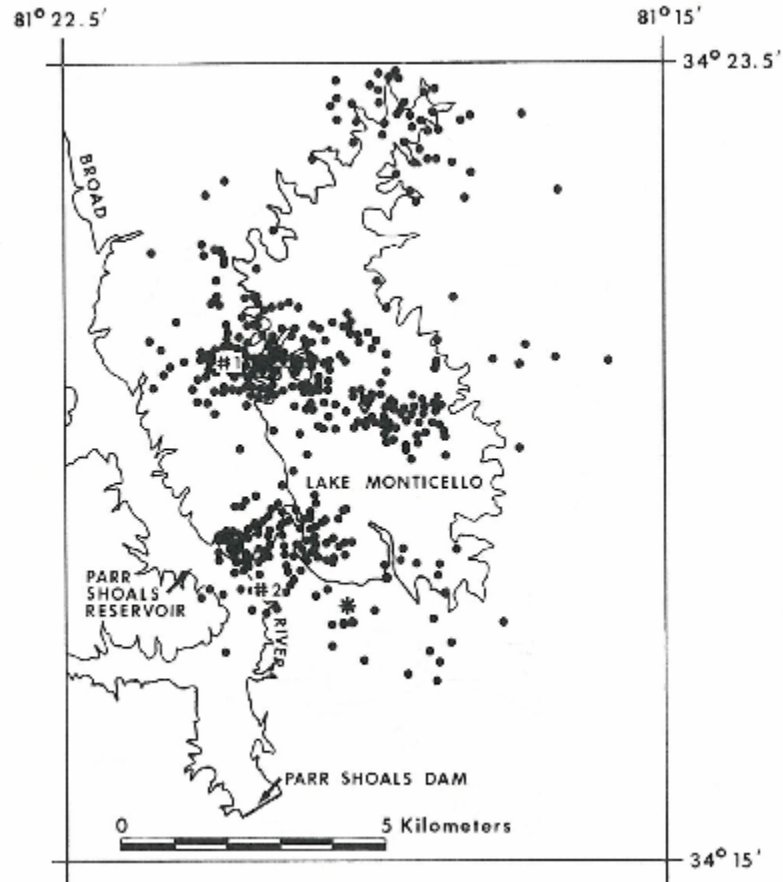
Figure 2.5.2-202. Distribution of Reservoir-Induced Seismicity from June 1978 to September 1979 (modified after Secor et al. 1982, Reference 266)
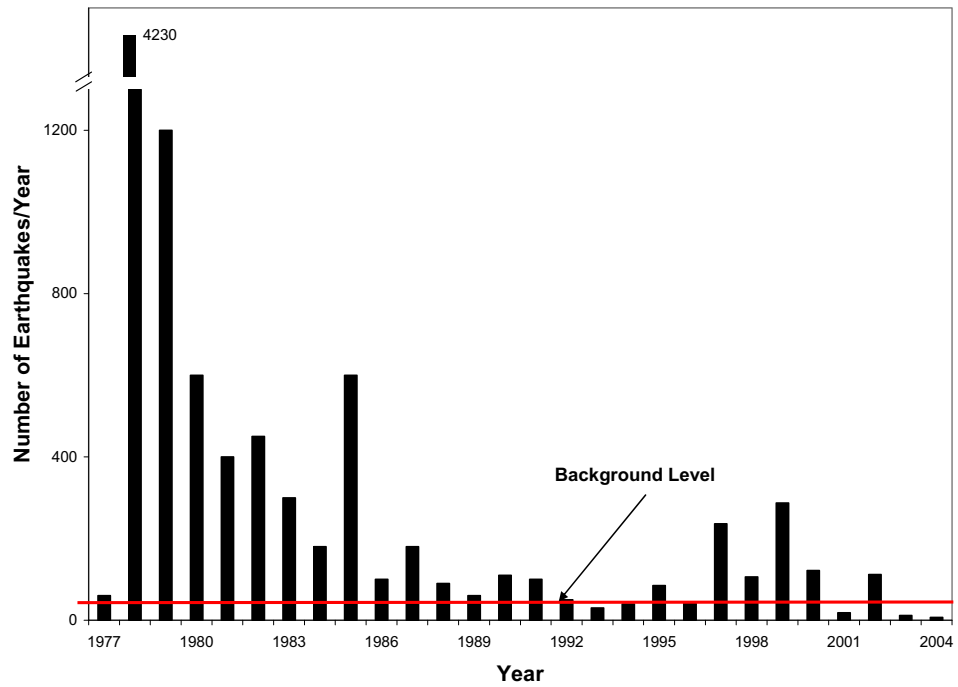
Figure 2.5.2-203. Annual Number of Earthquakes Recorded at Monticello Reservoir from 1977 to 2004 (References 222 and 276)
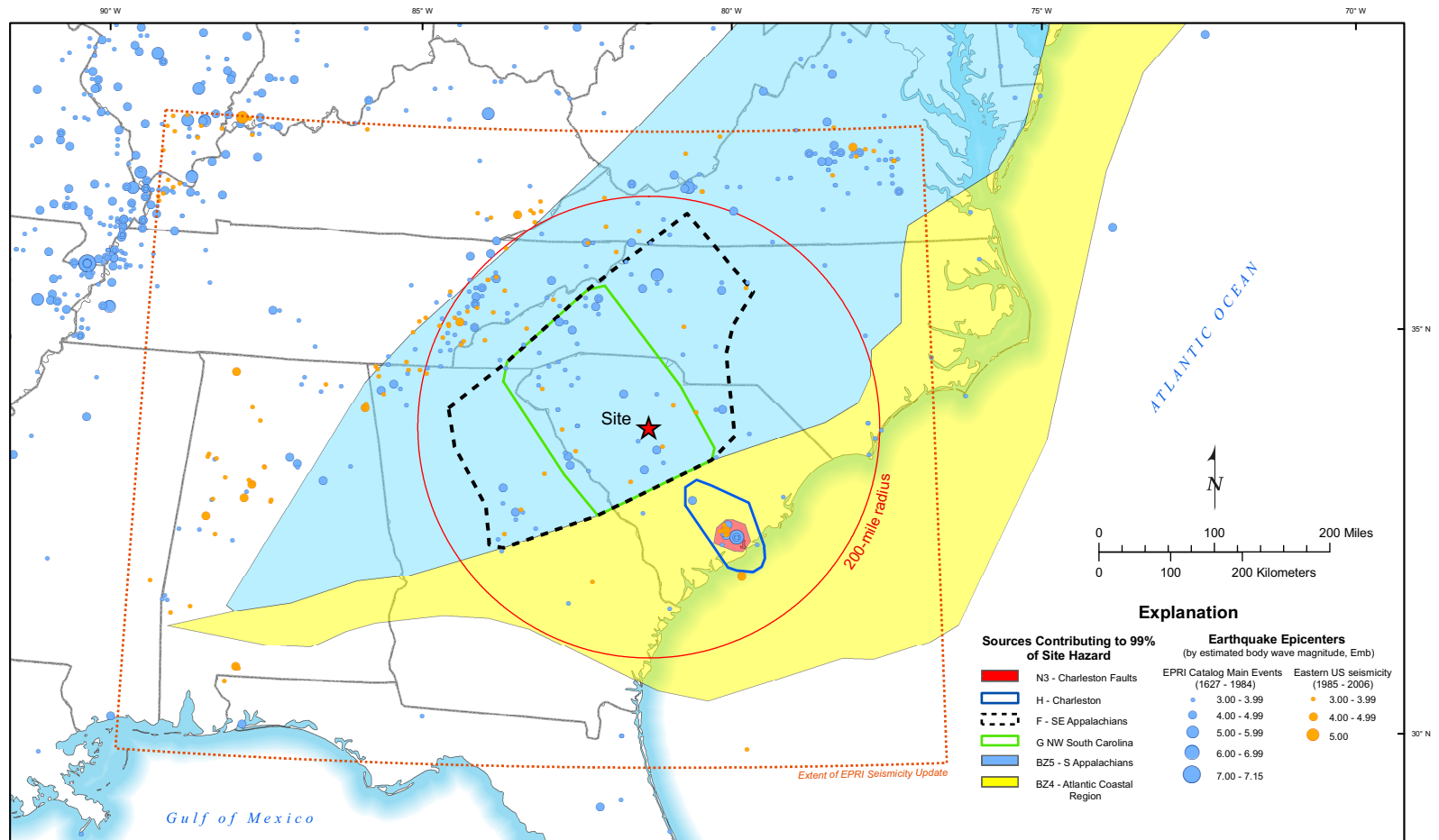
Figure 2.5.2-204.   EPRI Seismic Source Zones From Bechtel Team
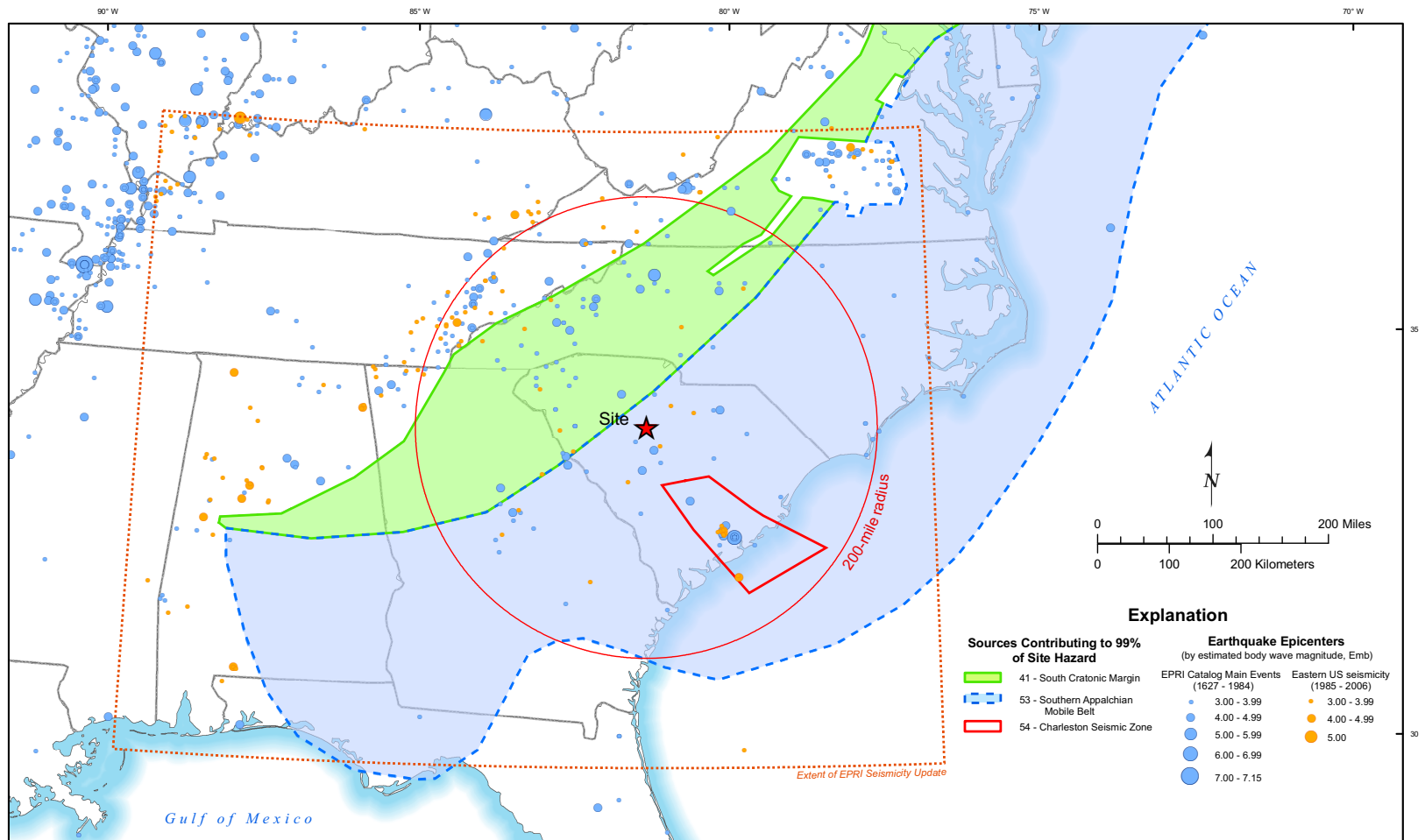
Figure 2.5.2-205.   EPRI Seismic Source Zones From Dames & Moore Team
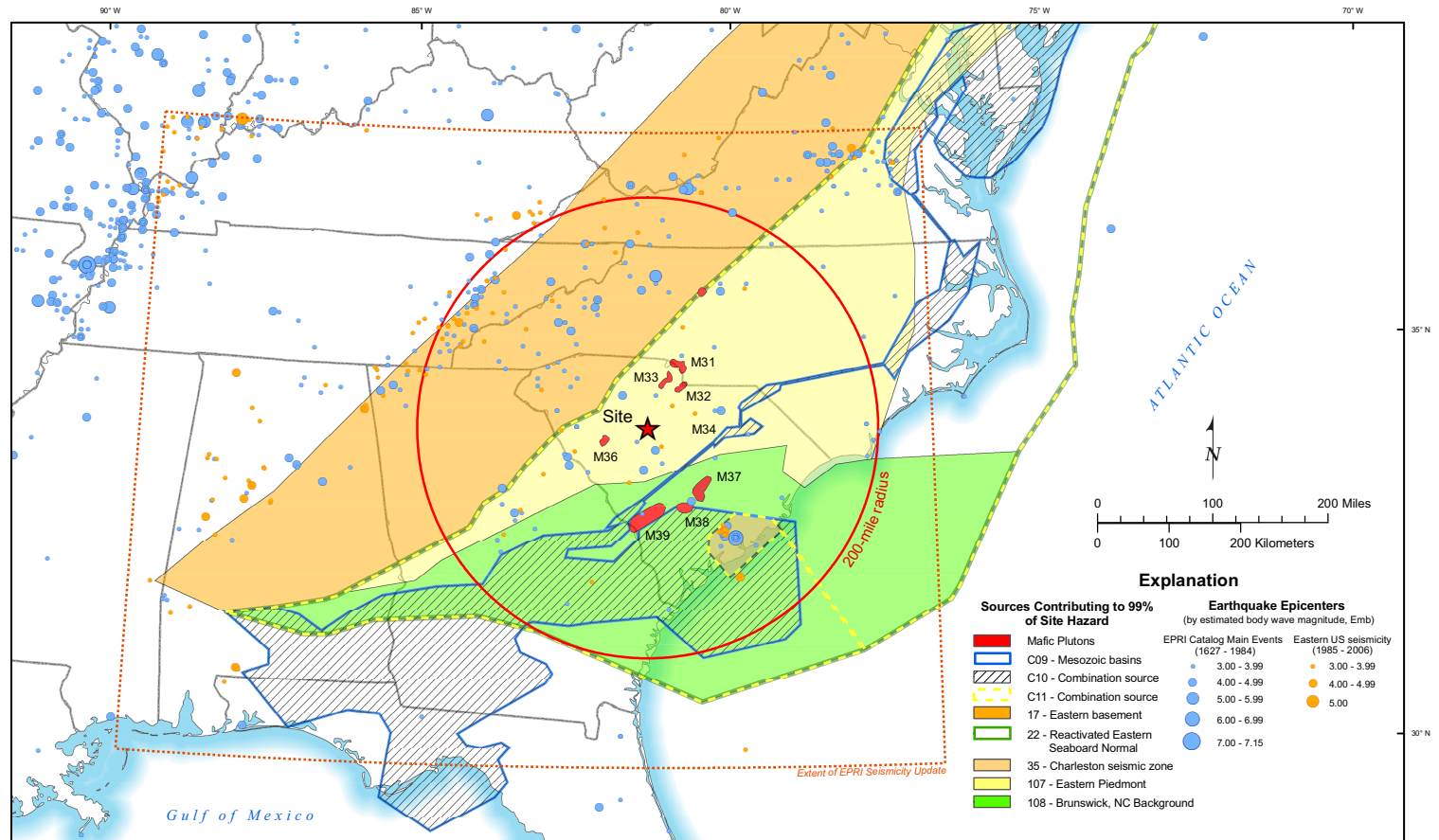
Figure 2.5.2-206. EPRI Seismic Source Zones From Law Engineering Team
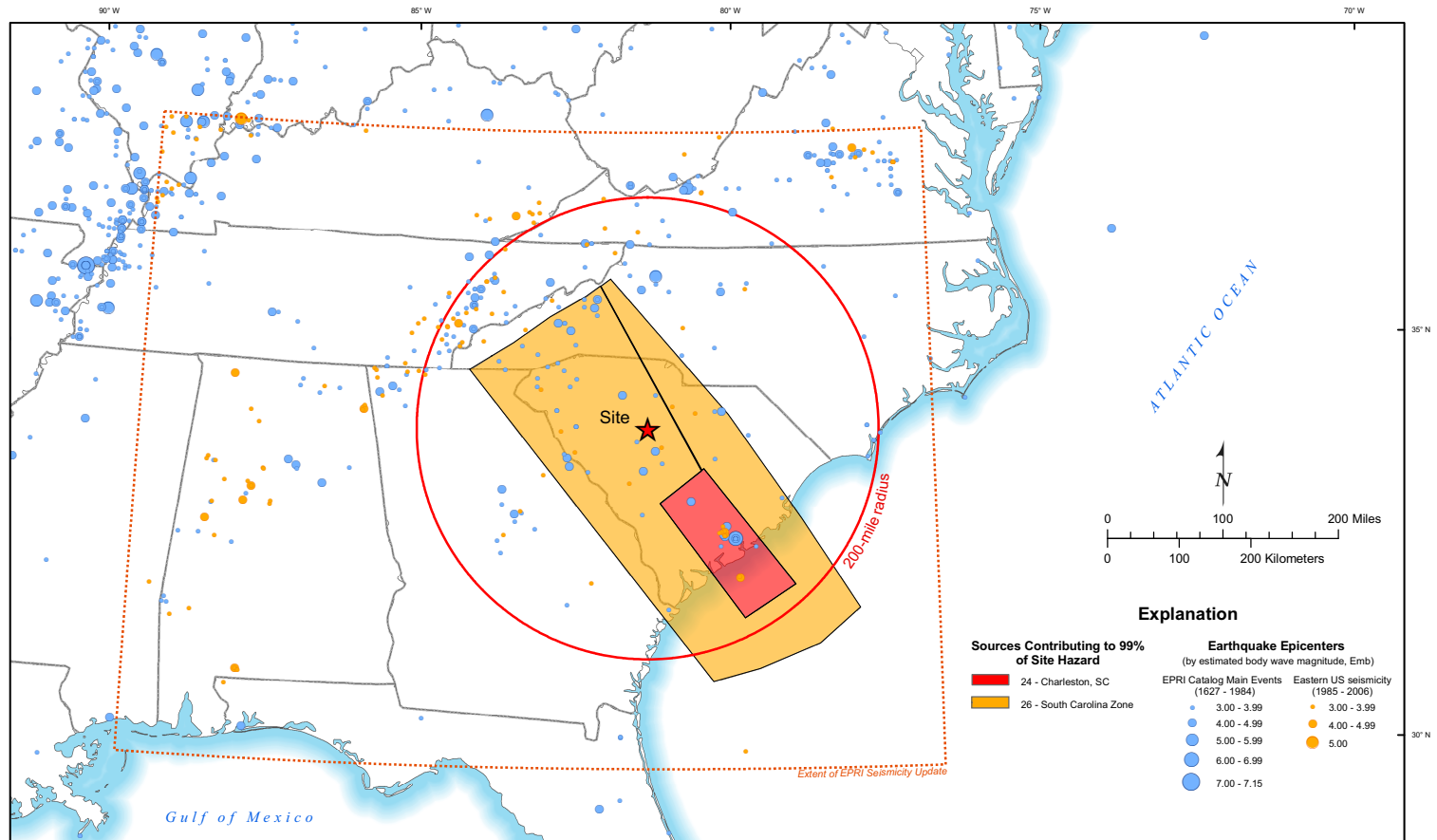
Figure 2.5.2-207.   EPRI Seismic Source Zones From Rondout Team
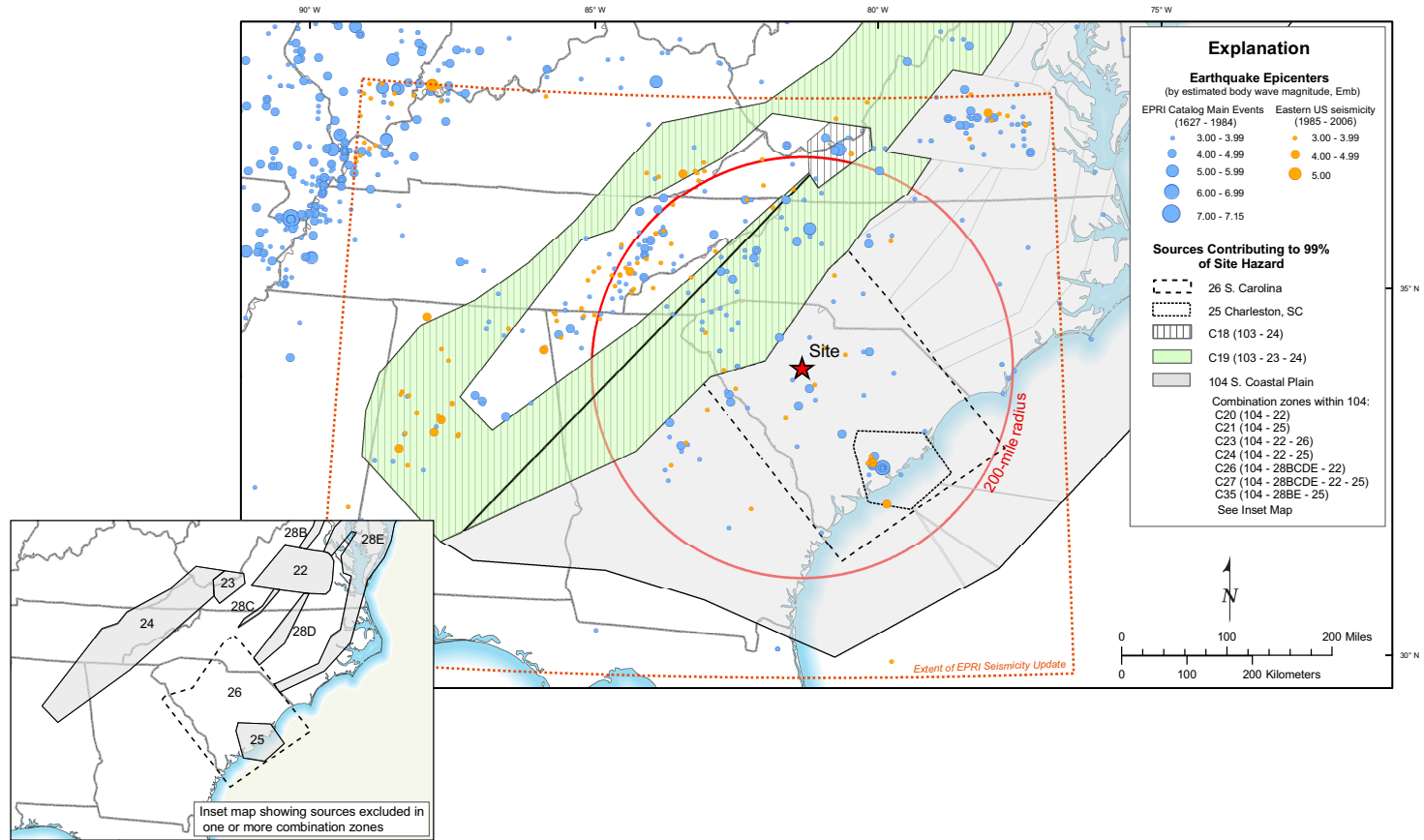
Figure 2.5.2-208. EPRI Seismic Source Zones From Weston Geophysical Team
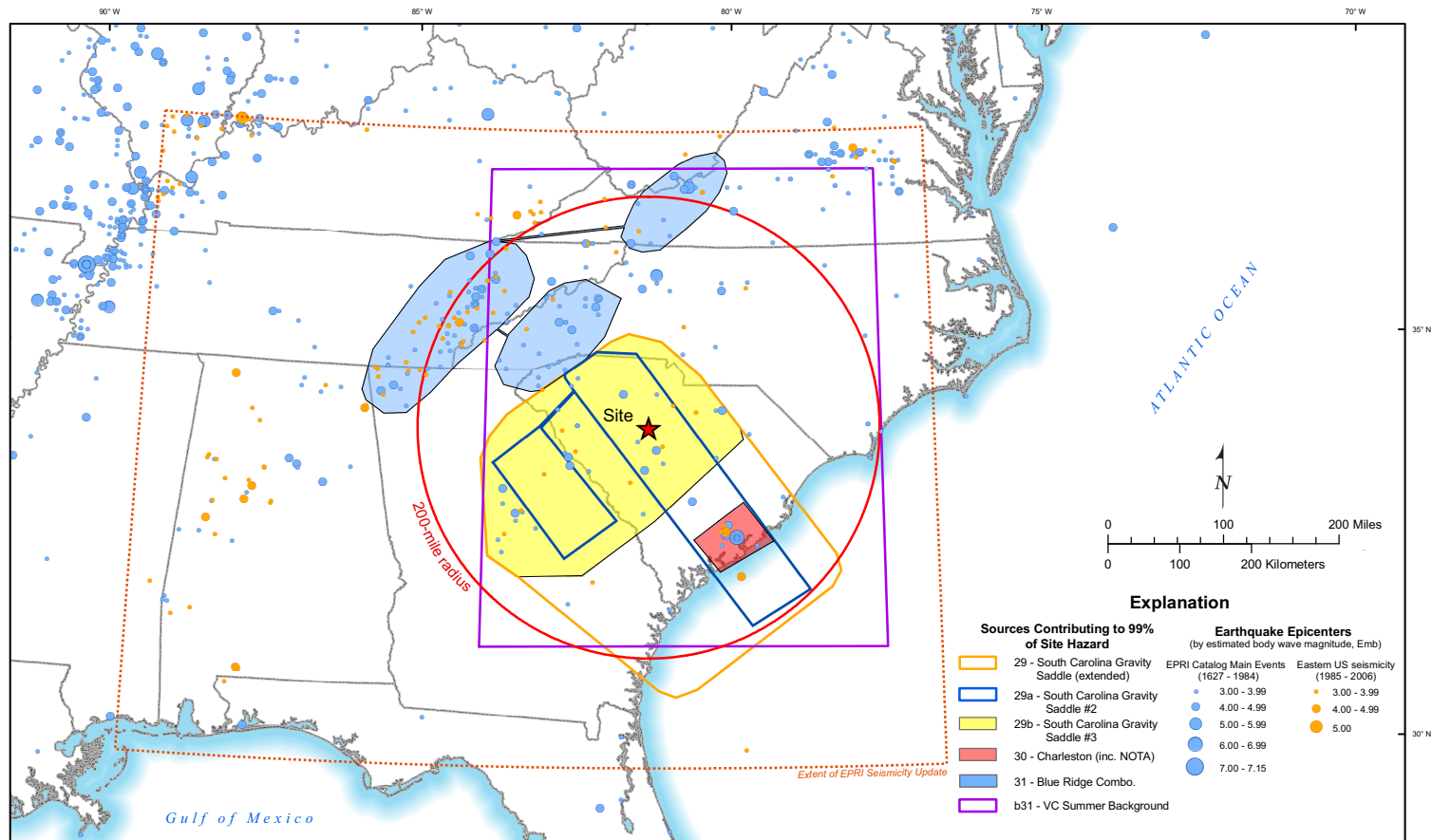
Figure 2.5.2-209. EPRI Seismic Source Zones From Woodward-Clyde Team.
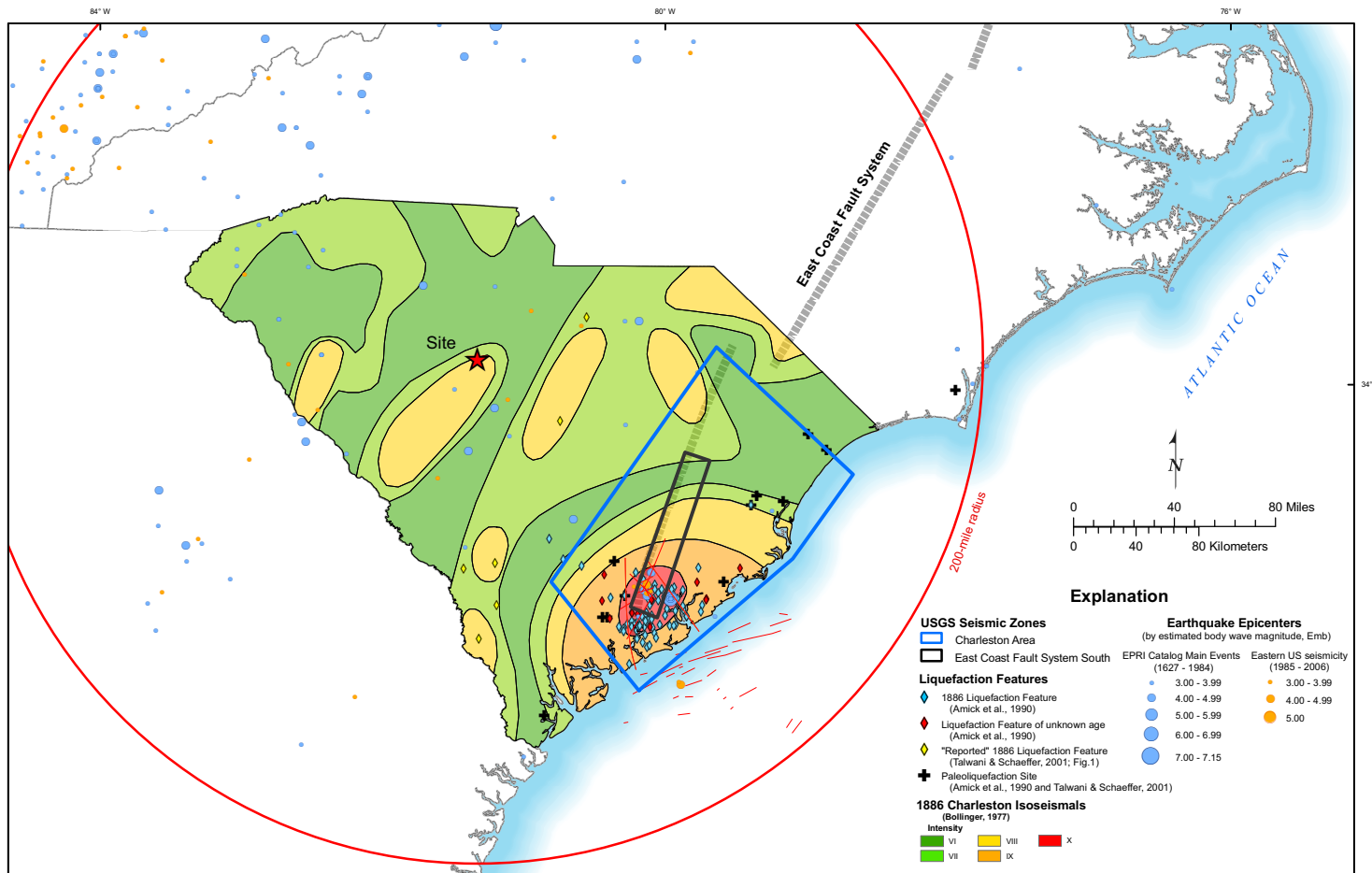
Figure 2.5.2-210.   USGS Charleston Model
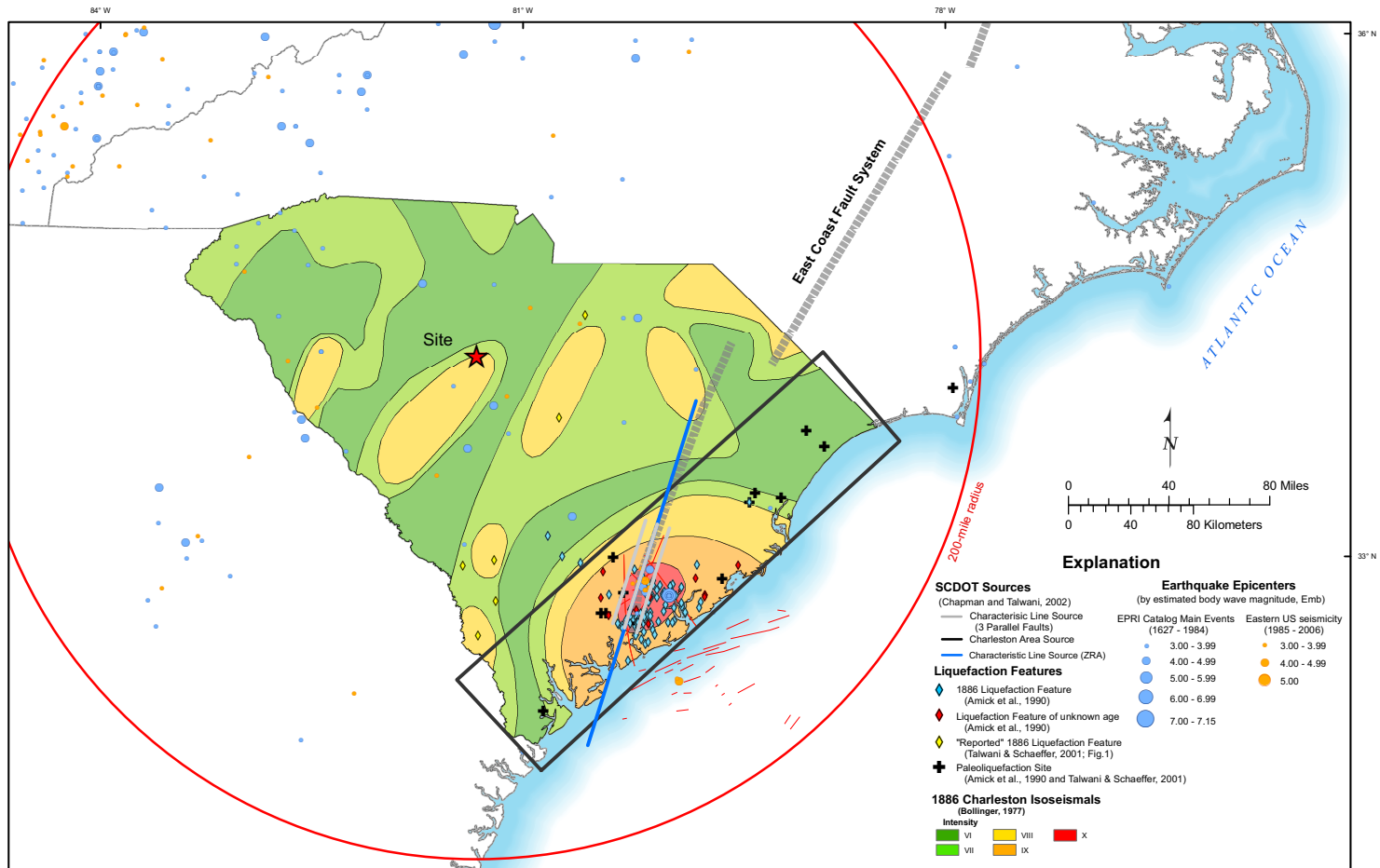
Figure 2.5.2-211. SCDOT Charleston Model
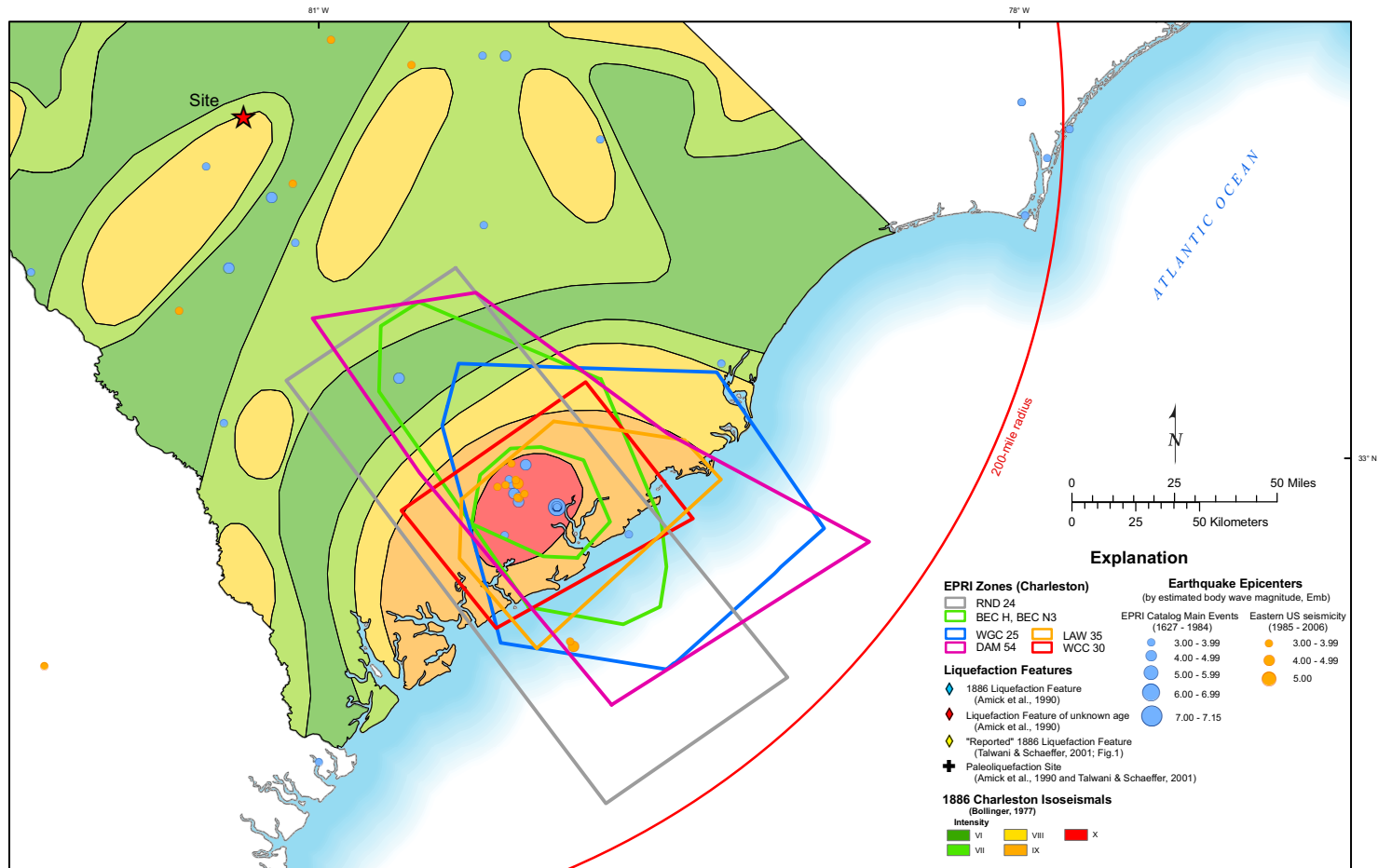
Figure 2.5.2-212. EPRI Representations of Charleston Seismic Source
Note: Woodward-Clyde source 29 is located outside the area of this figure. Figure 2.5.2-209 shows Woodward-Clyde source 29.
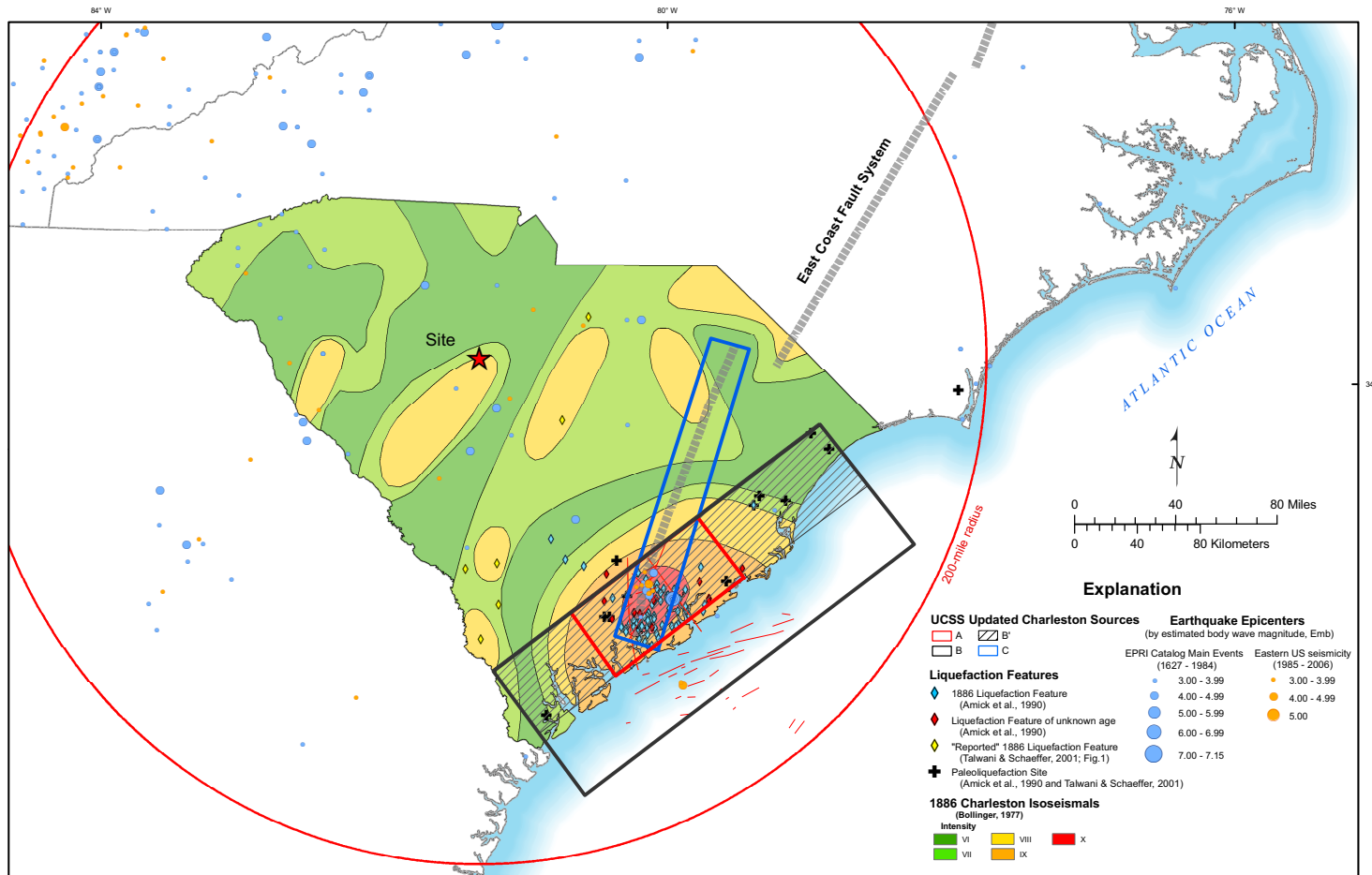
Figure 2.5.2-213.   UCSS Model
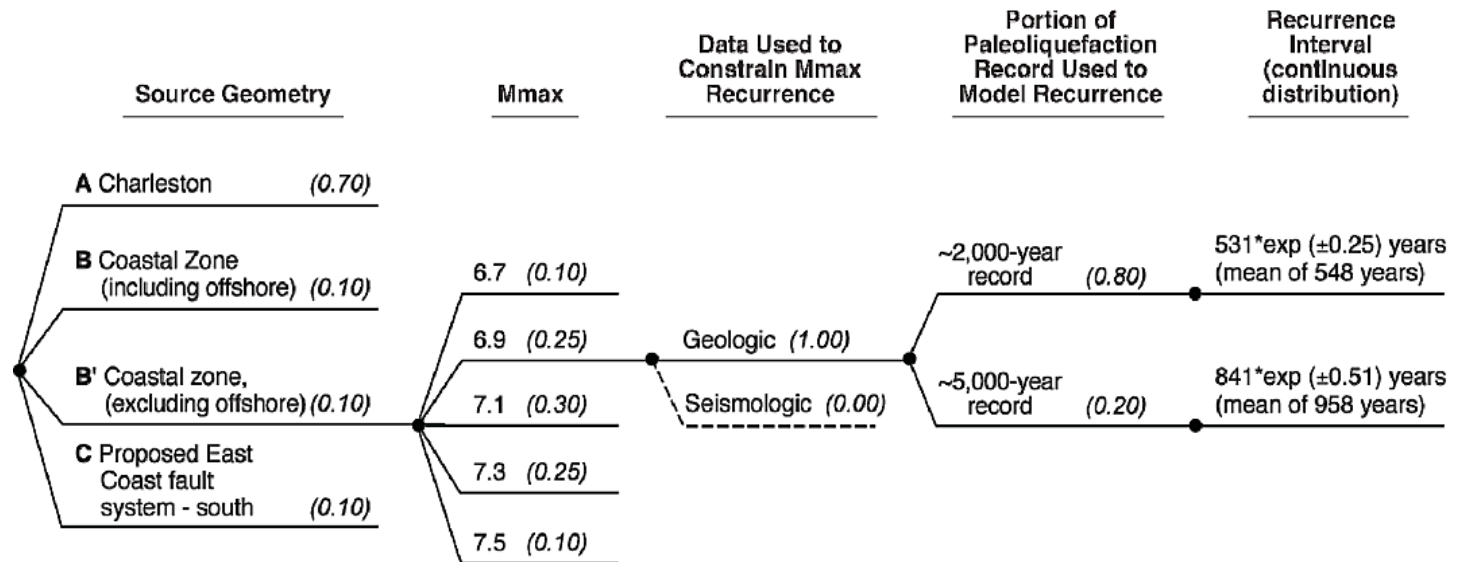
Figure 2.5.2-214. UCSS Logic Tree With Weights For Each Branch
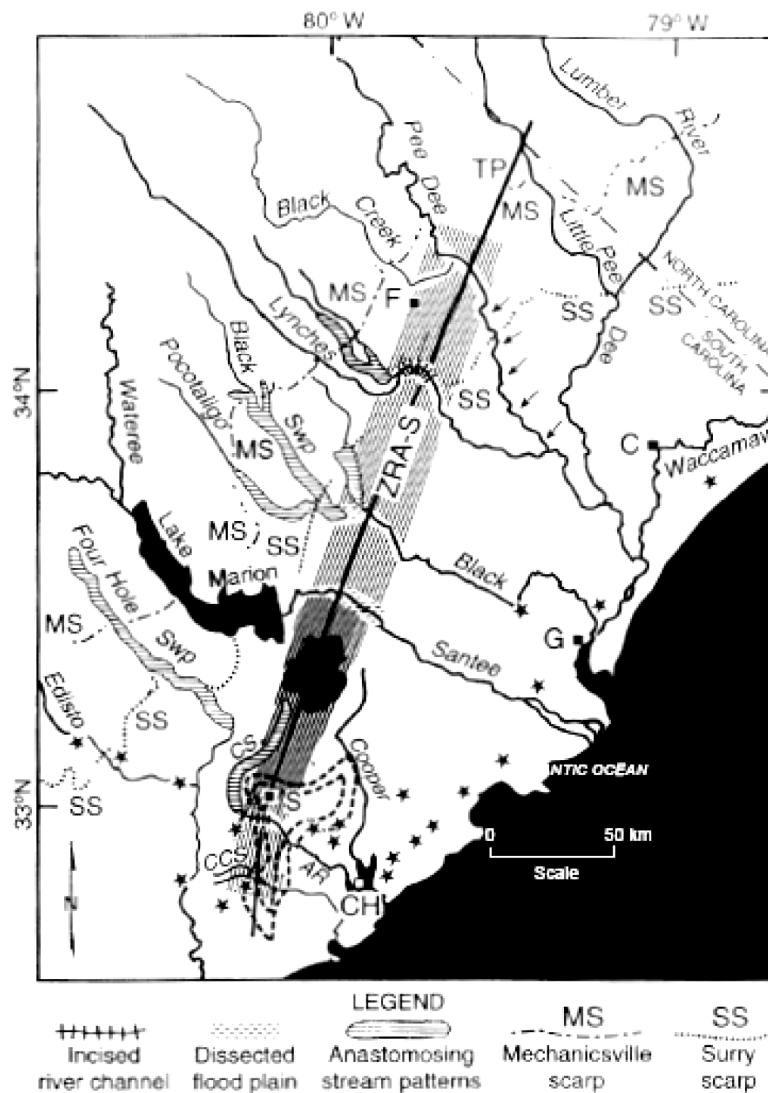
Map of ZRA-S from Marple and Talwani (2000). Figure shows southern zone of river anomalies (ZRA-S; striped area), anastomosing stream patterns, pre 1886 sandblow sites (stars), and topographic profile (TP, bold line) approximately along the ZRA-S axis. Arrows along Pee Dee River denote reach flowing against southwest valley wall. Closed dashed contours near Summerville are highest-intensity isoseismals of the 1886 Charleston, South Carolina, earthquake (from Dutton, 1889). Abbreviations are as follows: AR - Ashley River; C - Conway; CCS - Caw Caw Swamp; CH - Charleston; CS - Cypress Swamp; F - Florence; G - Georgetown; LM - Lake Moultrie; MS - Mechanicsville littoral scarp; S - Summerville; SS - Surry littoral scarp.

Figure 2.5.2-215. Map of ZRA-S from Marple and Talwani (Reference 250)
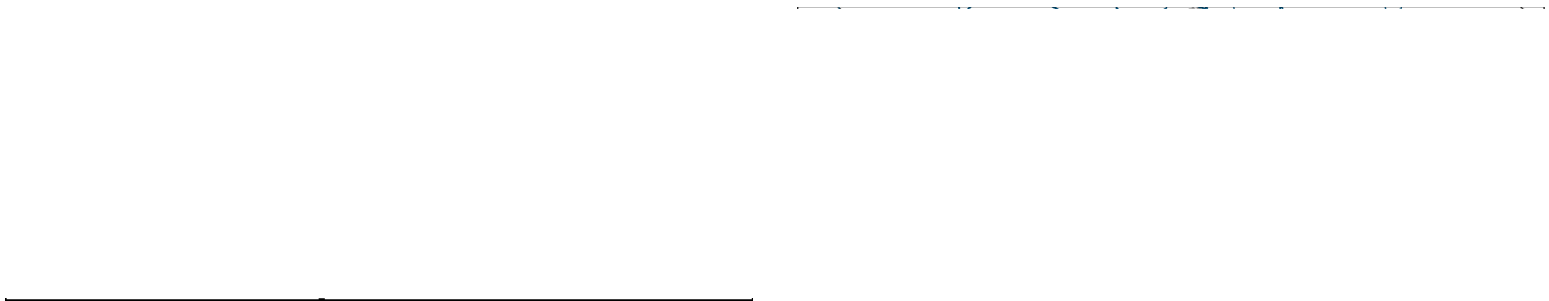
Figure 2.5.2-216.   Geographic Distribution of Liquefaction Features Associated with Charleston Earthquakes

Source: Exelon 2006
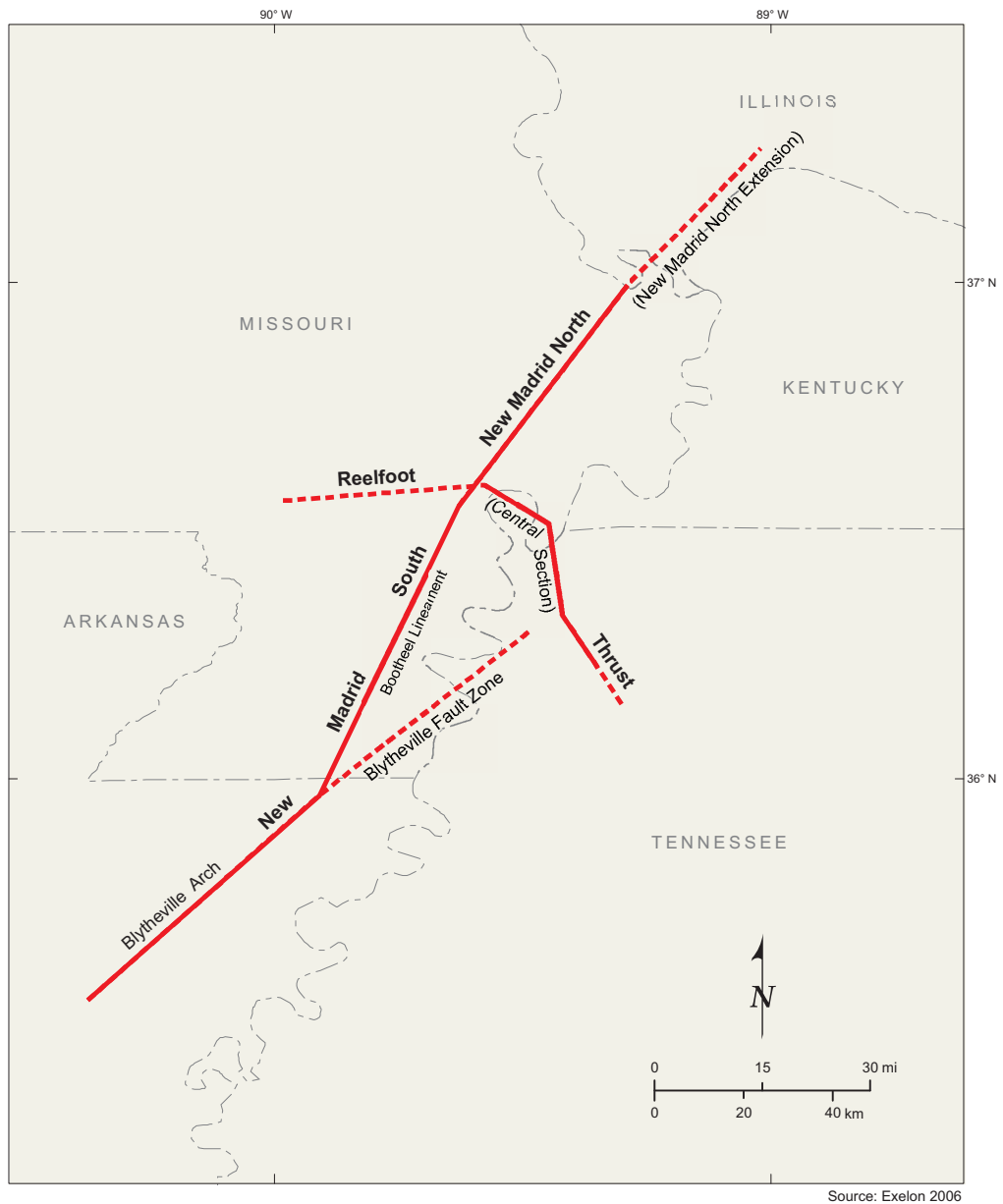
Figure 2.5.2-217. New Madrid Faults from Clinton ESP Source Model
Source: Reference 238

Southern New Madrid Source (NS)	Northern New Madrid Source (NN)	Reelfoot Fault (RF)	Characteristic Magnitudes for NM south, Reelfoot fault, and NM north	Rupture Sequence Model	Earthquake Recurrence Model	Repeat Time Coefficient of Variation	Equivalent Annual Frequency

Full Length (RF) (0.7)

New Madrid north (NN) (0.7)

Central Section (RFS) (0.3)

7.8, 7.7, 7.5 (0.1667)
7.9, 7.8, 7.6 (0.1667)
7.6, 7.8, 7.5 (0.25)
7.2, 7.4, 7.2 (0.0833)
7.2, 7.4, 7.0 (0.1667)
7.3, 7.5, 7.0 (0.1667)

Blytheville Arch/ Bootheel Lineament (BA/BL) (0.6)

New Madrid north plus extension (NN + NNE) (0.3)

Model A (0.667)
Model B (0.333)

Poisson (0.5) — N/A
Renewal (0.5)

0.3 (0.2)
0.5 (0.5)
0.7 (0.3)

Full Length (RF) (0.7)

New Madrid north (NN) (0.7)

Central Section (RFS) (0.3)

7.8, 7.7, 7.5 (0.1667)
7.9, 7.8, 7.6 (0.1667)
7.6, 7.8, 7.5 (0.25)
7.2, 7.4, 7.2 (0.0833)
7.2, 7.4, 7.0 (0.1667)
7.3, 7.5, 7.0 (0.1667)

Blytheville Arch/ Blytheville fault zone (BA/BFZ) (0.4)

New Madrid north plus extension (NN + NNE) (0.3)

Model A (0.667)
Model B (0.333)

Poisson (0.5) — N/A
Renewal (0.5)

0.3 (0.2)
0.5 (0.5)
0.7 (0.3)

Figure 2.5.2-218.   New Madrid Logic Tree From the Clinton ESP Source Model

Source: Reference 238
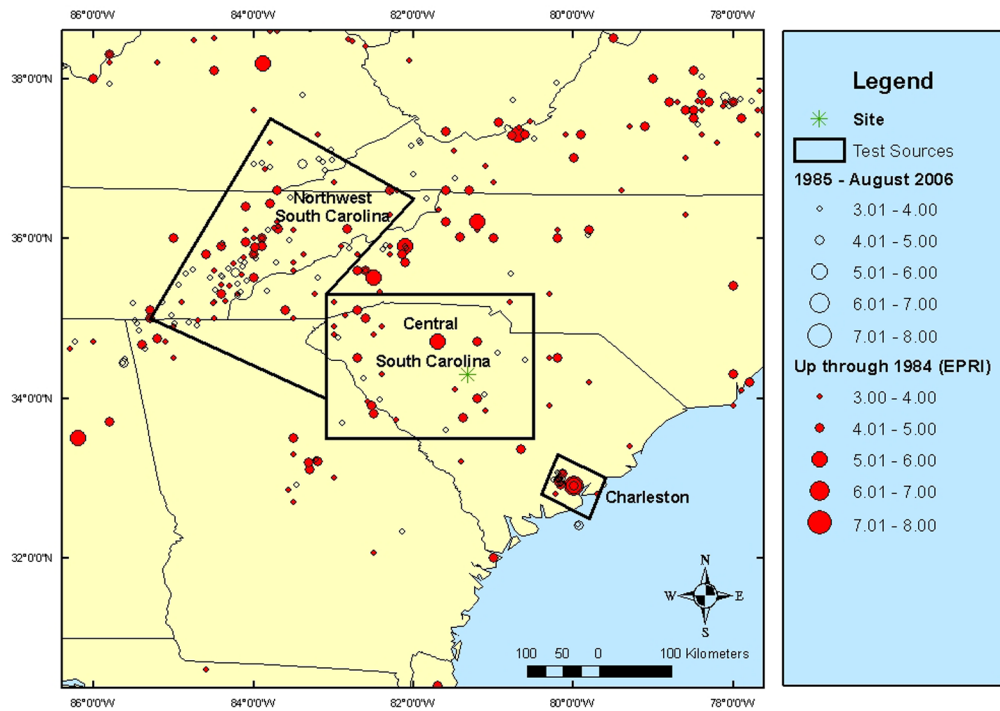
Figure 2.5.2-219. **Historical Seismicity in the Region of Units 2 and 3 Site and Three Areas Used to Test the Effects of Additional Seismicity**

Note: Earthquake epicenters are scaled to Rmb magnitude. For EPRI seismicity, only MAIN epicenters are plotted.
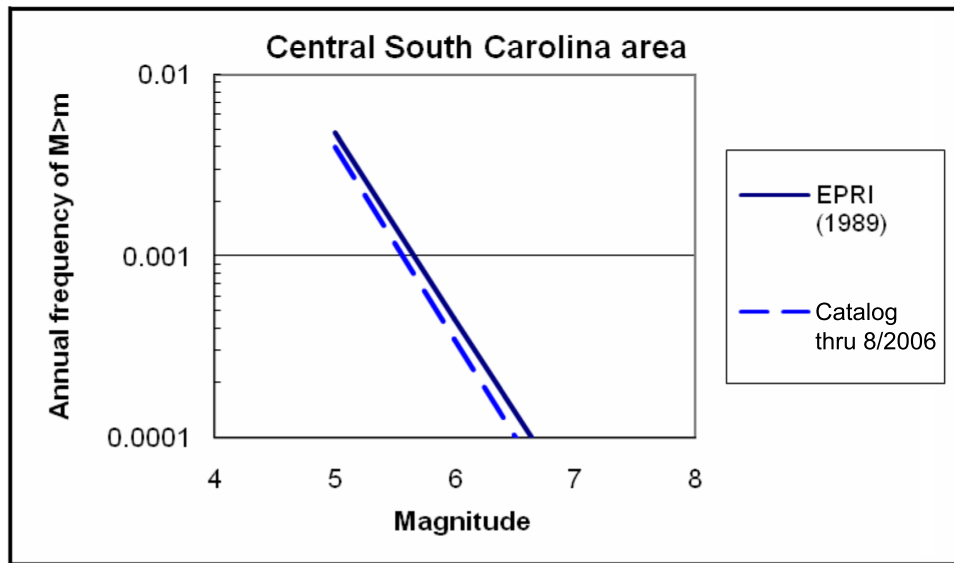
Figure 2.5.2-220. Earthquake Occurrence Rates for EPRI (1989) Catalog and for Catalog Extended through August 2006 for Central South Carolina Area
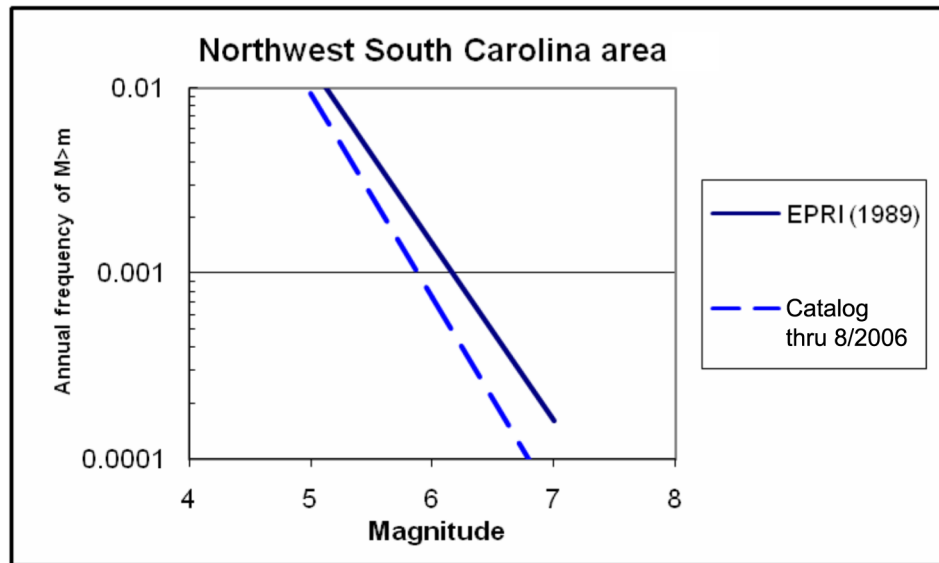
Figure 2.5.2-221. Earthquake Occurrence Rates for EPRI (1989) Catalog and for Catalog Extended through August 2006 for Northwestern South Carolina Area
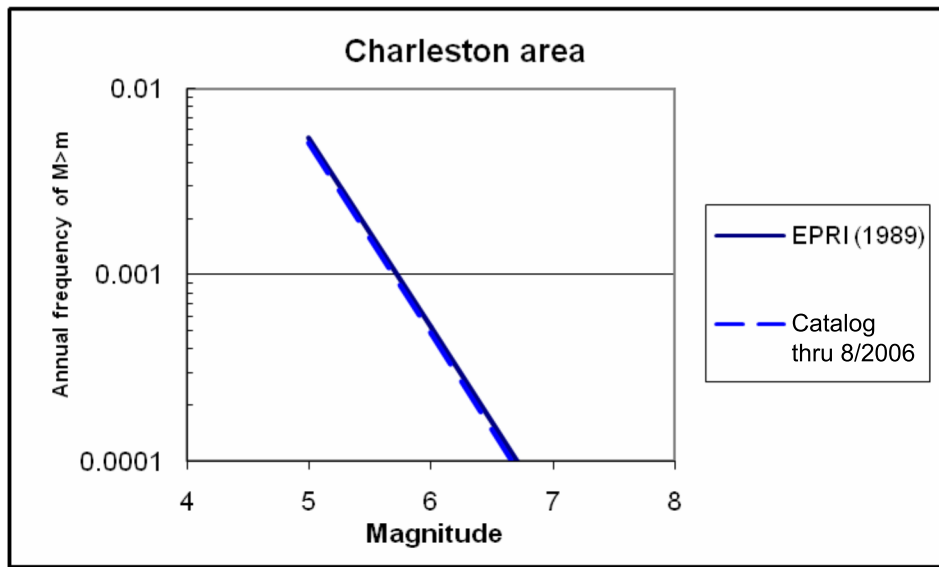
Figure 2.5.2-222. **Earthquake Occurrence Rates for EPRI (1989) Catalog and for Catalog Extended through August 2006 for Charleston Area**
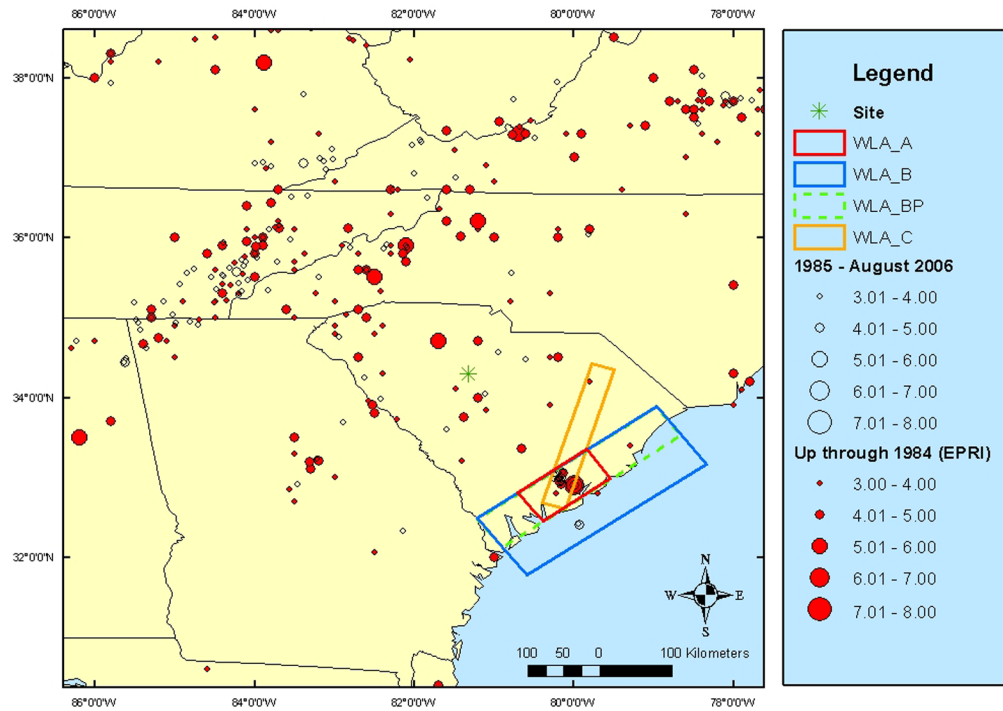
Figure 2.5.2-223. Geometry of Four Sources Used in UCSS Model
Note: Earthquake epicenters are scaled to Rmb magnitude. For EPRI seismicity, only MAIN epicenters are plotted. WLA_BP is equivalent to B'.
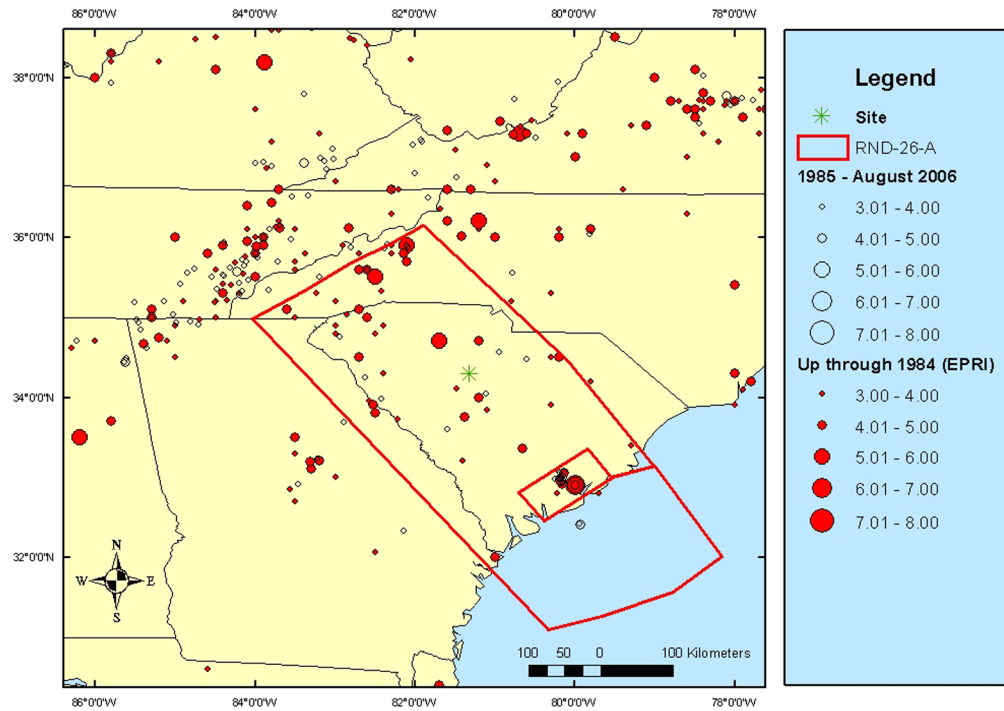
Figure 2.5.2-224. Geometry of Revised Rondout Source RND-26-A
Note: Earthquake epicenters are scaled to Rmb magnitude. For EPRI seismicity, only MAIN
        epicenters are plotted.
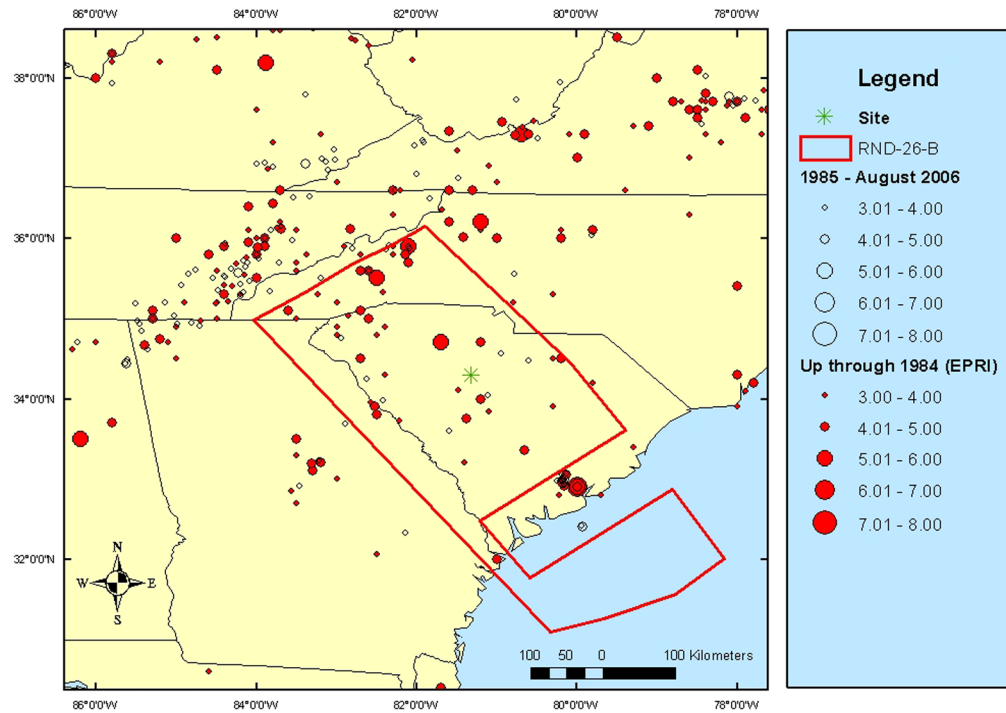
Figure 2.5.2-225.   Geometry of Revised Rondout Source RND-26-B
Note: Earthquake epicenters are scaled to Rmb magnitude. For EPRI seismicity, only MAIN
epicenters are plotted.
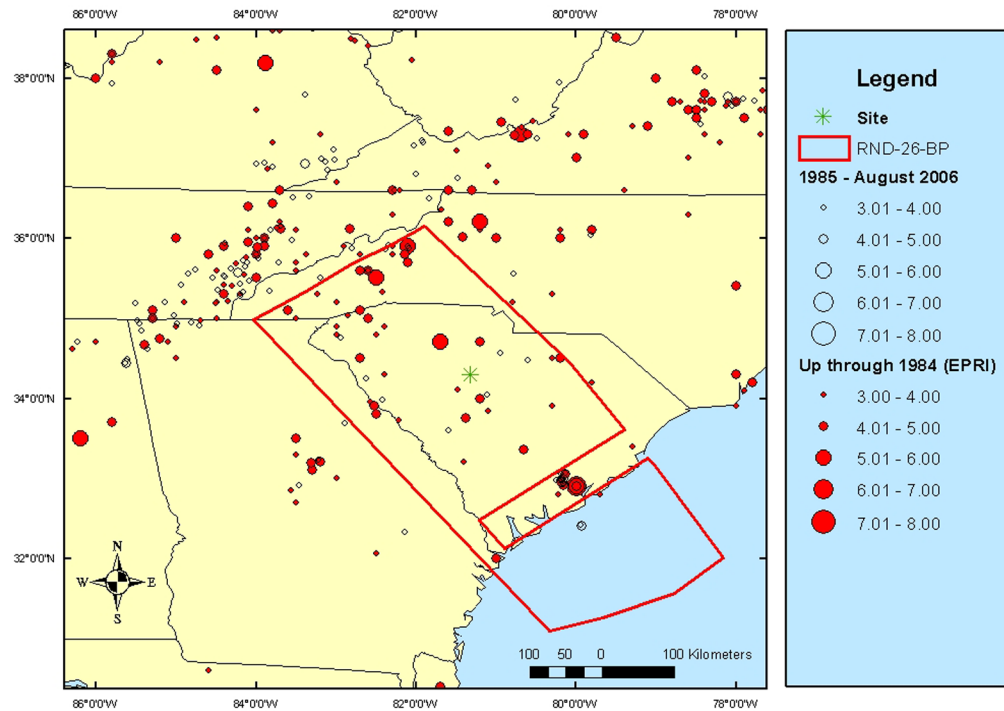
Figure 2.5.2-226. Geometry of Revised Rondout Source RND-26-BP
Notes:
Earthquake epicenters are scaled to Rmb magnitude. For EPRI seismicity, only MAIN epicenters are plotted.
BP is equivalent to B'.
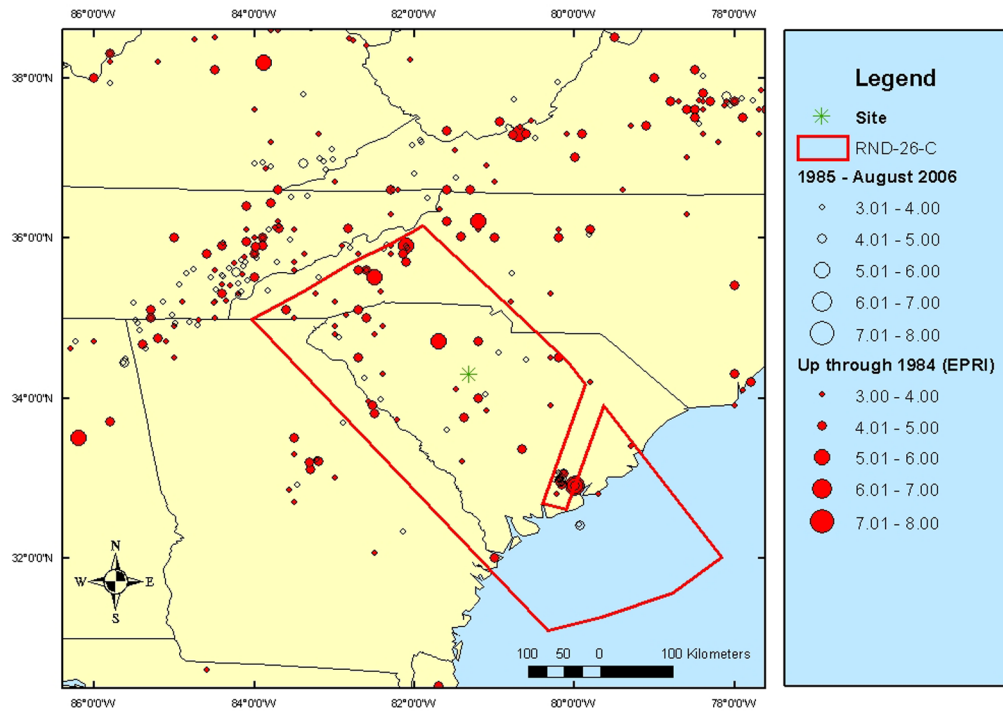
Figure 2.5.2-227. Geometry of Revised Rondout Source RND-26-C
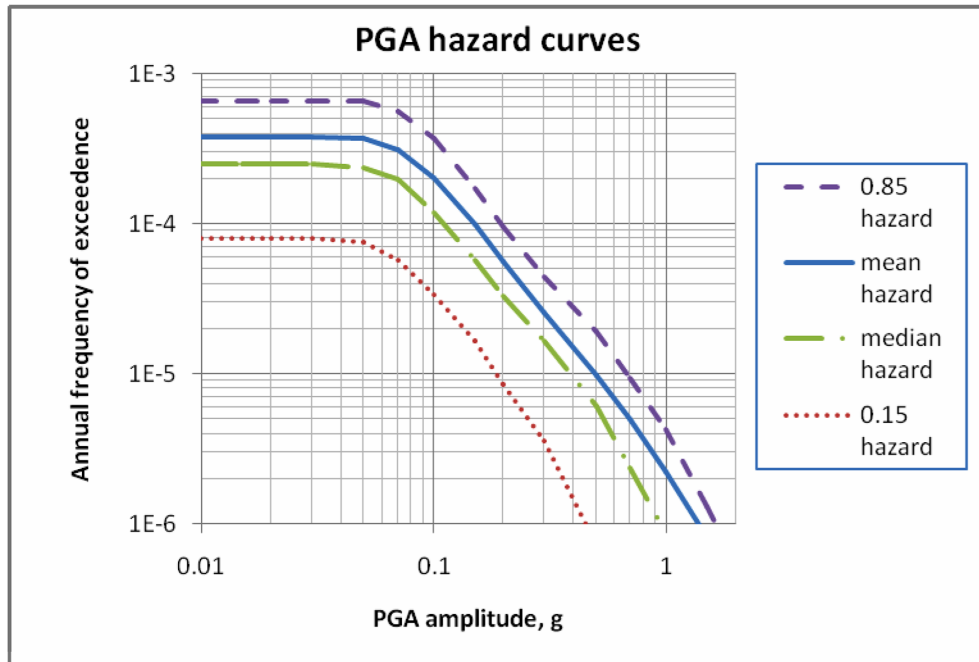
Figure 2.5.2-228. Mean and Fractile PGA Seismic Hazard Curves
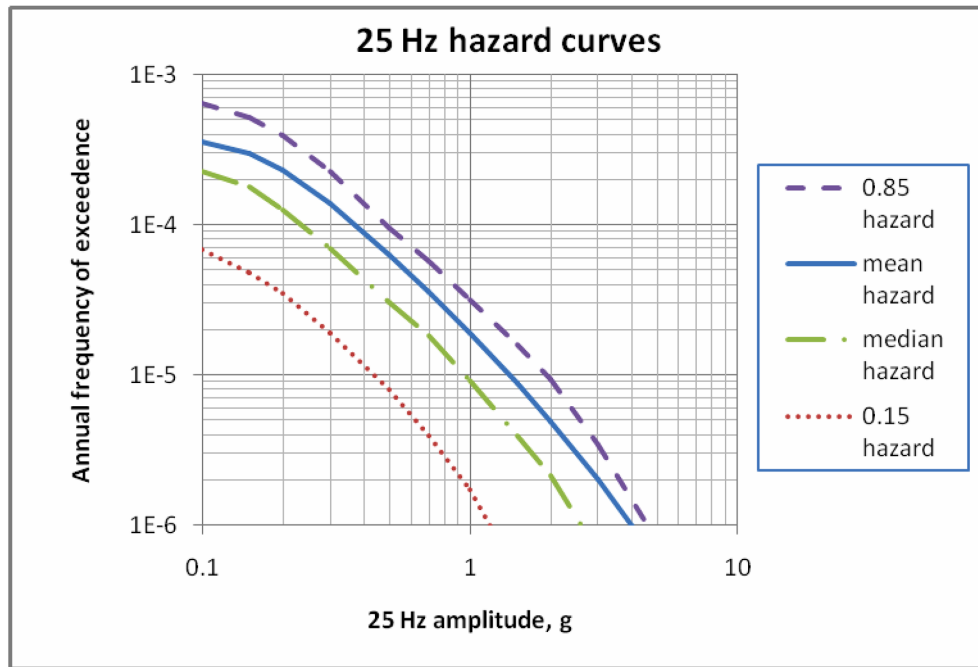
Figure 2.5.2-229.   Mean and Fractile 25 Hz Seismic Hazard Curves
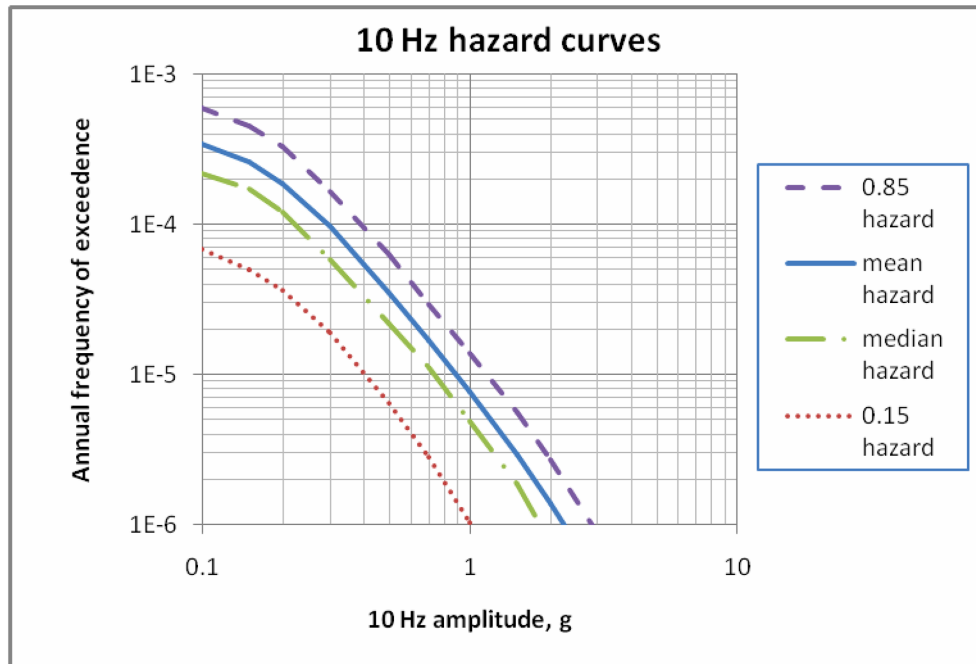
Figure 2.5.2-230. Mean and Fractile 10 Hz Seismic Hazard Curves
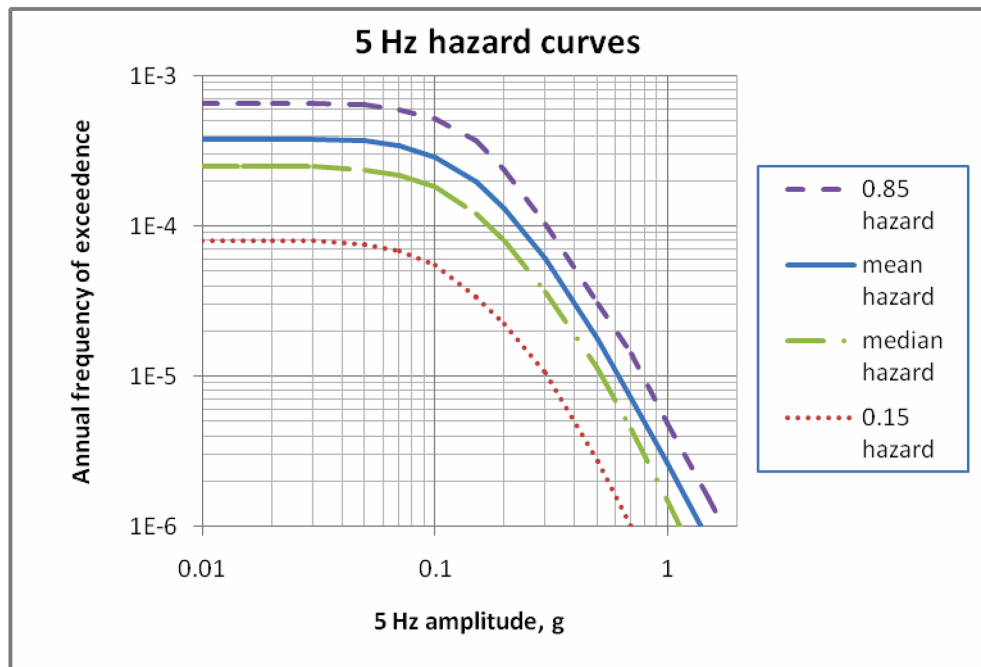
Figure 2.5.2-231. Mean and Fractile 5 Hz Seismic Hazard Curves
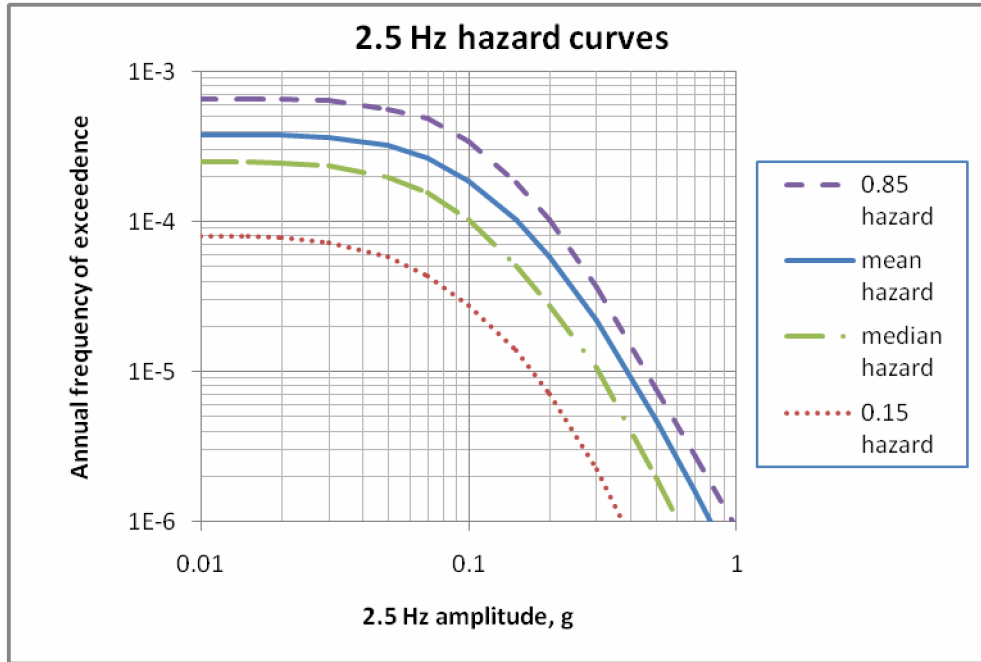
Figure 2.5.2-232.   Mean and Fractile 2.5 Hz Seismic Hazard Curves
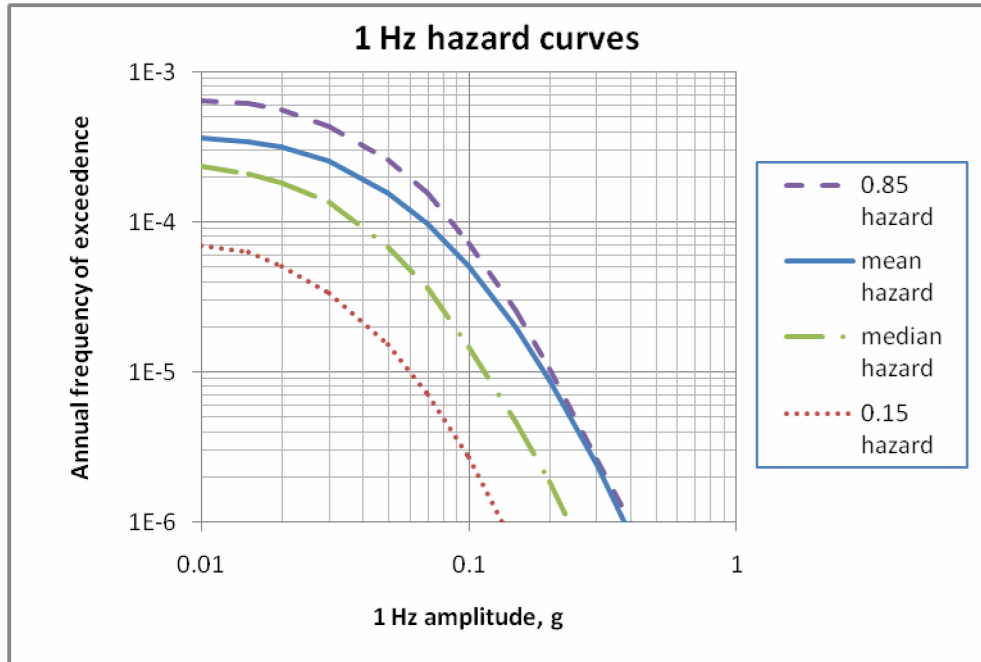
Figure 2.5.2-233.   Mean and Fractile 1 Hz Seismic Hazard Curves
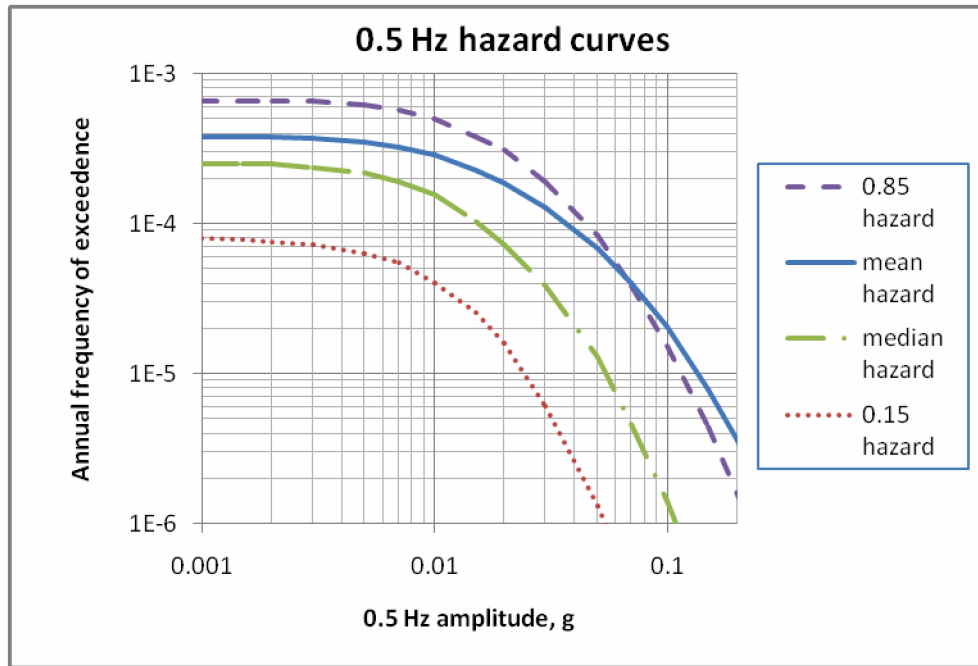
Figure 2.5.2-234. Mean and Fractile 0.5 Hz Seismic Hazard Curves
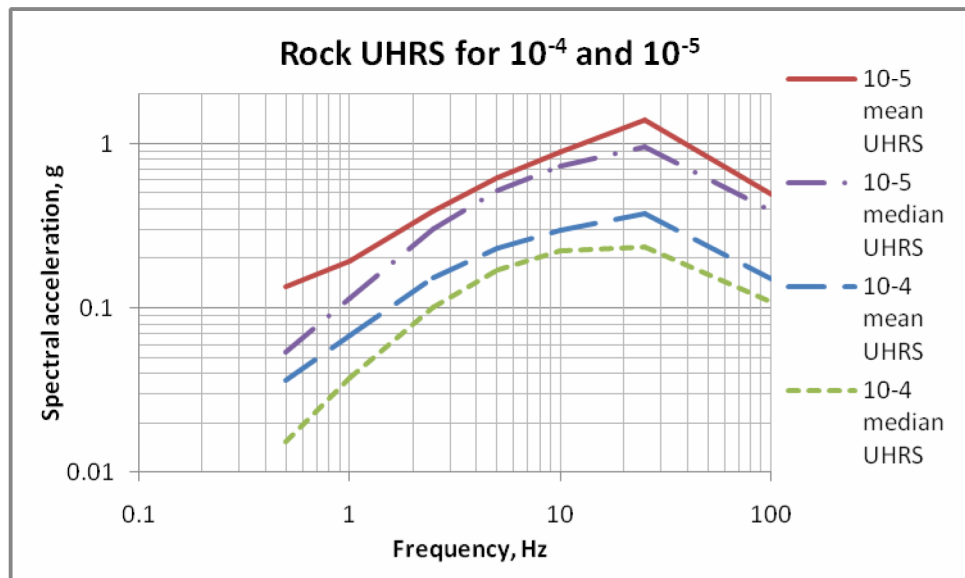
Figure 2.5.2-235. Mean and Median Uniform Hazard Response Spectra

1hz + 2.5hz, 1E-4
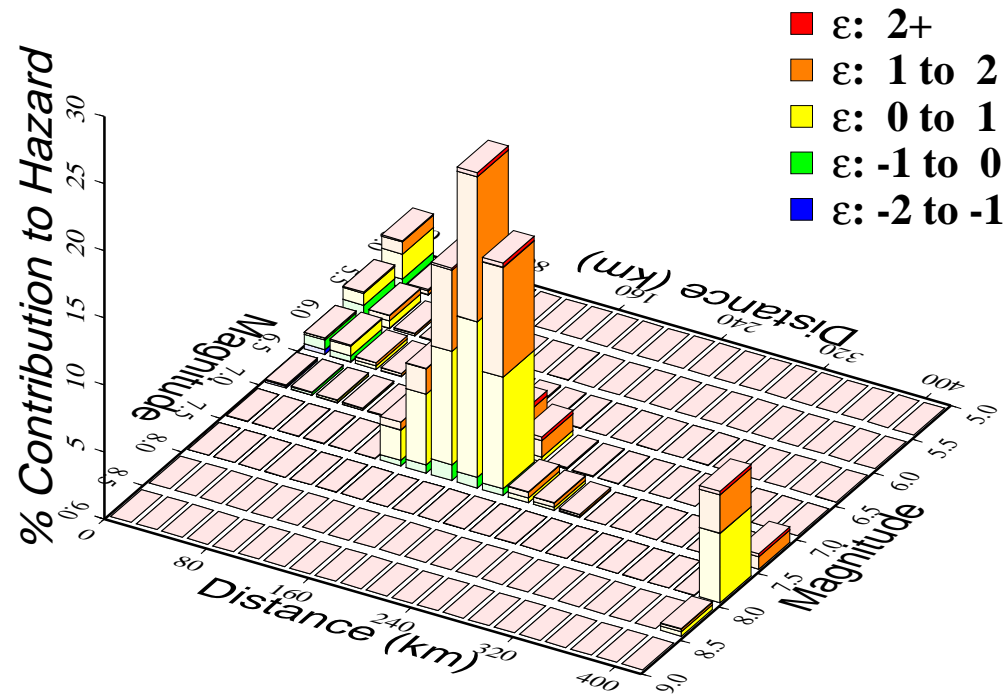
Figure 2.5.2-236. M and R Deaggregation for 1 and 2.5 Hz at 10^{-4} Annual Frequency of Exceedance

5hz + 10hz, 1E-4
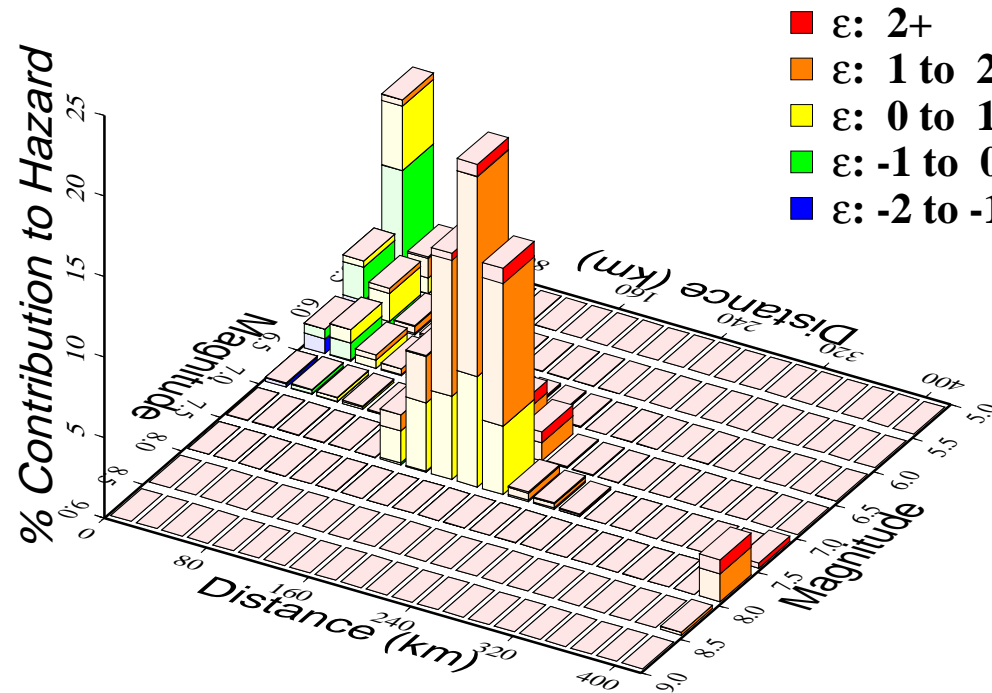
Figure 2.5.2-237. M and R Deaggregation for 5 and 10 Hz at 10^{-4} Annual Frequency of Exceedance

1hz + 2.5hz, 1E-5
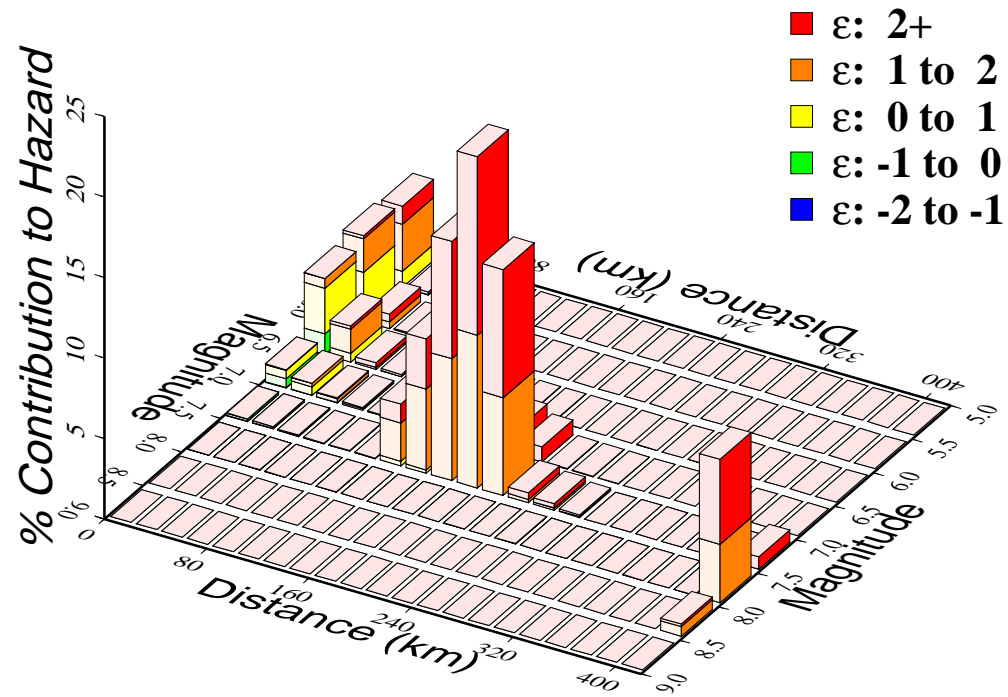
Figure 2.5.2-238. M and R Deaggregation for 1 and 2.5 Hz at 10^{-5} Annual Frequency of Exceedance

5hz + 10hz, 1E-5
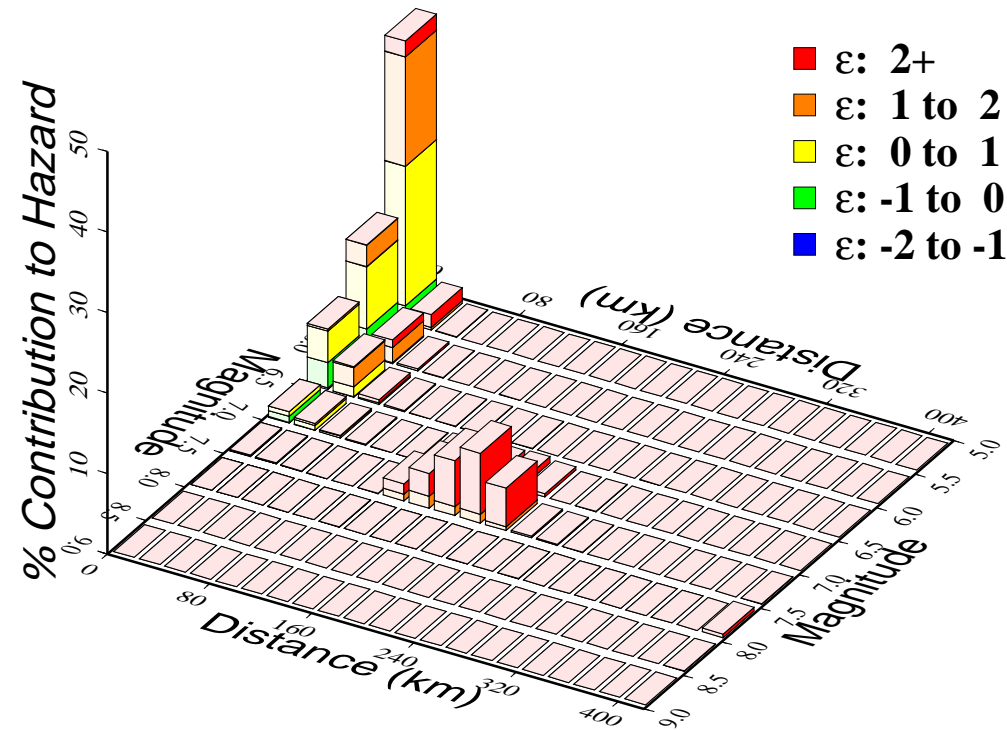
Figure 2.5.2-239. M and R Deaggregation for 5 and 10 Hz at 10^{-5} Annual Frequency of Exceedance

1hz + 2.5hz, 1E-6
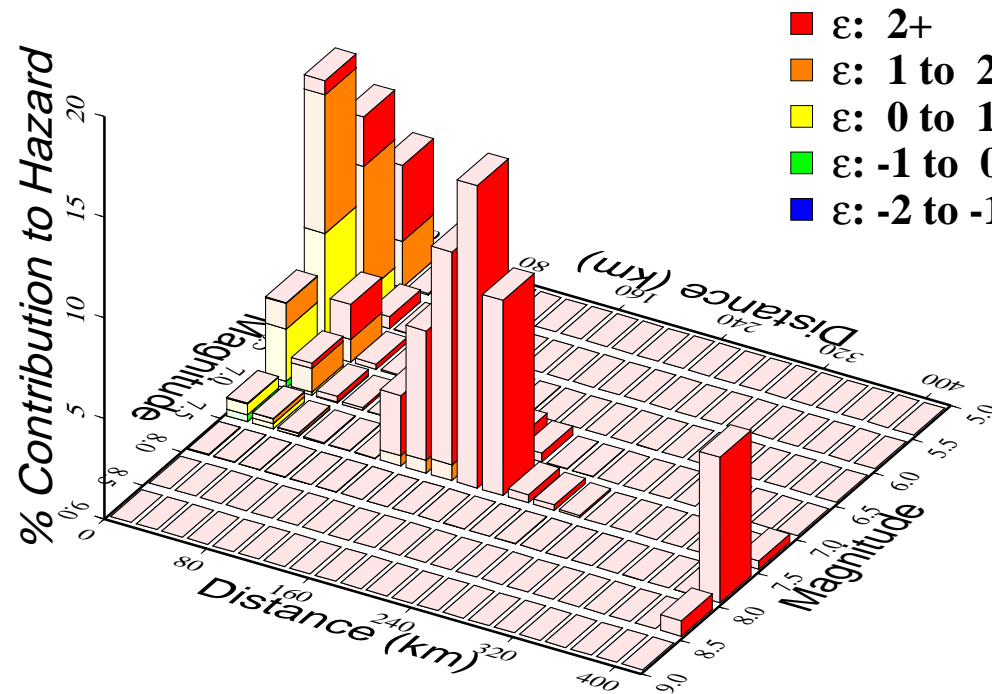
Figure 2.5.2-240. M and R Deaggregation for 1 and 2.5 Hz at 10^{-6} Annual Frequency of Exceedance
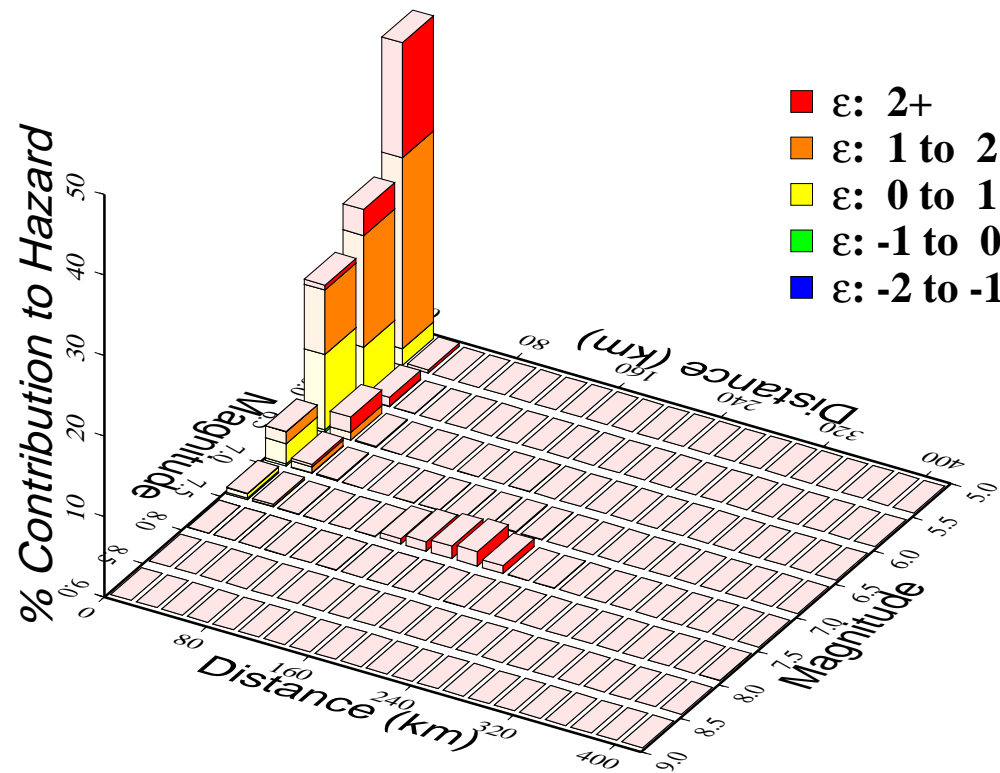
Figure 2.5.2-241. M and R Deaggregation for 5 and 10 Hz at 10^{-6} Annual Frequency of Exceedance
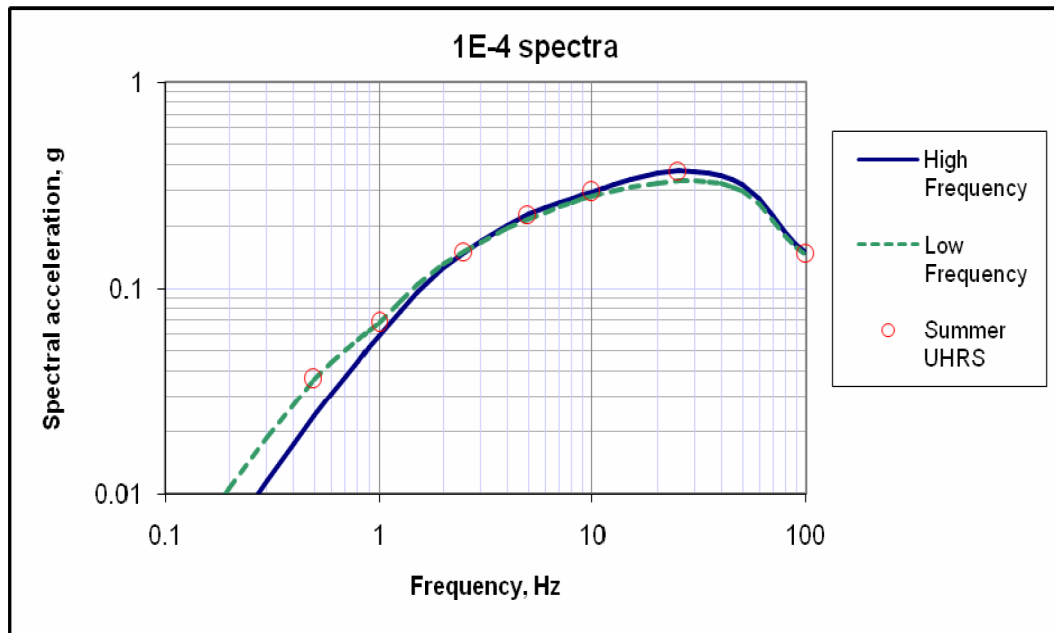
Figure 2.5.2-242. Smooth 10⁻⁴ UHRS for HF and LF Earthquakes
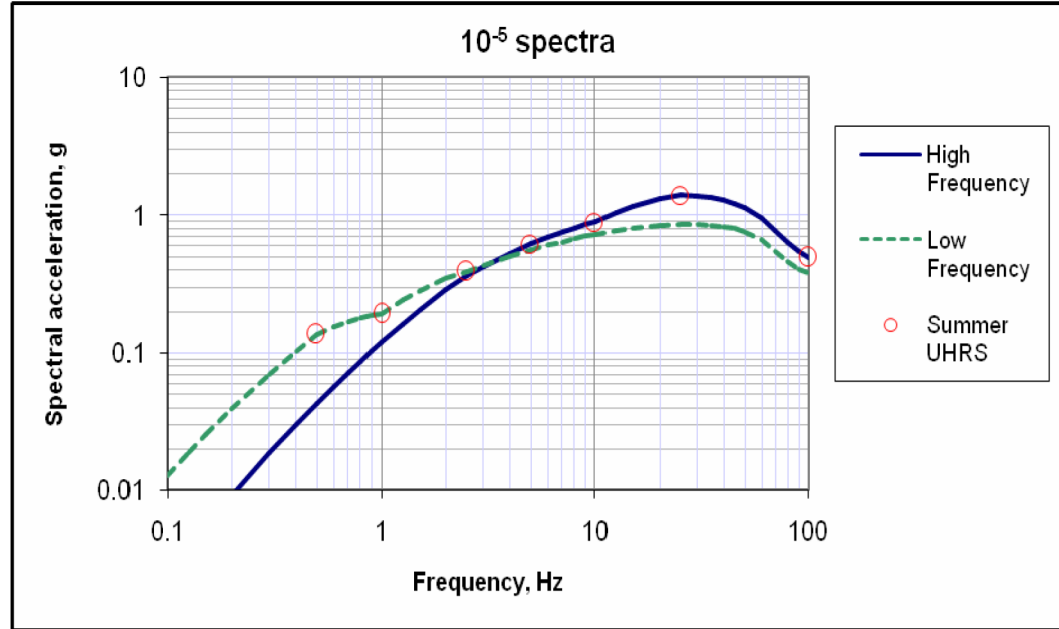
Figure 2.5.2-243. Smooth 10⁻⁵ UHRS for HF and LF Earthquakes
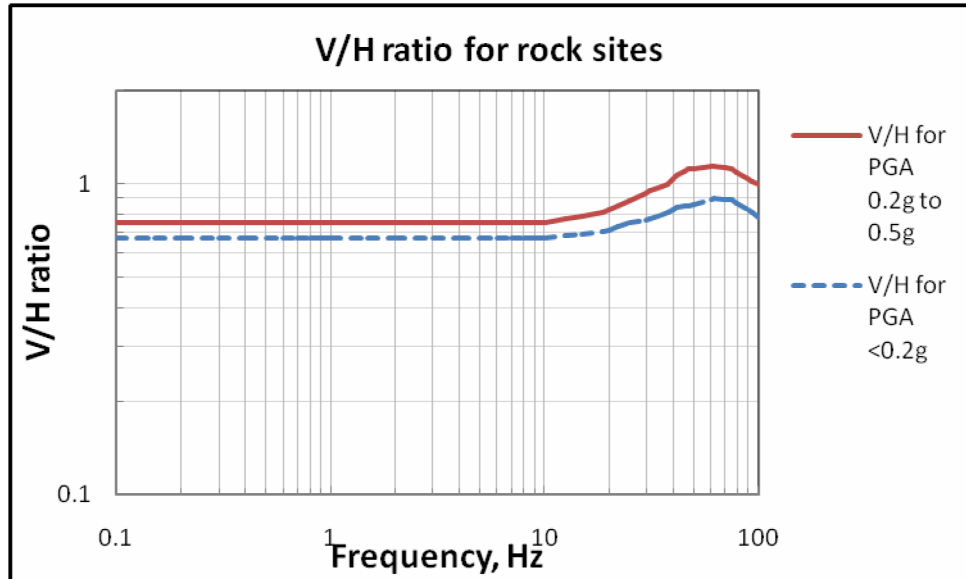
Figure 2.5.2-244. V/H Ratios for Hard Rock Sites for PGA<0.2g and for 0.2g≤PGA<0.5g
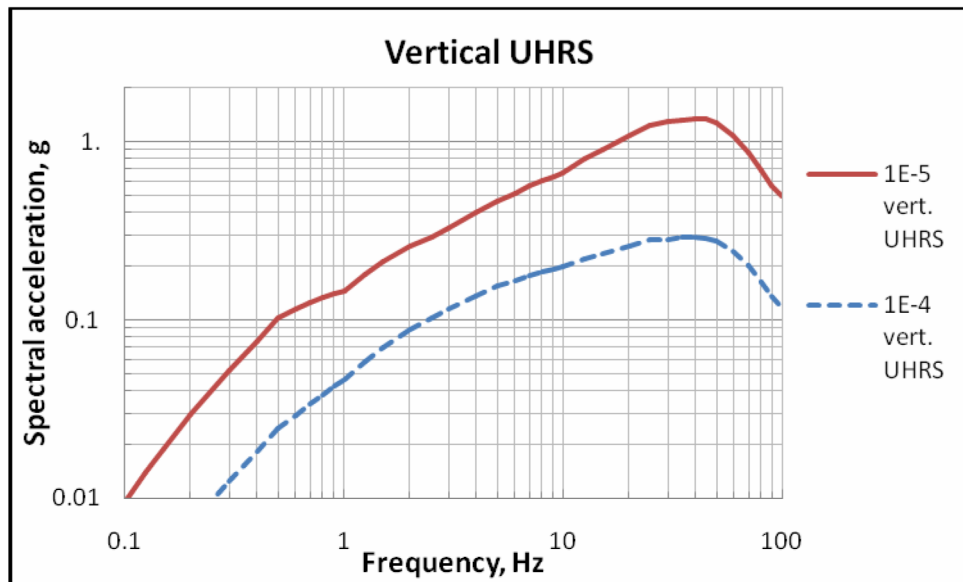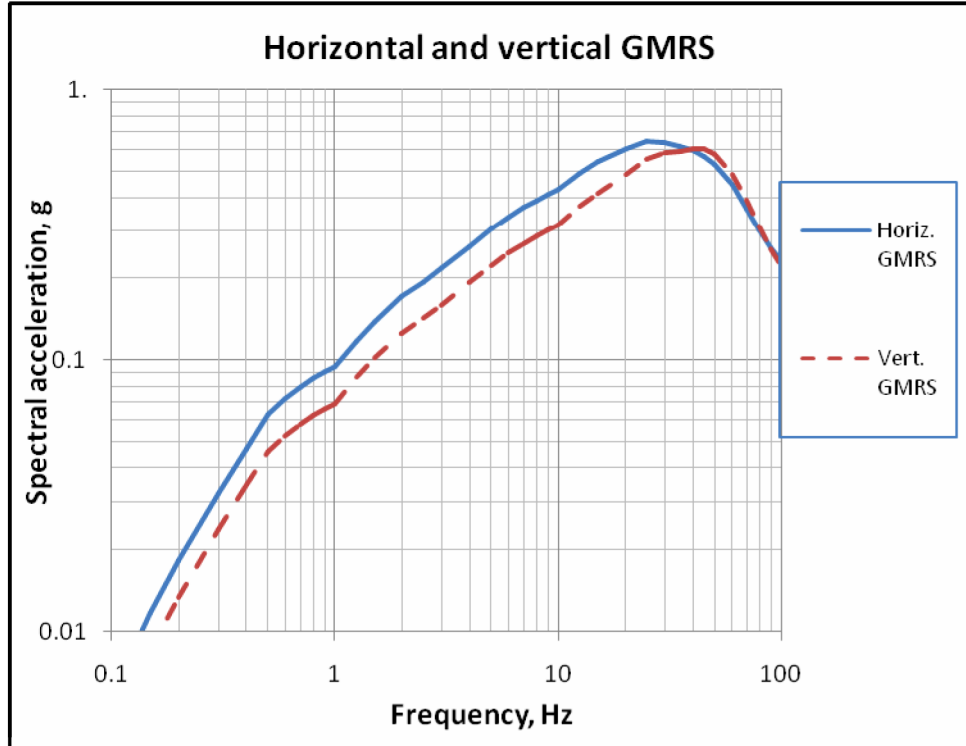
Figure 2.5.2-245. Vertical 10^{-4} and 10^{-5} UHRS

Figure 2.5.2-246. Horizontal and Vertical GMRS